University Medical Center Ulm

Department of Neurosurgery

Prof. Dr. med. Christian Rainer Wirtz

Tumor cell metabolism as a therapeutic target in glioblastoma - Characterization of the anti-neoplastic activity of a combined treatment with ONC201/TIC10 and 2-Deoxyglucose

Dissertation zur Erlangung des Doktorgrades der Medizin der Medizinischen Fakultät der Universität Ulm

Maximilian Pruss
born in Frankfurt am Main, Germany

2021

Current Dean: Prof. Dr. Thomas Wirth

First supervisor: Prof. Dr. Georg Karpel-Massler

Second supervisor: PD Mike-Andrew Westhoff, PhD

Day doctorate awarded: 13.01.2023

The data of this dissertation was published as:

"Dual metabolic reprogramming by ONC201/TIC10 and 2-Deoxyglucose induces energy depletion and synergistic anti-cancer activity in glioblastoma"

In the British Journal of Cancer in March 2020

Maximilian Pruss[1], Annika Dwucet[1], Mine Tanriover[1], Michal Hlavac[1], Richard Eric Kast[2], Klaus-Michael Debatin[3], Christian Rainer Wirtz[1], Marc-Eric Halatsch[1], Markus David Siegelin[4], Mike-Andrew Westhoff[3] and Georg Karpel-Massler[1]

[1] Department of Neurological Surgery, Ulm University Medical Center, Ulm, Germany;

[2] IIAIG, Study Center, Burlington, VT, USA;

[3] Department of Pediatric and Adolescent Medicine, Ulm University Medical Center, Ulm, Germany

[4] Department of Pathology and Cell Biology, Columbia University Medical Center, New York, NY, USA

Correspondence: Georg Karpel-Massler (georg.karpel@gmail.com)

Reuse under CC BY 4.0, https://creativecommons.org/licenses/by/4.0/

Table of Contents

ABBREVIATIONS VI

1. INTRODUCTION 1

1.1 GLIOBLASTOMA 1
1.2 MULTI-TARGETING AS A THERAPEUTIC STRATEGY IN GLIOBLASTOMA 4
1.3 CANCER CELL METABOLISM AS A TARGET IN GLIOBLASTOMA 7
1.4 IMIPRIDONES AS POTENTIAL ANTI-GLIOBLASTOMA THERAPEUTICS 14
1.5 2-DEOXYGLUCOSE 18
1.6 AIM OF THE STUDY 20

2. MATERIALS AND METHODS 21

2.1 MATERIALS 21
2.1.1 CELL LINES 21
2.1.2 CELL CULTURE MEDIA, SUPPLEMENTS AND REAGENTS 21
2.1.3 TREATMENT REAGENTS 22
2.1.4 CELL VIABILITY ASSAYS 22
2.1.5 SOFT AGAR ASSAY 23
2.1.6 CELLTITER-GLO® ASSAY 23
2.1.7 STAINING FOR CARBOXYFLUORESCIN DIACETATE SUCCINIMIDYL ESTER (CFSE) 24
2.1.8 MEASUREMENT OF CELL DEATH AND CELL CYCLE ANALYSIS 24
2.1.9 REAL-TIME PCR AND CDNA SYNTHESIS 24
2.1.10 WESTERN BLOT ANALYSIS 25
2.1.11 PHOSPHO-KINASE ARRAY 30
2.1.12 EXTRACELLULAR FLUX ANALYSIS 30
2.1.13 CELL MIGRATION/MOTILITY ASSAYS 30
2.1.14 CHORION ALLANTOIC MEMBRANE (CAM) ASSAY/TOXICITY STUDY IN CHICKEN EMBRYOS 31
2.1.15 CONSUMABLES 31
2.1.16 APPLIANCES 32
2.1.17 SOFTWARE 32
2.2 METHODS 33
2.2.1 CELL CULTURE 33
2.2.2 DETERMINATION OF CELL NUMBERS 34
2.2.3 TREATMENT OF CELLS 34
2.2.4 CELL VIABILITY ASSAYS 34
2.2.5 SOFT AGAR ASSAY 35
2.2.6 CELLTITER-GLO® ASSAY 36
2.2.7 STAINING FOR CARBOXYFLUORESCIN DIACETATE SUCCINIMIDYL ESTER (CFSE) 36
2.2.8 MEASUREMENT OF CELL DEATH AND CELL CYCLE ANALYSIS 36
2.2.9 REAL-TIME PCR AND CDNA SYNTHESIS 37
2.2.10 WESTERN BLOT ANALYSIS 38
2.2.11 PHOSPHO-KINASE ARRAY 39
2.2.12 EXTRACELLULAR FLUX ANALYSIS 41
2.2.13 CELL MIGRATION/MOTILITY ASSAYS 41

2.2.14 CHORION ALLANTOIC MEMBRANE (CAM) ASSAY 42
2.2.15 TOXICITY STUDY IN CHICKEN EMBRYOS 43
2.2.16 STATISTICAL ANALYSIS 43

3. RESULTS 44

3.1 TREATMENT WITH ONC201/TIC10 SUPPRESSES OXPHOS IN GLIOBLASTOMA CELLS .. 44
3.2 ONC201/TIC10 DOWN-REGULATES PROTEIN EXPRESSION OF RESPIRATORY CHAIN COMPLEXES 47
3.3 TREATMENT WITH ONC201/TIC10 ENHANCES THE GLYCOLYTIC RATE OF GLIOBLASTOMA CELLS 51
3.4 TREATMENT WITH ONC201/TIC10 LEADS TO AN ENHANCED ACTIVATION OF THE SERINE-ONE CARBON-GLYCINE (SOG) PATHWAY 53
3.5 COMBINED TREATMENT WITH ONC201/TIC10 AND 2-DEOXYGLUCOSE LEADS TO A SYNERGISTIC REDUCTION OF THE CELL VIABILITY OF GLIOBLASTOMA CELLS 54
3.6 COMBINED TREATMENT WITH ONC201/TIC10 AND 2-DG LEADS TO AN ENHANCED INHIBITION OF ANCHORAGE-INDEPENDENT GROWTH 57
3.7 THE COMBINATION TREATMENT LEADS TO SUPPRESSION OF ATP LEVELS 58
3.8 TREATMENT WITH ONC201/TIC10 AND 2-DG ACTIVATES AMPK AND INDUCES A HYPO-PHOSPHORYLATED STATE 60
3.9 THE COMBINATION TREATMENT INDUCES CYTOSTASIS IN GLIOBLASTOMA CELLS 64
3.10 COMBINED TREATMENT WITH ONC201/TIC10 AND 2-DG HAS MARKED ANTI-MIGRATORY EFFECTS ON GLIOBLASTOMA CELLS 69
3.11 COMBINED TREATMENT WITH ONC201/TIC10 AND 2-DG LEADS TO AN INHIBITION OF TUMOR GROWTH ON THE CHORION ALLANTOIC MEMBRANE 74
3.12 THE COMBINATION TREATMENT WITH ONC201/TIC10 AND 2-DG HAS A LOW TOXICITY IN NORMAL HUMAN CELLS AND SHOWS NO ORGAN TOXICITY IN CHICKEN EMBRYOS 76

4. DISCUSSION 80

5. SUMMARY 86

6. BIBLIOGRAPHY 87

Abbreviations

^{18}F-FDG	^{18}F-fluorodeoxyglucose
^{18}F-FDG-6-P	^{18}F-FDG-6-phosphate
2-DG	2-deoxyglucose
2-DG-6-P	2-deoxyglucose-6-phosphate
3-BP	3-bromopyruvate
2-HG	2-R-2-hydroxyglutarate
ACL	ATP-citrate lyase
AKT	Protein kinase B
APS	ammonium persulfate
ATP	adenosine triphosphate
ATRX	alpha thalassemia/mental retardation syndrome X-linked
Bcl-2	B-cell lymphoma-2
BSA	Bovine Serum Albumin
CAC	citric acid cycle
CAM	chorion allantoic membrane
cDNA	complementary DNA
CFSE	carboxyfluorescin diacetate succinimidyl ester
CSC	cancer stem cells
D-2-HG	D-2-hydroxyglutarate
DAPI	4’6-diamidino-2-phenylindole
DDT	DL-dithiothreitol
DMSO	dimethyl sulfoxide
DPBS	Dulbecco’s Phosphate Buffered Saline
DR4/DR5	death receptor 4/5
DRD2/4	dopamine receptor D2/3
ECAR	extracellular acidification rate
EDTA	Ethylenediaminetetraacetic acid

EGFR	epidermal growth factor receptor
EGFRm	EGFR-mutated
EGFRvIII	mutated EGFR subtype
eIF2α	eukaryotic initiation factor 2α
ERK	extracellular signal-regulated kinase
Foxo3a	Forkhead box O 3a
FBS	Fetal Bovine Serum
FCCP	carbonyl cyanide-4 (trifluoromethoxy) phenylhydrazone
GAPDH	glyceraldehyde 3-phosphate dehydrogenase
GLS	glutaminase
GLUT	glucose transporter
HCC	hepatocellular carcinoma
HK	hexokinase
HK2	hexokinase 2
HRP	horseradish peroxidase
IC_{50}	half maximal inhibitory concentration
IDH	isocitrate dehydrogenase
IDH1	isocitrate dehydrogenase-1
IDH2	isocitrate dehydrogenase-2
ISR	integrated stress response
LOH	loss of heterozygosity
MAPK	mitogen-activated protein kinase
MAC	membrane attack complex
Mcl-1	myeloid cell leukemia 1
MDM2	mouse double minute 2
MGMT	O^6-methylguanine-methyltransferase
min	minute
mTOR	mammalian target of rapamycin
mTORC1	mammalian target of rapamycin complex 1
MTT	3-(4,5-Dimethythiazol-2-yl)-2,5-diphenyl tetrazolium bromide

MW	molecular weight
NAD+	oxidized nicotinamide adenine dinucleotide
NADH	reduced nicotinamide adenine dinucleotide
NADP+	oxidized nicotinamide adenine dinucleotide phosphate
NADPH	reduced nicotinamide adenine dinucleotide phosphate
NAMPT	nicotinamide phosphoribosyl-transferase
OCR	oxygen consumption rates
OXPHOS	oxidative phosphorylation
PBS	Phosphate Buffered Saline
PDGFA	platelet-derived growth factor A
PDGFRa	platelet-derived growth factor receptor alpha
PDH	pyruvate dehydrogenase
PDX	patient derived xenograft
PEP	phosphoenolpyruvate
PET	positron emission tomography
PI	propidium iodide
PI3K	phosphatidylinositol-3-kinase
PKM2	pyruvate kinase M2
PTEN	phosphatase and tensin homolog
RAC1	Ras-related C3 botulinum toxin substrate 1
rpm	revolutions per minute
RT	room temperature
PCR	polymerase chain reaction
RTK	receptor tyrosine kinase
SD	standard deviation
SDS	sodium dodecyl sulfate
SOG	serine-one carbon-glycine
TAE	Tris Acetate EDTA
TEMED	N,N,N’-Tetramethyl ethylene diamine
TERT	telomerase reverse transcriptase gene
TIC10	TRAIL-inducing compound 10

TILs	tumor-infiltrating lymphocytes
TMZ	temozolomide
TP53	tumor suppressor protein 53
TRAIL	TNF-related apoptosis-inducing ligand
v/v	volume percent
wtEGFR	wild-type EGFR
wtIDH	wild-type IDH

1. Introduction

1.1 Glioblastoma

Glioblastoma accounts for over 65% of all malignant brain tumors, most of the time being a primary lesion and of IDH wild type status. In only about 5% of cases patients are diagnosed with a preceding low-grade glioma that progressed secondarily to a IDH mutant glioblastoma [21,43].

In the current WHO grading system, the glioblastoma is classified as a grade IV tumor being the most aggressive, invasive and undifferentiated type of glioma. Despite being a rare tumor with a global incidence of less than 10 people per 100,000, its mean survival rate of 15 months after diagnosis makes it an important public health issue [38]. Glioblastomas can occur at any age, but the peak incidence is in the age group 55 to 60 years with a slightly higher incidence in men compared to women. More than half of the patients diagnosed with a primary glioblastoma present with a clinical history between 3-6 months, yet if it progresses secondarily from a low-grade glioma the clinical history may extend to several [46]. The clinical signs and symptoms of a glioblastoma can result from different mechanisms. The loss of brain tissue from necrosis can give rise to focal neurological deficits (40-60%) and cognitive impairments depending on the location of the glioblastoma. Secondarily the gradually growing tumor and its increasing surrounding edema increases the intracranial pressure and can cause a deviation of intracranial contents resulting in usually unilateral and progressively worsening headaches (30-50%). Moreover, the patient can also present with seizures of focal onset, which are either simple partial, complex partial or generalized ones [57].

As mentioned before, glioblastoma is classified into primary (IDH wild type) and secondary glioblastomas (IDH mutant), where the primary type forms *de novo* with no clinical or histological evidence of a malignant precursor and the secondary glioblastoma develops from a low-grade diffuse astrocytoma (Grade II) or an anaplastic astrocytoma (Grade III) [62]. Genetic alterations commonly occurring in primary glioblastomas are EGFR (epidermal growth factor receptor) and MDM2

(mouse double minute 2) overexpression, chromosome p16 deletion and LOH (loss of heterozygosity) of chromosome 10q holding PTEN (phosphatase and tensin homolog) and TERT (telomerase reverse transcriptase gene) promoter mutation. Genetic characteristics of secondary glioblastomas besides the presence of mutations of IDH1/2 (isocitrate dehydrogenase-1 or 2) include the overexpression of PDGFA (platelet-derived growth factor A) and PDGFRa (platelet-derived growth factor receptor alpha), LOH of chromosome 19q, mutations of TP53 (tumor suppressor protein 53) and ATRX (alpha thalassemia/mental retardation syndrome X-linked). Those genetic alterations can be grouped into the oncogenic signaling pathway PI3K/AKT, which is altered in 88% of Glioblastomas and p53 pathway, altered in 87% of Glioblastomas [20,70].

The activation of PI3K (phosphatidylinositol-3-kinase), which is regulated by many growth factors and their receptors such as EGFR, generates phosphatidylinositol-3,4,5-triphosphate that consequently activates Akt [39]. Akt in turn activates mTOR (mammalian target of rapamycin) influencing the tumor cell growth and division. Tumor suppressor PTEN inhibits this pathway by blocking Akt signaling through the reduction of intracellular phosphatidylinositol-3,4,5-triphosphate. P53 is a tumor suppressor that responds to DNA damage and genotoxic and cytotoxic stress. It is not only important for tumor suppression itself, but is also regulating more than 2,500 genes, that are largely involved in tumor development, tumorigenesis and tumor invasion. Mutations in the p53 pathway are related to the development of both primary and secondary glioblastomas [39].

Histologically, glioblastoma is distinguished from low-grade gliomas through pseudopalisading necrosis, microvascular proliferation, increased mitotic activity and pleomorphic nuclei and cells [23,55]. On contrast enhanced T1-weighted magnetic resonance images, glioblastomas usually present as contrast enhancing tumors with a central irregular hypo-enhancement coherent with necrosis [35]. Commonly on T2-weighted images a hyperintense region surrounding the tumor, consistent with vasogenic edema is seen. Imaging features can also be of prognostic value, as the absence of edema, non-contrast-enhancing tumor, absence of satellite and multifocal lesions are shown to be significant predictors of longer survival [35].

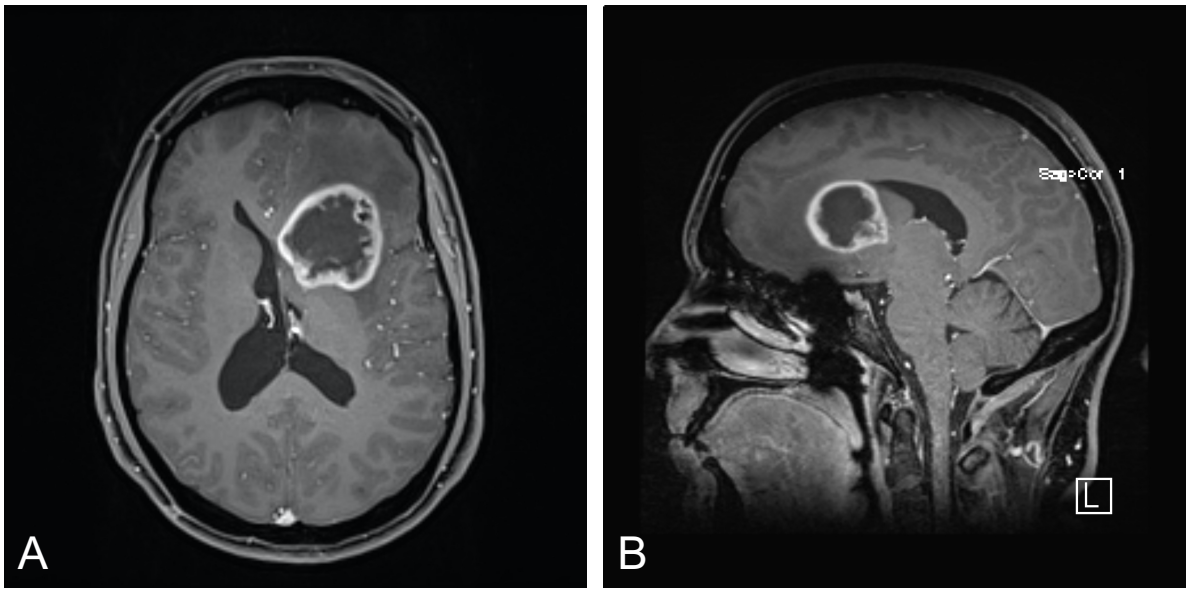

Figure 1: Glioblastoma on MRI (kindly provided by the Department of Diagnostic and Interventional Radiology, University Hospital Ulm)

A) Axial contrast-enhanced T1-weighted image showing an enhancing tumor with irregular hypo-enhancement coherent with necrosis and displacement of the lateral ventricle.

B) Sagittal contrast-enhanced T1-weighted image showing a hypo-intense region in the frontal lobe, which is suggestive of a vasogenic edema.

Another prognostic marker is the methylation status of the O^6-methylguanine-methyltransferase MGMT, a DNA repair protein that inhibits the cross-linkage of double-stranded DNA by alkylating agents, such as temozolomide (TMZ), through formation of O^6-methylguanine, ultimately causing cell death. Methylation of the MGMT promoter causes the silencing and inhibition of MGMT expression. Further, the mutation of IDH1 or IDH2, genes coding the expression of isocitrate dehydrogenase (IDH), where IDH1 is the more common mutation, is another positive prognostic marker. IDH is an enzyme in the citric acid cycle, which catalyses the oxidative decarboxylation of isocitrate to alpha-ketoglutarate and CO_2. Said mutations in the genes IDH1 and IDH2, which are frequently present in WHO grade II or III gliomas and in secondary glioblastomas, lead to a neo-function that results in the generation of 2-hydroxyglutarate [79]. Importantly, it has been shown that mutated IDH predicts a better response to TMZ in secondary

glioblastomas [64]. Together, the MGMT methylation and the the IDH mutation status predict an improved overall survival after treatment with TMZ and concomitant radiotherapy [7,43,64].

Unfortunately, despite first-line therapy that consists of a maximal safe surgical resection followed by radiotherapy with concomitant and adjuvant TMZ, the clinical course is grim in the vast majority of patients, as the invasive character of glioblastomas makes a recurrence inevitable [67]. Furthermore, in 95% of the cases the relapse occurs within two to three centimeters of the resection cavity and lesions can even be found in the contralateral hemisphere, which shows the importance of hampering the migratory capacity of tumor cells [18].

1.2 Multi-targeting as a therapeutic strategy in glioblastoma

Intratumoral heterogeneity presents a major obstacle for successful treatment of malignant diseases. It describes the synchronous presence of different tumor cell populations within the same tumor, that have distinct genetic, epigenetic and phenotypic features. This divergent development of subpopulations is presumably a main factor of therapy failure, occurrence of treatment resistance and also recurrence of the malignancy [26,65].

Genetic heterogeneity can result from the increased tolerance to genome instability of cancer cells, allowing them to endure DNA damage, chromosomal mutations and obtain therapy-induced mutations. TMZ treatment has been shown to be an exogenous source of mutations in glioblastoma, a highly heterogenous tumor, including RB1 and CDKN2A driver gene mutations, both of which lead to subclonal expansions making the tumor even more heterogenic. Besides that, continuous drug treatment in the presence of a resistant, non-dominant subclone can speed up tumoral growth by eliminating the chemotherapy-sensitive, dominant cell population and therefore, allow the resistant sub-population to expand and become the new dominant tumor-cell population [41,56,77].

It has been shown that different tumoral subclones can interact and even cooperate with each other. For instance, in glioblastoma, a subclone overexpressing EGFRvIII was identified to release cytokines to neighboring dominant cell populations expressing wtEGFR to promote tumor-growth [24]. Moreover, it has been described that in glioblastoma with significant EGFR expression, distinct cell populations can be present at the same time lacking EGFR and on the other hand express other receptor tyrosine kinases (RTK). This in turn, offers other potential mechanisms for proliferation and can compromise a treatment just targeting one of the expressed pathways [48].

Treatment-induced mutations also form an obstacle for targeted therapy, that acts on a specific molecule or group of molecules. Secondary mutations in the drug target can prevent the inhibition by disturbing the binding to the target [22,58]. Moreover, the cancer cells can avoid the targeted pathway by activating a parallel mechanism that can compensate for the targeted pathway; for instance, by altering signaling up-stream or down-stream to achieve resistance [56]. Furthermore, monotherapy with molecularly targeted agents has been evaluated in a multicenter, open-label, proof-of-concept, randomized, controlled phase 2 trial and it was shown that there was no significant difference in progression-free survival compared to the control group, which was treated with the physician's choice. Common alterations targeted in this study were mutations of the PI3K/AKT/mTOR pathway, where everolimus was used, PDGFRA mutation, where sorafenib was used or EGFR mutations, where erlotinib was given. Although molecularly targeted therapy needs time to produce an anti-tumor effect and the study just included heavily pretreated patients, who could deteriorate before being sufficiently exposed to the drug, the results still suggest that mono-targeted therapy seems insufficient [72].

A potential approach to tackle intratumoral heterogeneity would be to target multiple pathways simultaneously with drug combination therapies, which optimally would act synergistically and have a low side effect profile [28].

One approach for multi-targeted treatment is to find the genetic alteration conferring the resistance to an otherwise suitable anti-cancer agent and

consequently target this pathway in addition. For instance, HER/EGFR1 is overexpressed in over 50% of glioblastomas, which leads to increased tumorigenicity and tumor growth. Given that, it was suggested to use a HER1/EGFR-targeted agent such as Erlotinib, that inhibits PI3K/AKT (Protein kinase B) and MAPK (mitogen-activated protein kinase) pathways. Unfortunately, solitary use of the tyrosine kinase inihibitor Erlotinib was not successful in a clinical setting due to candidate resistance genes, such as RAC1 (Ras-related C3 botulinum toxin substrate 1), that is overexpressed in erlotinib-resistant glioblastoma cell lines and has a decreased expression in erlotinib-sensitive cell lines. RAC1 is a member of the rho family of GTPases regulating cellular functions such as migration survival and malignant transformation. In order to overcome this treatment-resistance, NSC23766, a small-molecule inhibitor specifically binding to RAC1, was added to Erlotinib and showed a synergistic antiproliferative effect [31]. Another example of multi-targeted therapy in Glioblastoma is the use of ABT263, together with small-molecule inhibitor GX15-070. ABT263 is an agent targeting the anti-apoptotic Bcl-2 (B-cell lymphoma-2) family proteins Bcl-2, Bcl-xL and Bcl-w. Avoiding apoptosis, the Glioblastoma cells up-regulate Mcl-1 (myeloid cell leukemia 1), another anti-apoptotic protein of the Bcl-2 family. Therefore, to negate this escape mechanism, the Mcl-1 inhibitor GX15-070 is introduced. The addition of GX15-070 showed a synergistic antiproliferative effect, an enhanced pro-apoptotic and antineoplastic effect of ABT263 in multiple cell-lines and *in vivo* [30].

In like manner, ONC201/TIC10 (TRAIL-inducing compound 10) can be used synergistically with the previously mentioned ABT263 to suppress the upregulation of Mcl-1 and yields increased anti-cancer activity compared to mono-therapy [28]. Consequently, it is of utmost importance to address the heterogeneity and dynamics of not only Glioblastoma, but all the heterogenic malignancies to improve therapeutic strategies and potentially discover a cure.

1.3 Cancer cell metabolism as a target in glioblastoma

Cancer cells, like all other cells, need to import nutrients, such as glucose and glutamine, to match the needs for survival and proliferation. Those nutrients are then either used anabolic as building blocks or as energy sources. Otto Warburg first described the phenomenon of tumors fermenting higher levels of glucose to lactate in the presence of oxygen, whereas normal cells preferentially use mitochondria to oxidize glucose and to produce energy, namely ATP (Adenosine triphosphate) [75]. This aerobic glycolysis was therefore termed the Warburg effect. Although Warburg speculated that the increased rate of glycolysis is due to dysfunctional mitochondria, unable to perform the oxidative phosphorylation, it is now proven that mitochondria are functional and therefore the metabolism is presumably metabolically reprogrammed and dynamic [49,50]. In reality, a large part of cancer cells, mainly the quiescent subpopulations, still utilizes mitochondrial oxidative phosphorylation as its source of ATP. Nonetheless, in proliferating cells the aerobic ATP production comes secondary to the synthesis of anabolic precursors through glycolysis [76].

In addition to anabolic precursor and energy production, proliferating cells are in a great need of reducing equivalents, specifically NADPH (reduced nicotinamide adenine dinucleotide phosphate), which are increasingly synthesized in the oxidative branch of the pentose phosphate pathway, a pathway parallel to glycolysis. Through an increased rate of aerobic glycolysis, cancer cells therefore also generate more NADPH from NADP+ (oxidized nicotinamide adenine dinucleotide phosphate) that eventually can be used for fatty acid synthesis. Additionally, the reduction of pyruvate to lactate through lactate dehydrogenase regenerates NAD+ (oxidized nicotinamide adenine dinucleotide) from NADH (reduced nicotinamide adenine dinucleotide) which is needed to sustain the high rate of glycolysis as well as the CAC (citric acid cycle) [37].

Furthermore, the Warburg effect has an important impact on the tumoral microenvironment, due to the elevated glucose metabolism resulting in increased acidity. As a result, there will be an inevitable acid diffusion into surrounding

stroma causing an acid-base imbalance that favors not only tumor growth but also invasion of tumor cells into the surrounding brain tissue [73]. It was shown that a decreased peritumoral pH is associated with degradation of extracellular matrix as well as apoptosis and necrosis that only affects healthy tissues, because of an acquired resistance of tumor cells to acidity [15]. Additionally, a high rate of glycolysis decreases the availability of glucose for TILs (tumor-infiltrating lymphocytes) which depend on a sufficient supply for their anti-tumoral activity [37].

PET (positron emission tomography) imaging can make use of the Warburg effect for cancer diagnosis, staging and observing treatment response by giving the patient a radioisotope-labelled glucose tracer, specifically ^{18}F-fluorodeoxyglucose (^{18}F-FDG). ^{18}F-FDG is then transported into the cell by GLUTs (glucose transporters) which are increased in many tumors presenting aerobic glycolysis, particularly GLUT1 and GLUT3 and phosphorylated by hexokinase (HK) to ^{18}F-FDG-6-phosphate (^{18}F-FDG-6-P), that becomes trapped and labels the tumor [50]. Similarly, ^{18}F-labeled glutamine is used in PET scans, to reveal tumors with an increased glutamine uptake. This is useful in regions, that are characterized by an already high glucose utilization, such as the brain, where the use of ^{18}F-FDG would be not suitable. It raises the question to how the cancer cells can utilize such an increased amount of glucose and glutamine, since nutrient uptake is normally regulated by growth factors and extracellular stimuli [49].

The activation of the PI3K/Akt pathway downstream of RTK increases GLUT1 expression on the cell surface and its glucose uptake. Afterwards, the Akt-induced activation of phosphofructokinase-1 facilitates the commitment of glucose to the glycolytic metabolism. Pyruvate dehydrogenase (PDH) then transforms pyruvate into mitochondrial Acetyl-CoA which needs to be condensed to Citrate. Next, the mitochondrial Citrate can be moved into the cytosol where it is converted back into Acetyl-CoA by the Akt-activated ATP-citrate lyase (ACL). The cytoplasmic Acetyl-CoA acts then as a component for lipid synthesis. The increased lipid production in cancer allows the cell to change the membrane composition in favor of saturated fatty acids, that are more resistant to oxidative stress. Downstream of Akt, the

protein complex mTORC1 is also activated, which transcriptionally enhances protein synthesis and mitochondrial biogenesis. The transcription factor c-Myc which is often overexpressed in cancer, increases cellular glutamine uptake and its mitochondrial conversion into Glutamate by enhancing the expression of Glutaminase (GLS). Therefore, c-Myc enhances cellular proliferation by supplying nitrogen and carbon sources but also by promoting mitochondrial biogenesis and nucleotide/amino acid synthesis through transcriptional regulation. High glutamine levels are crucial for cancer cell progression, as a deprivation can lead to cell-cycle arrest in the S phase [49,76].

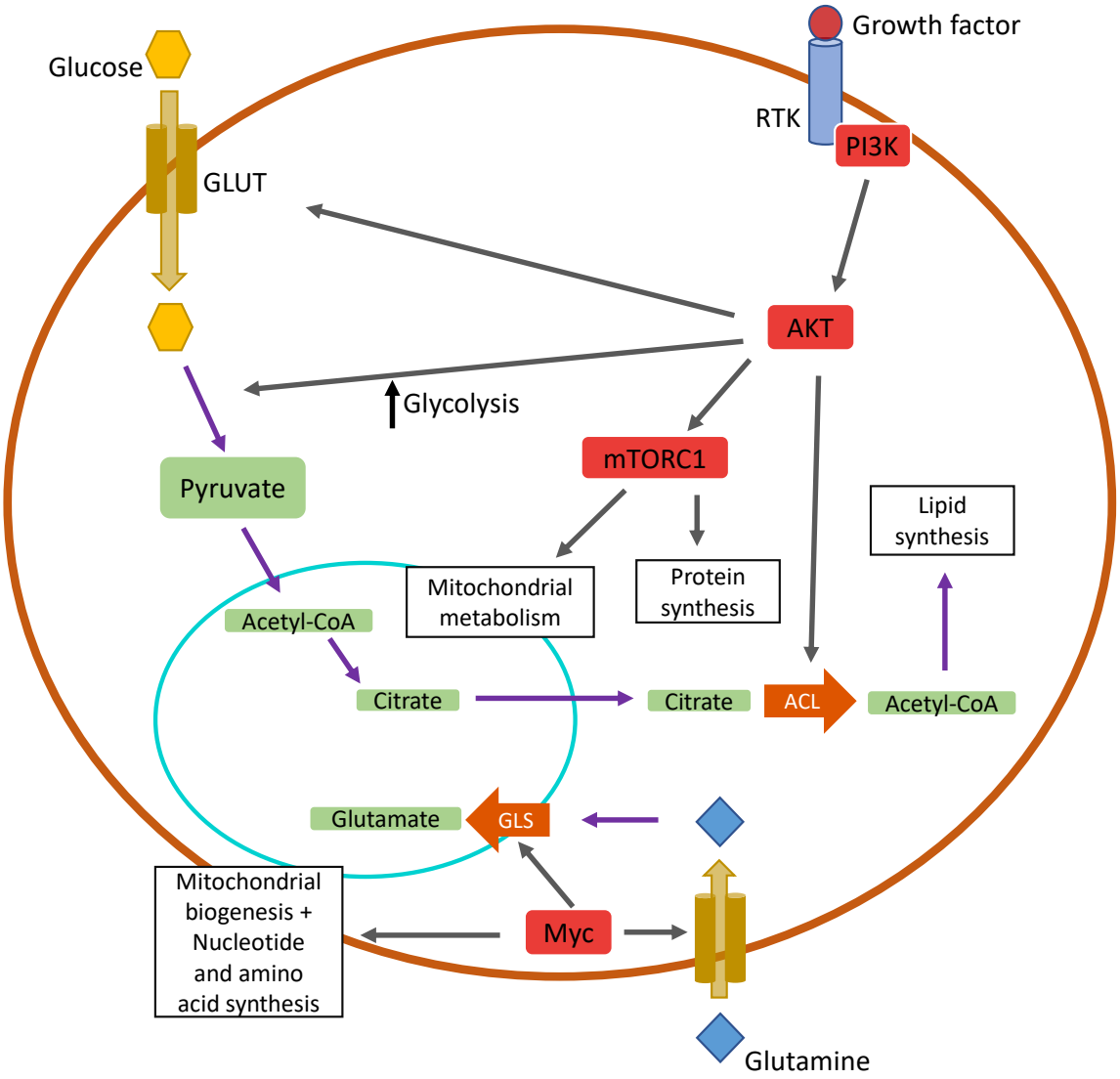

Figure 2: Overview of oncogenic reprogramming of cancer cell metabolism

PI3K/Akt signaling enhances glucose uptake through GLUT and increases rate of glycolysis. Akt also activates ATP-citrate lyase (ACL) to convert citrate into cytoplasmic Acetyl-CoA for lipid synthesis. mTORC1 enhances mitochondrial metabolism and protein synthesis. Myc increases mitochondrial biogenesis and nucleotide/amino acid synthesis [76].

In addition to enhancing certain pathways and increasing the expression of transcription factors, proliferating cancer cells have been shown to selectively overexpress particular isoforms of metabolic enzymes. For instance, PKM2 (pyruvate kinase M2), a glycolytic enzyme that converts phosphoenolpyruvate (PEP) to pyruvate and additionally generates ATP that is preferentially expressed in embryonic tissues and proliferating cancer cells. On the contrary, the PKM1

isoform is normally predominant in most differentiated tissues and paradoxically also has a higher enzymatic activity and a lower sensitivity to inhibition by tyrosine kinase. In vivo, it was shown that PKM2-expressing cells have a significant growth advantage compared to PKM1-expressing cells using a xenograft model [11]. It was demonstrated that a reduced cytoplasmic PKM2 activity leads to an enhanced anabolic metabolism through increased glycolytic intermediates. For example, the accumulation of 3-phosphoglycerate intermediate is used for the serine synthetic pathway of glycolysis. The enzyme serine dehydratase can then convert it into pyruvate, further explaining how the less active PKM2 isomer can result in a higher outcome of pyruvate. Therefore, through both forms of PKM2, the inactivated and the activated one, it can benefit the cancer cell metabolism depending on the extracellular nutrient availability by either enhancing the branching anabolic glycolytic pathways or direct production of pyruvate [76].

Furthermore, mutations of IDH1/2, specifically missense mutations of R132 in IDH-1 or R172 in IDH-2, which reduce the CAC metabolite isocitrate to D-2-hydroxyglutarate (2-HG) rather than α-ketoglutarate, the product of cells expressing the IDH-wild-type form, have a striking effect on tumor survival. The oncometabolite 2-HG was found to suppress both innate and adaptive immunity. Specifically, it inhibited complement activation in a dose-dependent manner, reduced MAC (membrane attack complex)-mediated cellular injury and reduced complement-mediated opsonization and phagocytosis. Additionally, IDH mutations were found to be associated with a decreased number of TILs [81]. Another important key point to remember is, that cancer cells do not only reprogram their metabolism to survive under difficult circumstances. Cancer cells can select which pathway is best for their survival depending on their surroundings. For instance, it has been shown that with high levels of glucose in the culture media the oxidative phosphorylation is down-regulated, according to the Warburg effect. In contrast, under lower-level glucose concentrations, tumor-cells switch towards higher rates of oxidative phosphorylation, therefore neglecting the glycolytic pathway. This was demonstrated in vitro with multiple cancer cell lines using extracellular flux analysis to determine oxygen consumption rates (OCR) as an

indicator for oxidative phosphorylation and extracellular acidification rates (ECAR) as an indicator for the glycolytic rate. When providing cells with high glucose concentrations (25 mM), either aerobic glycolysis was used, meaning low OCR and high ECAR-rates, oxidative phosphorylation, showing high OCR with low ECAR-rates, or something in between. In contrast, when provided a low concentration of glucose (1 mM), all tested cell lines exhibited a high-moderate OCR with very low ECAR, proving that the metabolism of the evaluated cell lines can switch between these two energy-producing pathways depending on the provided environment. As a clinical consequence, it would not be enough to deprive the tumor of just its glucose or its oxygen source, when targeting the cancer cell metabolism [50].

Considering that the cancer cell metabolism is crucial for the growth and survival response, it is suggestive to attempt targeting it in cancer therapy. However, there are certain issues to consider when choosing a therapeutic target. For instance, when one inhibits an enzyme or a signaling pathway in tumor tissue, it may also have adverse effects on the physiological functions of normal tissues in the body. One approach to avoid this problem, is to target a specific pathway that is dysregulated in the malignancy. However, a major obstacle is represented by the fact that targeting only one pathway will in most cases not suffice because the cancer cells will respond by adapting their metabolism to develop resistance by using compensatory pathways. Accordingly, targeting multiple different metabolic pathways simultaneously or combining an anti-metabolic treatment with another anti-cancer therapy seems more promising.

An appealing strategy is to target glycolysis, due to the increased glycolytic rate seen in cancer cells when compared to normal tissue and its essential role in proliferation and tumor development [12].

However, due to the possible compensatory up-regulation of mitochondrial oxidative phosphorylation, creating a profound state of energy deprivation, appears to be more efficient but also potentially more toxic.

In pre-clinical studies, promising results regarding the inhibition of growth, migration and invasion of ovarian cancer cells were shown when treated with the combination of metformin and 2-DG. The anti-hyperglycemic agent metformin,

used mainly as first-line medication for type II diabetes, inhibits the complex I of the electron transport chain and ATP synthase, thereby directly limiting mitochondrial respiration. Additionally, 2-DG acts as a glucose analog and competitively inhibits glycolysis. The combination of both substances led to a major ATP depletion in both tested cell lines of about 90%, thus initiating intense metabolic stress. Moreover, it was demonstrated that ATP-levels also decreased by either treatment alone, indicating that both oxidative phosphorylation and glycolysis are needed for the tumor to sustain energy supply. Consequently, the results suggested that targeting two metabolic pathways of ovarian cancer simultaneously deemed to be auspicious [83].

2-DG has also been reported to be effective in hepatocellular carcinoma (HCC). When 2-DG was combined with the standard treatment sorafenib, which is a protein kinase inhibitor with activity against multiple protein kinases, including VEGFR, PDGFR and RAF kinases, a synergistic anti-proliferative in both sorafenib-sensitive and sorafenib-resistant HCC cell lines was observed. Furthermore, the glycolysis inhibitor 3-bromopyruvate which acts on hexokinase 2 has shown promising anti-neoplastic effects in vitro and in vivo and thus, has been approved by the FDA for HCC therapy [36].

In another preclinical study, it has been tested whether a dual inhibition of glycolysis and OXPHOS would inhibit the growth of lung cancer cell lines carrying an EGFR mutation. For the suppression of glycolysis, the EGFR inhibitor osimertinib and for targeting OXPHOS the biguanide drug phenformin were used. The combination therapy with osimertinib and phenformin led to enhanced apoptotic and metabolic stress which significantly reduced the development of drug resistance to osimertinib [40].

Targeting the metabolism of glioblastoma as an addition to chemotherapy was already investigated in 1985 by Dranoff and colleagues in *in vitro* experiments. They used acivicin, a glutamine analog and inhibitor of gamma-glutamyl transferase to target the glutamine metabolism synergistically with the use of L-asparaginase or 5-fluorouracil as cytostatic chemotherapeutic agents [14]. Furthermore, the use of nicotinamide phos- phoribosyl-transferase (NAMPT) inhibitors, which deplete the

NAD+ required for the glyceraldehyde 3-phosphate dehydrogenase (GAPDH) step of glycolysis, has been shown to be a potential strategy to counter the increased glycolytic drive in myc amplified glioblastoma cells. Myc is an oncoprotein often overexpressed in glioblastoma, that contributes to malignancy by driving cellular proliferation, blocking differentiation and increasing cell migration [71]. In like manner, Ishida and colleagues have shown that increased levels of c-myc, a member of the proto-oncogene family of myc, predict enhanced susceptibility to metabolic reprogramming through dual AKT/ERK inhibition by the use of imipridones, to enhance anti-tumor activity [25].

Overall, targeting tumor metabolism, especially the dual blockade of glycolysis and OXPHOS blocks the cellular energy supply and decreases cancer cell proliferation, tumor growth and can even delay therapy resistance, making it an encouraging treatment strategy to battle cancer.

1.4 Imipridones as potential anti-glioblastoma therapeutics

ONC201/TIC10 is the founding compound of a class of drugs termed imipridones. It was rediscovered as a potential anti-cancer agent in a luciferase reporter screen for small molecule inducers of TNF-related apoptosis-inducing ligand (TRAIL) gene transcription after initially being patented for the treatment of central nervous system disorders in 1973 [1]. TRAIL gene regulation has been described for various transcription factors, predominantly being tumor suppressors such as Forkhead box O 3a (Foxo3a) and p53, but due to the common inactivation of p53 in late stage cancers, the screen was conducted for compounds with a mechanism of action independent of p53 activation status [3]. TRAIL is an endogenous protein, inducing tumor-specific apoptosis through binding to death receptors 4 or 5 at the surface of tumor cells and subsequently engaging the extrinsic apoptotic pathway [2,16]. As a consequence, to test the cancer therapeutic properties of TRAIL, initially, a soluble form of TRAIL was created. This recombinant TRAIL protein was shown to

have anti-cancer properties in vitro and in vivo and further led to the implementation of clinical trials [74]. While the use recombinant TRAIL seemed in the beginning promising, several undesirable drug properties, such as poor biodistribution, instability and short serum half-life were described [13]. Therefore it was hypothesized that an up-regulation of the TRAIL gene expression by a small molecule could enhance pharmacokinetic properties by increasing endogenous TRAIL production, which is a more stable product with an improved biodistribution and half-life [2]. The previously mentioned transcription factor Foxo3a plays an important role in tumor suppression through induction of cell cycle arrest and repairing damaged DNA. In tumor cells, Foxo3a expression is often down-regulated due to an increased activity of the PI3K/Akt pathway. Akt hereby directly phosphorylates the Foxo3a transcription factor, leading to its relocalization from the nucleus into the cytoplasm and consequently inhibiting its transcription [19]. Moreover, it has been described that the RAS/ERK pathway, which has been shown to promote cell growth and tumorigenesis, reduces Foxo3a transcription in a similar way through its phosphorylation by extracellular signal-regulated kinase (ERK), therefore decreasing its stability and increasing the affinity to be degraded by mouse double minute 2 homolog (MDM2), a ligase that has an important role in cancer development through degradation of tumor suppressor proteins [80]. Thus, targeting those two pathways, commonly up-regulated in cancer, could increase TRAIL gene expression and consequently have an anti-tumor effect.

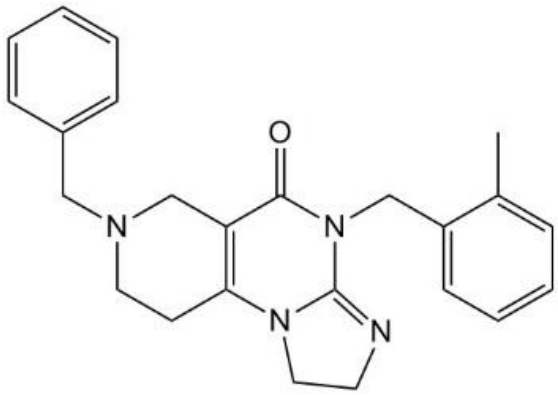

Figure 3: Chemical structure of the angular/active form of ONC201/TIC10

(Made with ChemDraw Professional 16.0, Perkin Elmer)

The previously mentioned screen was conducted in TRAIL-resistant Bax-null HCT116 human colon cancer cells and identified the compound ONC201/TIC10 to be a TRAIL-inducing compound. ONC201/TIC10 was shown to enhance TRAIL mRNA expression in a dose-dependent manner and to promote TRAIL protein expression on the cell surface of various different cancer cell lines independently of p53 expression [2]. This effect of ONC201/TIC10 was shown to be Foxo3a-dependent through a combined inhibition of the pro-survival kinases Akt and ERK indicated by a dose-dependent down-regulation of pAkt, pMEK and its downstream target pERK on the protein-level [2].

In addition, ONC201/TIC10 was shown to exert its anti-tumor effects through an early integrated stress response (ISR), which was shown to be associated with phosphorylation of eukaryotic initiation factor 2α (eIF2α), up-regulation of ATF-4 and subsequent enhanced expression of the pro-apoptotic protein CHOP and its target gene DR5 [1].

Notably, while the large recombinant TRAIL molecule was shown not to be able to cross the blood-brain barrier, the small molecule ONC201/TIC10 displayed blood-brain barrier penetration. This led to the investigation, whether ONC201/TIC10 could be a potential compound for glioblastoma therapy. Further analyses showed that ONC201/TIC10 had significant cytotoxic effect on multiple glioblastoma cell lines and also orthotopic xenograft models [2]. In addition, Allen and colleagues have described ONC201/TIC10 to be highly effective against temozolomide-resistant glioblastoma cell lines in vitro, as well as in murine subcutaneous xenografts [1]. Moreover, ONC201/TIC10 presents favorable drug characteristics to be used in combination therapies. The compound has a half-life of about 6-11 hours and its pharmacodynamic effect, that commences hours after the single-dose administration, persists significantly longer than its pharmacokinetic activity. This allows ONC201/TIC10 to be administered prior to another anti-cancer agent, that acts in a synergistic manner with the compound, using a schedule to minimize drug-drug interactions while preserving its combinatorial strengths [1]. In this turn, Karpel-Massler and colleagues have presented data showing synergistic pro-apoptotic activity of ONC201/TIC10 and the BH3-mimetic ABT263. In this study,

ONC201/TIC10 was observed to significantly down-regulate Mcl-1 expression and its interacting proteins, which have been described as key resistance factors to BH3-mimetics. Therefore, the data suggest that ONC201/TIC10 sensitizes glioblastoma cells to ABT263 through down-regulation of Mcl-1 [28].

Ishida and colleagues have presented data suggesting that the efficacy of ONC201/TIC10 to induce apoptosis and to inhibit the proliferation in glioblastoma cells and patient derived xenograft (PDX) model systems to be c-myc dependent. High levels of the c-myc protein were associated with an increased rate of apoptosis and inhibition of proliferation. In addition, their findings suggest enhanced c-myc degradation, likely through regulation of the proteasomal pathway, after treatment with the compound [25]. Importantly, Ishida and colleagues also discovered an alteration of the cancer cell metabolism following the treatment with ONC201/TIC10, namely the suppression of glycolysis and oxidative phosphorylation. On the other hand, through the suppression of these two essential energetic pathways, the tested glioblastoma cell lines were up-regulating the serine-one carbon-glycine pathway in a compensatory manner [25].

Another mechanism of action that has been described for ONC201/TIC10, is the selective inhibition of the G-protein-coupled receptor dopamine receptor D2 and 3 (DRD2 and 3). DRD2 and 3 are often overexpressed in gliomas, contributing to the ISR activation and anti-cancer activity [34].

The promising results obtained with ONC201/TIC10 from pre-clinical studies led to several clinical trials. Chi and colleagues have tested ONC201/TIC10 in patients with recurrent H3 K27M-mutant diffuse mid-line glioma, which is a distinct grade IV glioma with an elevated DRD2 expression and unmethylated MGMT promoter and therefore more likely to be resistant to temozolomide. Their data suggested a clinical benefit in pediatric and adult patients with no dose-limiting toxicities or treatment discontinuation due to side effects [10]. Arrillaga-Romany and colleagues have also presented data suggesting achievable therapeutic concentrations in the brain and anti-tumor activity in a phase 2 study of 17 patients with recurrent glioblastoma previously treated with temozolomide and radiotherapy. Furthermore, they have shown that the treatment with

ONC201/TIC10 was well-tolerated by all except of one patient whose adverse event was manageable [4].

In the light of these results, the repurposed drug ONC201/TIC10, that acts simultaneously on multiple vital pathways of cancer cells in a still not fully understood way, holds enough potential to be further investigated. In addition, ONC201/TIC10 has been shown to act favorably in combination with other agents making it a potentially suitable compound to evade the adaptive mechanisms of cancer through further inhibition of additional pathways.

1.5 2-deoxyglucose

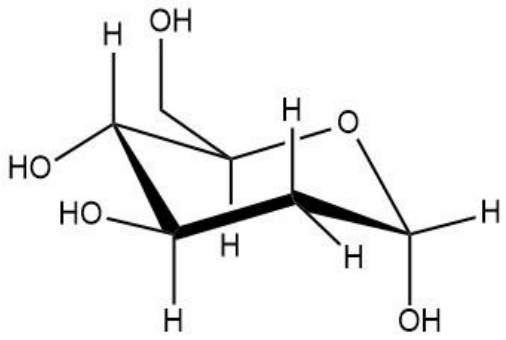

Figure 4: Chemical structure of 2-deoxyglucose

(Made with ChemDraw Professional 16.0, Perkin Elmer)

2-deoxyglucose represents a glucose analogue which is chemically characterized by replacement of the hydroxyl group at the second carbon group with a hydrogen atom. It competes with glucose for uptake and is a competitive inhibitor of HK. 2-DG is phosphorylated by HK, the enzyme facilitating the first step of glycolysis the conversion to 2-deoxyglucose-6-phosphate (2-DG-6-P), a metabolite that is not utilized by the downstream glycolytic enzyme phosphoglucose isomerase. 2-DG-P accumulates in the cytoplasm and therefore causes a product inhibition of HK [27,63,78]. In addition to its effects on the tumor glycolytic metabolism, 2-DG has been described to induce a suppression of ERK phosphorylation in a subset of Non-

Small Cell Lung Cancer Cells and to sensitize cancer-cells to death receptor-mediated apoptosis, pathways that are also targeted by ONC201/TIC10 at different levels [45,68]. Importantly, 2-DG is able to penetrate the blood-brain barrier, sharing the same cerebral transport systems as glucose and has already been tested in clinical settings in multiple studies [6,47]. For instance, 2-DG was already tested in phase I clinical trials, where it was either given alone or in combination for the treatment of advanced solid tumors and was described to have a good tolerability with most side effects being attributed to hypoglycemia [54,66]. Most interestingly, clinical studies have shown that the use of 2-DG in combination with radiotherapy is feasible and safe in the treatment of glioblastoma [42]. 2-DG hereby not only sensitizes the tumor to radiation but at the same time also protects the healthy tissue against radiotoxicity [60]. It was shown that 2-DG inhibits the repair of radiation-induced DNA double-strand breaks in yeast and in healthy tissue such as spleen, thymus and bone marrow of mice that received whole-body irradiation, a protective effect of 2-DG was observed [17,61,69]. The molecular mechanism of 2-DG's differential effects on healthy and tumor tissue is yet to be fully understood. However, the favorable safety profile and its ability to increase the radiosensitivity of tumors makes 2-DG an interesting compound to be used in glioblastoma therapy [60].

2-DG has already been investigated as part of combination therapies against different cancers in vitro. Zhang and colleagues have demonstrated that the treatment of acute myeloid leukemia and multiple myeloma cells with 2-DG leads to a decreased expression of the anti-apoptotic protein Mcl-1 and weakens its interaction with Bak. As a consequence, these cells were sensitized to the treatment with ABT-263/737 and subsequently apoptosis was induced [82]. Kim and colleagues have also conducted a study combining metformin with 2-DG, showing that the combination therapy led to a decreased invasive capacity and a potential survival benefit in a murine orthotopic glioblastoma xenograft model [33]. Consequently, 2-DG has strong potential to be investigated in combinatorial treatment strategies targeting the cellular metabolism of glioblastomas.

1.6 Aim of the study

In this study we investigated the effect of the therapy with ONC201/TIC10 combined with 2-DG on established and primary cultured glioblastoma cells. We examined whether a metabolic reprogramming through targeting the oxidative phosphorylation with ONC201/TIC10 and glycolysis with 2-DG would affect the cellular viability of glioblastoma cells and how it affects the energetic state of the cells. Furthermore, we examined the effects our treatment on the migratory capacity of glioblastoma cells, their ability to form colonies, characteristics of drug-drug interaction and activation of protein kinase signaling pathways. Finally, we examined possible side effects on healthy tissues in multiple organs of chicken embryos and on normal cells such as primary astrocyte-enriched brain cells, human fibroblasts and human mesenchymal stem cells.

2. Materials and Methods

2.1 Materials

2.1.1 Cell lines

Cell line	
A172	ATCC 02/2011, Manassas, VA, USA
U251	Sigma Aldrich 01/2017, St. Louis, MO, USA
ULM-GBM-PC38	Primary tumor material, Department of Neurosurgery, Ulm University Medical Center
ULM-GBM-PC40	
ULM-GBM-PC128	
Human fibroblasts	kindly provided by Dr. Markus Hönicka, Department of Cardiac Surgery, Ulm University Medical Center
Human mesenchymal stem cells	
Primary astrocyte-enriched brain cells	kindly provided by Dr. Matthias Schneider, Department of Neurosurgery, University of Bonn Medical Center

The identities of the glioblastoma cell lines, that were purchased, were confirmed by the respective source of purchase. The initial stocks were expanded, frozen and stored in liquid nitrogen. Fresh aliquots were thawed every 6 weeks.

2.1.2 Cell culture media, supplements and reagents

Cell culture medium:	
1 x DMEM with 4.5 g/L D-Glucose, L-Glutamine, Pyruvate	Life Technologies, Paisley, UK
10% Fetal Bovine Serum (FBS) 20% FBS for ULM-GBM-PC128	Life Technologies, Grand Island, USA

1,5% FBS for Treatment	
1% Penicillin-Streptomycin (10,000 U/mL)	Life Technologies, Grand Island, USA

Cell culture reagents:	
1x Dulbecco's Phosphate Buffered Saline (DPBS)	Life Technologies, Paisley, UK
Trypan Blue	Sigma-Aldrich, Steinheim, Germany
Trypsin/ Ethylenediaminetetraacetic acid (Trypsin/ EDTA)	Biochrom AG, Berlin, Germany

2.1.3 Treatment reagents

Reagent	
ONC201/TIC10	Kindly provided by Oncoceutics Inc., Philadelphia, PA, USA
2-DG	Sigma Aldrich, St. Louis, MO, USA

A 10mM stock solution was prepared for ONC201/TIC10 with DMSO. For 2-DG the 500mM stock solution was prepared with sterile water. All stock solutions were stored at -20°C. For all experiments, final concentrations of DMSO were below 0.1% (v/v).

2.1.4 Cell viability assays

Product:	
3-(4,5-Dimethythiazol-2-yl)-2,5-diphenyl tetrazolium bromide (MTT) powder	Sigma-Aldrich, Steinheim, Germany

RPMI Medium 1640 (1X) without L-Glutamine, Phenol Red	Life Technologies, Paisley, UK
Isopropyl alcohol	VWR, Leuven, Belgium

MTT solution (5x):	
10 mg/ml MTT powder in DPBS	Sigma-Aldrich, Steinheim, Germany

MTT working solution (1x):
20% MTT solution (5x)
80% RPMI Medium 1640 (1x) without L-Glutamine, Phenol Red

Appliances:	
Microplate Reader EL800	BioTek, Highland Park, USA

2.1.5 Soft agar assay

Product:	
0.9% low-melting agarose (base layer)	Biozym Scientific GmbH
0.35% agarose (top layer)	Biozym Scientific GmbH

Both the base- and top layer were containing 10% FBS, antibiotics and respective treatment reagents or corresponding solvents

2.1.6 CellTiter-Glo® assay

Reagent:	
CellTiter-Glo® Reagent	Promega, Madison, WI, USA

2.1.7 Staining for carboxyfluorescin diacetate succinimidyl ester (CFSE)

Product:	
CellTrace™ CFSE cell proliferation kit	Molecular Probes, Inc., Eugene, OR, USA

2.1.8 Measurement of cell death and cell cycle analysis

Propidium iodide (PI) staining buffer:	
0.05% trisodiumcitrate-dihydrate	Carl Roth, Karlsruhe, Germany
0.05% triton-X 100	Sigma Aldrich, St. Louis, MO, USA
0.05mg/ml PI	Sigma Aldrich, St. Louis, MO, USA

Consumables and Appliances:	
Fluorescence-activated cell sorting (FACS) tubes, 5ml, 75x12mm, PS	Sarstedt, Nümbrecht, Germany
FACSCalibur	Becton Dickinson, Heidelberg, Germany
FACS Clean	BD Biosciences, San José, USA
FACS Flow	BD Biosciences, San José, USA
FACS Rinse	BD Biosciences, San José, USA

2.1.9 Real-time PCR and cDNA synthesis

RNA Isolation, Reverse transcription and PCR amplification:	
Maxwell 16 LEV simplyRNA Cells Kit	Promega, Madison, WI, USA
Maxwell 16 LEV simply RNA Tissue Kit	Promega, Madison, WI, USA
Maxwell 16 IVD Instrument	Promega, Madison, WI, USA
cDNA Synthese Kit	Biozym Scientific GmbH
C1000 Touch Thermal Cycler	Bio-Rad, Munich, Germany

LightCycler	Thermo Fisher Scientific, Waltham, Massachusetts, USA
MicroAmp™ Fast Optical 96-Well Reaction Plate, 0.1ml	Thermo Fisher Scientific, Waltham, Massachusetts, USA
SYBR Green (SG)	Bio-Rad, Munich, Germany
Standard Primers	Eurofins Genomics Germany GmbH, Ebersberg, Germany

PCR-Primers:		
Gene	Forward sequence	Reverse sequence
PHGDH	CTT ACC AGT GCC TTC TCT CCA C	GCT TAG GCA GTT CCC AGC ATT C
PSAT1	ACT TCC TGT CCA AGC CAG TGG A	CTG CAC CTT GTA TTC CAG GAC C
PSPH	GAC AGC ACG GTC ATC AGA GAA G	CGC TCT GTG AGA GCA GCT TTG A
18S	AGT CCC TGC CCT TTG TAC ACA	GAT CCG AGG GCC TCA CTA AAC

2.1.10 Western blot analysis

Cell lysis buffer:	
30mM Tris-Hydrochloride (pH 7.4)	Roth, Karlsruhe, Germany
150mM NaCl	Sigma-Aldrich, Steinheim, Germany
1%Triton X-100	Sigma-Aldrich, Steinheim, Germany
10% Glycerol	Roth, Karlsruhe, Germany
1 tablet cOmplete™ Protease Inhibitor Cocktail per 50ml lysis buffer	Roche, Mannheim, Germany

10% Sodium dodecyl sulfate (SDS):

20g SDS	Serva, Heidelberg, Germany
200ml deionized water	Department of Neurosurgery, Ulm University Medical Center, Germany

10% Ammonium persulfate (APS):	
5g APS	Bio-Rad, Munich, Germany
50ml deionized water	Department of Neurosurgery, Ulm University Medical Center, Germany

1.5M Tris (pH 8.8):	
90.86g Tris Base (Trizma® Base)	Sigma Aldrich, St. Louis, MO, USA
Deionized water added up to a total volume of 500ml	Department of Neurosurgery, Ulm University Medical Center, Germany
pH adjustment by adding of HCl	Merck, Darmstadt, Germany

1M Tris (pH 6.8):	
78.80g Tris HCl	Roth, Karlsruhe, Germany
Deionized water added up to a total volume of 500ml	Department of Neurosurgery, Ulm University Medical Center, Germany
pH adjustment by adding NaOH	Merck, Darmstadt, Germany

12% resolving gel (30ml):	
12ml 30% Polyacrylamide Rotiphorese	Roth, Karlsruhe, Germany
9.9ml deionized water	Department of Neurosurgery, Ulm University Medical Center, Germany
7.5ml 1.5M Tris pH 8.8	
300µl 10% SDS	
300µl 10% APS	
12µl N,N,N'-Tetramethyl ethylene diamine (TEMED)	Serva, Heidelberg, Germany

5% stacking gel (10ml):	
1.7ml 30% Polyacrylamide Rotiphorese	Roth, Karlsruhe, Germany
6.8ml deionized water	Department of Neurosurgery, Ulm University Medical Center, Germany
1.25ml 1.0M Tris pH 6.8	
100µl 10% SDS	
100µl 10% APS	
10µl TEMED	Serva, Heidelberg, Germany

Upper Gel Buffer (pH 6.8):	
0.5M Tris Base (Trizma® Base)	Sigma Aldrich, St. Louis, MO, USA
0.4% SDS	Serva, Heidelberg, Germany
deionized water	Department of Neurosurgery, Ulm University Medical Center, Germany
pH adjustment by adding HCl	Merck, Darmstadt, Germany

SDS Loading buffer (6x):	
7ml Upper Gel Buffer	
3.8ml Glycerol	Roth, Karlsruhe, Germany
1g SDS	Serva, Heidelberg, Germany
930µl DL-Dithiothreitol (DDT)	Sigma-Aldrich, Steinheim, Germany
1.2mg Bromphenol-Blue	Merck, Darmstadt, Germany

Running buffer:	
125mM Tris Base (Trizma® Base)	Sigma Aldrich, St. Louis, MO, USA
950mM Glycine	Roth, Karlsruhe, Germany
0.5% SDS	Serva, Heidelberg, Germany

Running buffer was diluted 1:5 in deionized water before use	Department of Neurosurgery, Ulm University Medical Center, Germany

Blotting buffer:	
25mM Tris Base (Trizma® Base)	Sigma Aldrich, St. Louis, MO, USA
190mM Glycine	Roth, Karlsruhe, Germany
0.1% SDS	Serva, Heidelberg, Germany
20% Methanol	Sigma-Aldrich, Steinheim, Germany

Phosphate Buffered Saline (PBS) (10x) (pH 7.4)	
400g NaCl	Sigma-Aldrich, Steinheim, Germany
72g Na_2HPO_4 x $2H_2O$	VWR, Leuven, Belgium
10g KCl	Merck, Darmstadt, Germany
10g KH_2PO_4	Sigma-Aldrich, Steinheim, Germany
Fill up to 5l with deionized water	Department of Neurosurgery, Ulm University Medical Center, Germany
pH adjustment by adding NaOH	Merck, Darmstadt, Germany
PBS was diluted 1:10 in deionized water before use	Department of Neurosurgery, Ulm University Medical Center, Germany

Wash buffer – PBS-Tween 20 (PBS-T) (1x):	
1l PBS 1x	
1ml Tween 20	Merck, Darmstadt, Germany

Blocking solution:	
5% milk powder	Roth, Karlsruhe, Germany
Diluted in PBS-T	

Primary Antibody solution:	
0.02% NAN_3	Sigma-Aldrich, Steinheim, Germany

5% Bovine Serum Albumin (BSA) Fraction V	PAA Laboratories, Coelbe, Germany
Diluted in PBS-T	

Protein marker:	
Page Ruler™ Prestained Protein Ladder	Thermo Scientific, Rockford, USA

Primary Antibodies	MW (kDa)	Dilution	
Total OXPHOS human WB antibody cocktail	18; 22; 29; 48; 54	1:1000	#ab110411, Abcam, Cambridge, U.K.
Human caspase-3	19/17; 30	1:1000	#9662; Cell Signaling Technology, Danvers, MA, USA
Human caspase-9	37/35; 47	1:1000	#9508T; clone C9, Cell Signaling Technology, Danvers, MA, USA
β-actin	40	1:2000	Clone AC15; Sigma Aldrich, St. Louis, MO, USA

Secondary Antibodies	Dilution	
Anti-mouse IgG, horseradish peroxidase (HRP)-linked Antibody	1:2000	#7076S; Cell Signaling Technology, Danvers, MA, USA
Anti-rabbit IgG, HRP-linked Antibody	1:2000	#7074S; Cell Signaling Technology, Danvers, MA, USA

Consumables and Appliances:	
Chemi Doc™ MP Imaging System	Bio-Rad, Munich, Germany
Electrophoresis gel chamber	Department of Neurosurgery, Ulm University Medical Center, Germany
Hybond ECL Nitrocellulose blotting membrane	GE Healthcare, Freiburg, Germany

Shaker Platform Polymax 1040	Heidolph, Schwabach, Germany
Trans-Blot SD Semi-Dry Transfer Cell	Bio-Rad, Munich, Germany
Whatman Blotting Paper	VWR GmbH, Darmstadt, Germany
Pierce™ ECL Western Blotting Substrate	Thermo Fisher Scientific, Waltham, Massachusetts, USA

2.1.11 Phospho-kinase array

Product:	
Proteome Profiler Human Phospho-Kinase Array Kit	#ARY003B; R&D Systems, Inc., Minneapolis, MN, USA

2.1.12 Extracellular flux analysis

Product:	
XF96 V3 PS cell culture microplates	Agilent Technologies INC., Wilmington, DE, USA
XF assay medium (pH adjusted to 7.5)	Agilent Technologies INC., Wilmington, DE, USA
Mito stress test kit	Agilent Technologies INC., Wilmington, DE, USA
Agilent Seahorse XFe96 analyzer	Agilent Technologies INC., Wilmington, DE, USA

2.1.13 Cell migration/motility assays

Transwell® assay:	
Transwell® membranes (pore size 8μm)	Corning Incorporated, Corning, NY, USA
4'6-diamidino-2-phenylindole (DAPI)	

2.1.14 Chorion allantoic membrane (CAM) assay/toxicity study in chicken embryos

Products:	
Fertilized Eggs	LSL Rhein-Main, Dieburg, Germany
Matrigel®	BD Biosciences, MA, USA
Silicone rings	Ulrich Medical, Ulm, Germany
Histosettes	VWR, Radnor, PA, USA
Microtome RM2135	Leica, Nußloch, Germany
Microtome Blades	Feather, Osaka, Japan
Microscope slides	VWR, Radnor, PA, USA

2.1.15 Consumables

Products:	
Combitips advanced (1ml, 2.5ml, 5ml, 10ml)	Eppendorf, Hamburg, Germany
CryoPure Tubes (1.8ml)	Sarstedt, Nümbrecht, Germany
Parafilm M	Sigma-Aldrich, Darmstadt, Germany
Pipette tip (10µl, 20µl, 100µl, 200µl, 1000µl)	Sarstedt, Nümbrecht, Germany
SafeSeal tubes (0.5ml, 1.5ml, 2ml)	Sarstedt, Nümbrecht, Germany
Serological pipettes (5ml, 10ml, 25ml)	Sarstedt, Nümbrecht, Germany
Tube 15ml, 120 x 17mm, PP	Sarstedt, Nümbrecht, Germany
Tube 50ml, 114 x 28mm, PP	Sarstedt, Nümbrecht, Germany
TC Plate 12 Well, Standard, Flat	Sarstedt, Nümbrecht, Germany
TC Plate 24 Well, Standard, Flat	Sarstedt, Nümbrecht, Germany
TC Plate 96 Well, Standard, Flat	Sarstedt, Nümbrecht, Germany
TC Flask T75, Standard, Ventilation Cap (red)	Sarstedt, Newton, MA, USA
Vasco Nitril long, M	B. Braun, Melsungen, Germany

2.1.16 Appliances

Products:	
Analytical balance BP221S	Sartorius, Goettingen, Germany
CC-12 microscope camera	Soft Imaging System GmbH, Münster, Germany
Centrifuge 5417R	Eppendorf, Hamburg, Germany
Heraeus Multifuge x3 FR	Thermo Scientific, Schwerte, Germany
Incubator: Hera Cell Heraeus	Thermo Scientific, Schwerte, Germany
Laminar Flow hood: Hera Safe KS	Thermo Scientific, Schwerte, Germany
Water bath W12	Medingen, Amsdorf, Germany
MasterCycler Gradient Thermal Cycler	Eppendorf, Hamburg, Germany
Microscope CK30	Olympus, Hamburg, Germany
Microscope AX70	Olympus, Hamburg, Germany
Multipette M4	Eppendorf, Hamburg, Germany
Neubauer Cell Counting Chamber	Optik Labor, Lancing, UK
Pipetboy acu-jet®	Integra Biosciences, Zizers, Switzerland
Thermomixer 5436	Eppendorf, Hamburg, Germany
VacuSafe	Integra Biosciences, Zizers, Switzerland
Vortex mixer, EU-plug	VWR, Leuven, Belgium
VWR pHenomenal	VWR, Leuven, Belgium
VWR™ Galaxy Mini Microcentrifuge	VWR, Leuven, Belgium
Zeiss Imager.M1	Zeiss, Göttingen, Germany
Zeiss Observer.Z1	Zeiss, Göttingen, Germany

2.1.17 Software

Software:	
Bio-1D software	Vilber Lourmat, Eberhardzell, Germany

Cell^F	Olympus, Hamburg, Germany
Cell Quest Pro	Becton Dickinson, Heidelberg, Germany
CompuSyn software	ComboSyn, Inc., Paramus, NJ, USA
GraphPad Prism 5.04	GraphPad, La Jolla, CA, USA
ImageJ	Rasband, W.S., U.S. National Institutes of Health, Bethesda, USA
Image Lab 6.0.1	Bio-Rad, Munich, Germany
Integrated BioDiagnostics	Ibidi, Martinsried, Germany
FlowJo V10	Tree Star, Ashland, OR, USA
FlowJo version 7.6.5	Tree Star, Ashland, OR, USA
MtrackJ plugin for ImageJ software	Rasband, W.S., U.S. National Institutes of Health, Bethesda, USA

2.2 Methods

2.2.1 Cell culture

Human glioblastoma cell lines were cultured in T75 culture flasks at 37°C with 5% CO_2 and 96% humidity. Cells were passaged twice a week in a ratio depending on the density of the monolayer in each flask. For passaging, the old culture medium was removed, and cells were briefly washed with 3-5ml of DPBS. Afterwards, approximately 3ml of Trypsin/EDTA were added and the flask was incubated, at 37°C with 5% CO_2 and 96% humidity, until all cells were detached. The cell suspension was then resuspended in approximately 7ml of culture medium and transferred into a 50ml tube to be centrifuged at 1300 revolutions per minute (rpm) for 5 minutes (min) at room temperature (RT). After being centrifuged, the supernatant was discarded, and the cell pellet was resuspended in fresh culture medium. Afterwards, the cell number was either determined for further utilization or a predetermined portion, with a volume appropriate for cell passaging, of the cell suspension was transferred into a new T75 flask containing about 20ml of culture medium.

2.2.2 Determination of cell numbers

To determine the cell concentration in a suspension per ml, 20µl of said cell suspension were diluted with 60µl of Trypan blue, to distinguish intact from dead cells. Afterwards, 10µl of the obtained solution was transferred to the Neubauer counting chamber and the intact cells were counted in the large squares of the chamber. The cell concentration per ml was calculated using the following formula:

$$\frac{counted\ cells}{4} \times\ dilution\ factor\ (1) \times\ 10^4 (2) = \frac{cell\ number}{ml}$$

(1) Dilution factor = 4

(2) Neubauer counting chamber factor

2.2.3 Treatment of cells

For all experiments, the cells were seeded with the culture medium according to the cell culturing protocol one day prior to treatment for appropriate attachment of the cells. The next day before stimulation of cells, the culture medium was exchanged for fresh culture medium containing 1.5% of FBS. Treatment concentrations were freshly prepared before stimulation and diluted in culture medium containing 1.5% FBS. Each experiment included a control treated with just the solvent of the respective substance.

2.2.4 Cell viability assays

In order to examine cellular viability, MTT assays were performed. For the assay, 3 x 10^3 cells/well/100µl DMEM with 10% FBS of U251 cells and 5 x 10^3 cells/well/100µl DMEM with 20% FBS of ULM-GBM-PC128 cells were seeded in a 96-well plate and allowed to get attached overnight at 37°C with 5% CO_2 and 96% humidity. The next day, prior to stimulation of the cells, the medium was exchanged with DMEM containing 1.5% FBS and the cells were treated with the reagents or corresponding solvents with following concentrations:

	C	C	C	C	C	C	C	C	C	C	
	DG10	DG5	DG2.5	DG1.25	DG0.625	T50	T25	T12.5	T6.25	T3.125	
	DG10	DG5	DG2.5	DG1.25	DG0.625	T50	T25	T12.5	T6.25	T3.125	
	DG10 T3.125	DG5 T6.25	DG2.5 T12.5	DG1.25 T25	DG0.625 T50	DG10 T50	DG5 T25	DG2.5 T12.5	DG1.25 T6.25	DG0.625 T3.125	
	G10 T3.125	G5 T6.25	G2.5 T12.5	G1.25 T25	G0.625 T50	G10 T50	G5 T25	G2.5 T12.5	G1.25 T6.25	G0.625 T3.125	
	C	C	C	C	C	C	C	C	C	C	

C – Control, which is treatment with both the solvents of ONC201/TIC10 and 2-DG

DG – Treatment with 2-DG with the concentration in mM

T – Treatment with ONC201/TIC10 with the concentration in μM

After 72h of treatment, the culture medium was aspirated and 100μl MTT working solution was added prior to incubation for 3h. In metabolically active cells, the MTT salt is converted into a dark purple colored formazan that accumulates inside the cells. The reaction was ended by adding 100μl of isopropanol to solubilize the cells and further spectrophotometric analysis. The mixture is then mixed by pipetting and afterwards the plate is placed on the shaker for 30min to ensure appropriate solubilization of the cells. Spectrophotometric analysis was performed at a wavelength of 550nm using the microplate reader EL800.

2.2.5 Soft agar assay

Anchorage-independent growth was examined using a soft agar assay. Six-well plates were coated with a base layer of 0.9% low-melting agarose containing 20% FBS, antibiotics and the respective agents or solvent. 2 x 10^4 cells were seeded in a top layer of 0.35% agarose, containing the same components as the base layer, and incubated for 21 days at 37°C with 5% CO_2 and 96% humidity. All colonies larger than 200μm in diameter were counted and images were taken at 4x microscopic magnification.

2.2.6 CellTiter-Glo® assay

The CellTiter-Glo® luminescent assay was used as instructed by the manufacturer's manual to determine cellular ATP levels. Cells were seeded in 96-well plates and were allowed to attach overnight at 37°C with 5% CO_2 and 96% humidity. Afterwards, the cells were stimulated for 72h with respective agents or solvent. Then, 100µl of CellTiter-Glo® Reagent was added to each well containing medium and cells. Further, the cells were shaken for 2 minutes to induce cell lysis. Cells were then incubated for 10 minutes at RT for signal stabilization prior to measuring the luminescence.

2.2.7 Staining for carboxyfluorescin diacetate succinimidyl ester (CFSE)

CFSE staining was carried out using the CellTrace™ CFSE cell proliferation kit as instructed by the manufacturer. Two x 10^6 cells were enzymatically detached, washed with PBS and centrifuged at 1300 rpm for 5 minutes. Subsequently, the supernatant was discarded before the cells were resuspended in 1800µl of PBS. Then 200µl CFSE in a concentration of 50µM were added to make up a final concentration of 5µM prior to incubation for 10 minutes at 37°C. The reaction was quenched by adding 10ml of DMEM containing 10% FBS and incubation at RT for a duration of 10 minutes prior to three steps of washing with 8ml of fresh DMEM and centrifugation at 1300 rpm. Finally, cells were seeded in 6-well plates at a density of 4.5 x 10^4 cells/well, allowed to attach overnight and stimulated with the respective reagents or solvent for 96h. Afterwards, cells were enzymatically detached, centrifuged and resuspended in 300µl of PBS at RT before flow cytometric analysis. FlowJo software (version 7.6.5) was used for data analysis.

2.2.8 Measurement of cell death and cell cycle analysis

Measurement of cell death was performed by using propidium iodide (PI) staining followed by flow cytometric analysis. Briefly, cells were seeded in 12-well plates at a density of 3 x 10^4 cells/well/1.5ml, allowed to attach over night at 37°C with 5%

CO_2 and 96% humidity prior to treatment with respective agents or solvent for 48h. Cells were then enzymatically detached, centrifuged for 5 minutes at 1800 rpm and washed twice with PBS. Afterwards, 300µl PI staining buffer was added, and the cells were incubated for 30 minutes at 4°C before flow cytometric analysis. Cell cycle analysis was performed using the FlowJo V10 cell cycle tool.

2.2.9 Real-time PCR and cDNA synthesis

To isolate total cellular mRNA from the glioblastoma cells and determine the RNA concentration, cells were collected from flasks and centrifuged for 5 minutes at 1800 rpm and 4°C and subsequently a solution is prepared to have a cell density of 5 x 10^5 cells/ml. The isolation of the mRNA was performed using the Maxwell® LEV simplyRNA Tissue Kit (Promega) and the Maxwell® 16 IVD Intrument (Promega) according to the manufacturers' instructions and the RNA concentration was measured using photometry. To synthesize complementary DNA (cDNA), reverse transcription was performed using the Biozym cDNA Synthesis Kit. One µg of RNA was mixed with 8µl of Master mix (Biozym) and water free of nucleases to a total volume of 20µl prior to incubation at 55°C for 50 minutes and further 5-minute incubation time at 99°C to inactivate the enzymes. Produced cDNA was stored at -20°C or directly used for RT-PCR.

For PCR the Roche LightCycler (ThermoFisher) was used according to the manufacturers' instructions with MicroAmp™ Fast Optical 96-Well Reaction Plates (life technologies). After subsequent denaturation at 95°C for 30 seconds, the SYBR Green Master Mix (Bio-Rad) was used for RT-PCR analysis with the following thermal settings according to the Roche LightCycler 480 fast standard mode:

35-40 cycles of:

95°C	5-15 seconds
60°C	10-30 seconds
60°C	60 seconds

Followed by:

65-95°C	10 minutes
0,5°C	finish

For evaluation of equal amounts of cDNA, the 18s gene was used as a control.

2.2.10 Western blot analysis

Western blot analysis was performed to determine the protein expression of the respiratory chain complexes I-V following treatment with the reagents. β-actin Western blot analysis was performed to confirm that equal amounts of protein were loaded. For the preparation of cell lysates cells were seeded with a density of 5 x 10^4 cells/well/1.5ml in 12-well plates and were allowed to attach overnight. Afterwards, cells were stimulated for 6 hours and 24 hours with respective reagents and solvent. For harvesting of the cell lysates, the culture medium was transferred to SafeSeal tubes and centrifuged for 5 minutes at 7000 rpm and RT. Meanwhile 100µl of SDS loading buffer and 500µl of lysis buffer was mixed and 50µl of this solution was added to each well. After centrifugation the supernatant was discarded, and the viscous cell-lysis product was scratched with a pipette tip from each well and added to the corresponding SafeSeal tube and resuspended with the cell pellet. Then, the samples were denaturated for 70 minutes at 70°C and 300 rpm with the Thermomixer 5436.

Afterwards, proteins were separated using polyacrylamide gel electrophoresis with a 12% resolving gel and a 5% stacking gel. The gel electrophoresis chamber was filled with running buffer and the protein samples were concentrated in the stacking gel at 80V, 400mA and 100W. Then, the samples were separated in the resolving gel overnight at 20V, 400mA and 100W. The next day, the separated proteins were transferred onto a nitrocellulose membrane with blotting buffer by Semi-dry blotting at 20V and x mA for 2 hours.

$$x = length\ (of\ the\ nitrocellulose\ membrane) \times width \times 2$$

Afterwards, the membrane was shortly washed with PBS-T and subsequently the transfer was blocked by incubating the membrane for 1 hour at RT in blocking

solution on a shaker. Then, the membrane was washed 3-4 times with PBS-T for 8-10 minutes prior to exposure with the primary antibody over night at 4°C on Shaker Platform Polymax 1040. The next day, the membrane was washed 3 times with PBS-T before being exposed to the horseradish peroxidase-coupled secondary antibody for 1 hour at RT on the Shaker Platform. Then, the membrane was again washed 3 times for 8-10 minutes with PBS-T prior to incubation with enhanced chemiluminescence (ECL) solution (Thermo Fisher Scientific) and subsequent visualization via enhanced chemoluminescence.

2.2.11 Phospho-kinase array

For establishing protein samples to use with the phospho-kinase array, 6 10cm-dishes per treatment were seeded with a cellular density of 2.76 x 10^6 to attach overnight. Then, the cells were treated for 24 hours or 48 hours prior to protein extraction. For the protein extraction, all steps were performed on ice. First, the dishes were scraped off with a cell scraper and the culture medium was collected in a test tube to be filled up to 50ml with PBS prior to centrifugation for 5 minutes with 1800 rpm at 4°C. Then, the supernatant was discarded, and the pellet was resuspended with 5ml of PBS before being centrifuged again using the same settings. Afterwards, the supernatant was again discarded, and the pellet was resuspended with 1ml of PBS prior to pooling all cells with the same treatment conditions in one test tube and subsequent centrifugation. Further, the supernatant was again discarded, and the cell pellet was resuspended with 1ml PBS before being transferred to a SafeSeal test tube and the last centrifugation step using the same settings. Then, the supernatant was discarded, and the resulting cell pellet was stored at -20°C until further utilization. Cell lysis buffer was added to the cell pellet and incubated for 30 minutes at 2-8°C prior to centrifugation for 20 minutes with 14000 rpm at 4°C. Finally, the supernatant was transferred to a new SafeSeal test tube to be checked for protein content. A BCA protein assay was used to quantify the total protein of said sample prior to the calculation of which volume of the sample was needed to obtain the 600µg of protein needed for the

phospho-kinase array. The human phospho-kinase array kit is divided into two membranes (A and B) to increase sensitivity and decrease cross-reactivity. Therefore, membranes A and B were kept in separate wells while handling them. First, the needed volume to obtain 600μg of protein was diluted to a final volume of 2ml (1 ml for each membrane A and B) with array buffer 1, which is a buffered protein base with preservatives, provided by R&D Systems. Afterwards, 1ml of array buffer 1 was added to each well of the 8-well dish provided by R&D systems and each of the 8 membranes was placed in a separate well to incubate for one hour on a rocking platform shaker. Then, the array buffer 1 was aspirated and 1ml of the lysate-array buffer mixture was added to each well (membrane A and B, for every treatment option) to be incubated overnight at 2-8°C. The next day, each membrane was removed and separated in two containers (one container for membranes A and one for membranes B) to be washed together with the provided wash buffer for 10 minutes and a total of three washes. Then, each membrane was placed again into the 8-well multi-dish after draining the washing buffer. Afterwards, 1ml of the mixed detection antibody cocktails A and B, containing 20μl of the antibody mixture and 980μl of array buffer 2/3 per 1 ml, was added to the corresponding wells and incubated for 2 hours at room temperature. Then, the membranes were again washed for a total of three times before being exposed to the streptavidin horseradish peroxidase-coupled secondary antibody and incubated for 30 minutes at room temperature. Afterwards, the washing steps were repeated again for 3 washes. Then, the membranes A and B were placed in separate plastic sheet protectors, 1ml of the provided chemi reagent mix was pipetted evenly on each membrane and air bubbles and excess reagent were removed. Finally, the results were visualized via enhanced chemiluminescence with exposure times of 5 or 10 minutes.

For quantitative analysis of the data, the Bio-1D software was used and the data was first normalized to the respective reference spot and secondly to the respective control.

2.2.12 Extracellular flux analysis

One x 10^4 cells were seeded onto XF96 V3 PS cell culture microplates (Agilent Technologies) and were allowed to attach overnight. After 24 hours cells were stimulated with the indicated treatments for 24 hours prior to being washed with XF assay medium, which contains 5mM of glucose (pH adjustment to 7.5). Then the mito stress test kit (Agilent Technologies) was used according to the manufacturers' instructions by applying serial injections of oligomycin at a concentration of 2μM, carbonyl cyanide-4 (trifluoromethoxy) phenylhydrazone (FCCP) at a concentration of 2μM and rotenone/antimycin A at a concentration of 0.5μM. The Agilent Seahorse XFe96 analyzer was used for all analyses and the data were normalized to cell content by staining with JanusGreen and measured with a standard microplate spectrophotometer.

2.2.13 Cell migration/motility assays

Transmembranous migration (Transwell®) and *in vitro* scratch assays were used to evaluate the directed and non-directed migration of cells. Cellular motility was examined through time-lapse live cell microscopic imaging.

For the transmembranous migration (Transwell®) assay, 3 x 10^4 cells were seeded onto Transwell® membranes with a pore size of 8μm in culture medium containing 1.5% FBS and were stimulated subsequently with respective substances or solvent. The wells were filled with culture medium containing 10-20% FBS, depending on the cell-line, and the respective substances or solvent. Thus, a culture medium gradient from 1.5% FBS above the membrane towards a 10-20% FBS content in the well was created, promoting cellular motility towards the more nutritious environment, additional to the gravitational gradient. This contrast gradient stimulated the cells to migrate towards the culture medium containing a higher amount of FBS. After 24 hours, the upper side of the membrane was washed and wiped with PBS three consecutive times. Then, the cells, which migrated to the bottom side of the membrane were fixed and stained with a solution containing 4'6'diamidino-2-phenylindole (DAPI) and methanol at a concentration of 1:2000.

Afterwards, the membranes were mounted, and the number of migrated cells was counted in for each membrane using the NIH ImageJ software.

For the Scratch assay, 1 x 10^5 cells/well/1.5ml were seeded in 12-well plates and were allowed to attach overnight. The next day, the cells sustained a scratch across the well which was carried out with a 200µl pipet tip prior to a washing step with PBS and subsequent stimulation with respective substances or solvent. Sequential microscopic images were taken at defined time points with a 10x magnification, taking photographs always at the exact same position of the well. Afterwards, the area of the scratch was further analyzed using the NIH ImageJ software.

For time-lapse live cell imaging, 4 x 10^4 cells/well/1.5ml were seeded in 12-well plates and were allowed to attach overnight. The next day, the cells were stimulated with respective substances or solvent and microscopic images at 10x magnification were taken with a live-imaging inverted video microscope every 30 minutes for 24 hours. During this time, cells were kept at 37°C with 5% CO_2 and 96% humidity. Analysis was performed by single-cell tracking with the MtrackJ plugin for the NIH ImageJ software. Afterwards, normalized wind-rose plots were obtained using the chemotaxis and migration tool from Integrated BioDiagnostics.

2.2.14 Chorion allantoic membrane (CAM) assay

To evaluate the effects of the tested substances and their combination on three-dimensional tumor formation and tumor cell invasion into a biologic membrane, CAM assays were performed. A 1:1 mixture of Matrigel® and serum-free medium containing 2 x 10^6 cells of the U251 cell line or 1 x 10^6 cells of the ULM-GBM-PC128 cell line was seeded onto the CAM of one-week old fertilized chicken eggs. After 24 hours, the treatment with respective substances or solvent was started and consisted of local application two times per day. Then, after 4 days after seeding, the tumor and its adjacent CAM were harvested and embedded in paraffin. For analysis, sections were obtained, stained with hematoxylin and eosin and evaluated microscopically. Microphotographs were taken at a 2.5x magnification and the tumor area was quantified using the NIH ImageJ software.

2.2.15 Toxicity study in chicken embryos

Five-day old chicken embryos were treated with the combination therapy or solvent twice per day for 5 days per week over a period of 11 days to assess the substances for organ and hematological toxicity. For determination of erythrocyte and leukocyte count, blood samples were collected. For morphological alterations of erythrocytes and leukocytes, blood smears were prepared and microphotographed at 20x magnification and were assessed by two independent observers. Organ samples were extracted and fixed in 10% PBS-buffered formalin for at least 24h. Then, tissues were embedded in paraffin and cut into 4μm thick sections before being stained with hematoxylin and eosin. 10x magnification was used for microphotographs and two independent observers assessed the organs for tissue damage.

2.2.16 Statistical analysis

The statistical significance of all experiments was assessed by using the Student's t-test with Prism version 5.04, if not stated otherwise. A p-value of ≤ 0.05 was considered statistically significant.

3. Results

3.1 Treatment with ONC201/TIC10 suppresses OXPHOS in glioblastoma cells

As it was previously described by Ishida and colleagues, imipridones like ONC201/TIC10 alter the cellular energy metabolism of glioblastoma cells [25]. For further investigation of how ONC201/TIC10 reprograms the energy metabolism of glioblastoma cells, extracellular flux analyses determining oxygen consumption rates (OCR) were performed. Our findings show, that treatment with ONC201/TIC10 leads to a significant reduction of mitochondrial respiration in U251 and A172 cells (Figure 5A and B, Figure 6). Further analysis of the mitochondrial respiration showed that especially the ATP-linked respiration was significantly affected. Interestingly, the effect of ONC201/TIC10 on the oxidative phosphorylation did not increase dose-dependently with treatments above 10μM ONC201/TIC10.

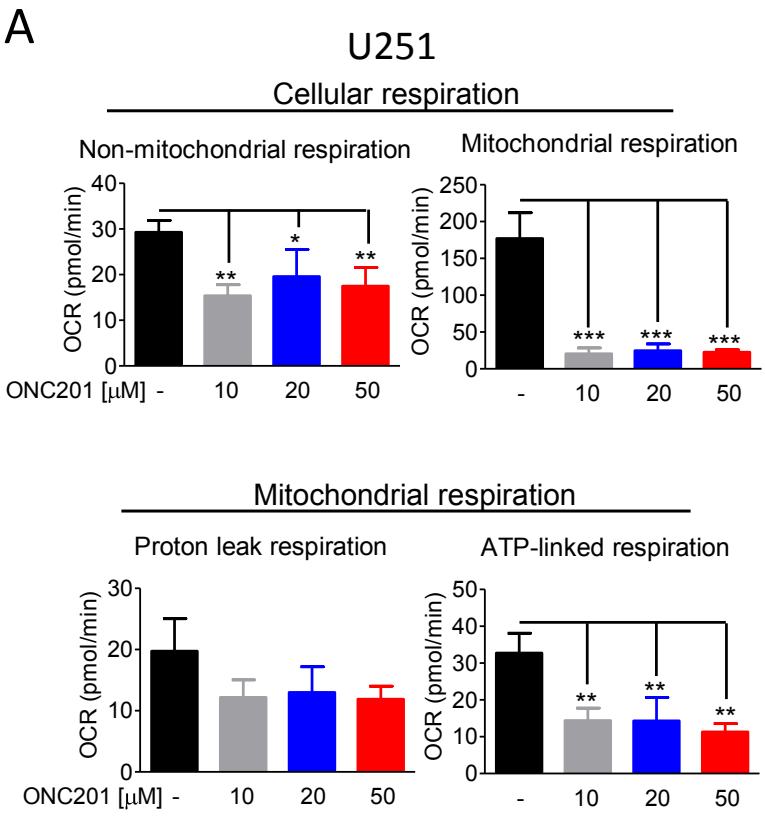

Figure 5 A: Treatment of glioblastoma cells with ONC201/TIC10 leads to alteration of energy metabolism by suppression of OXPHOS. A, U251 glioblastoma cells were treated as indicated for 24 hours prior to performing mitochondrial stress tests. Oligomycin, FCCP and rotenone/antimycin A were successively injected while continuous extracellular flux analysis was recording OCR. The inhibitors rotenone/antimycin A were used to dissect the total cellular respiration into mitochondrial and non-mitochondrial respiration. The ATP synthase inhibitor oligomycin was used to measure the portion of ATP-linked respiration and proton-leak (protons passing the mitochondrial membrane not coupled with ATP synthesis). Columns: mean; bars: SD; n=3 *p<0.05, **p<0.005 [53] (used according to CC BY 4.0 https://creativecommons.org/licenses/by/4.0/").

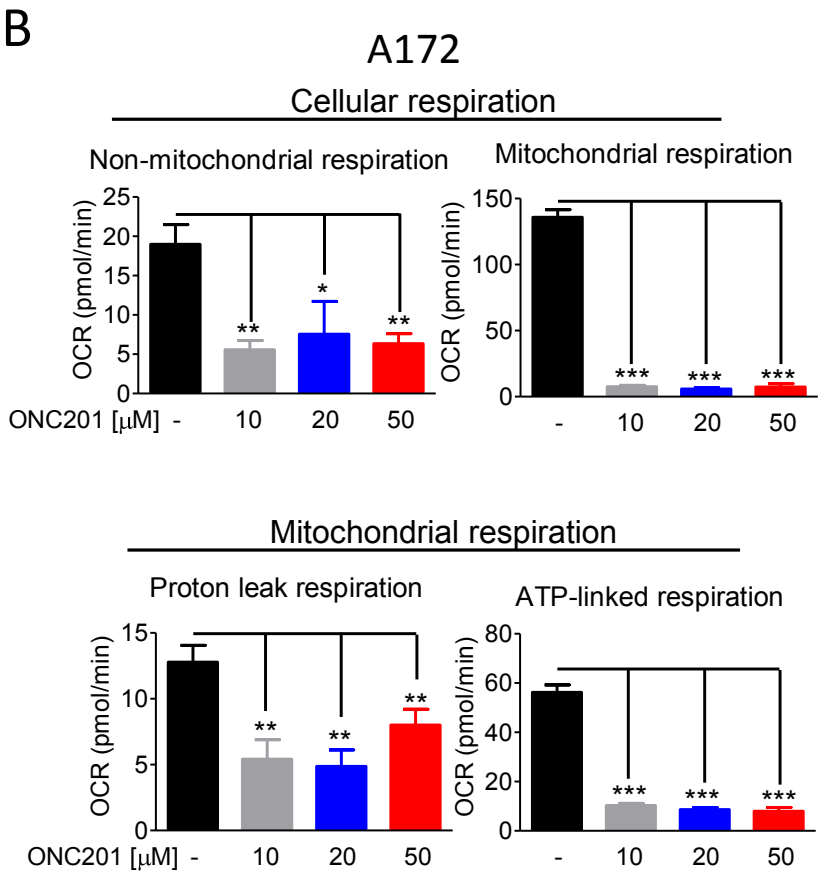

Figure 5 B: Treatment of glioblastoma cells with ONC201/TIC10 leads to alteration of energy metabolism by suppression of OXPHOS. B, A172 glioblastoma cells were treated as indicated for 24 hours prior to performing mitochondrial stress tests. Oligomycin, FCCP and rotenone/antimycin A were successively injected while continuous extracellular flux analysis was recording OCR. The inhibitors rotenone/antimycin A were used to dissect the total cellular respiration into mitochondrial and non-mitochondrial respiration. The ATP synthase inhibitor oligomycin was used to measure the portion of ATP-linked respiration and proton-leak (protons passing the mitochondrial membrane not coupled with ATP synthesis). Columns: mean; bars: SD; n=3 *p<0.05, **p<0.005 [53] (used according to CC BY 4.0 https://creativecommons.org/licenses/by/4.0/").

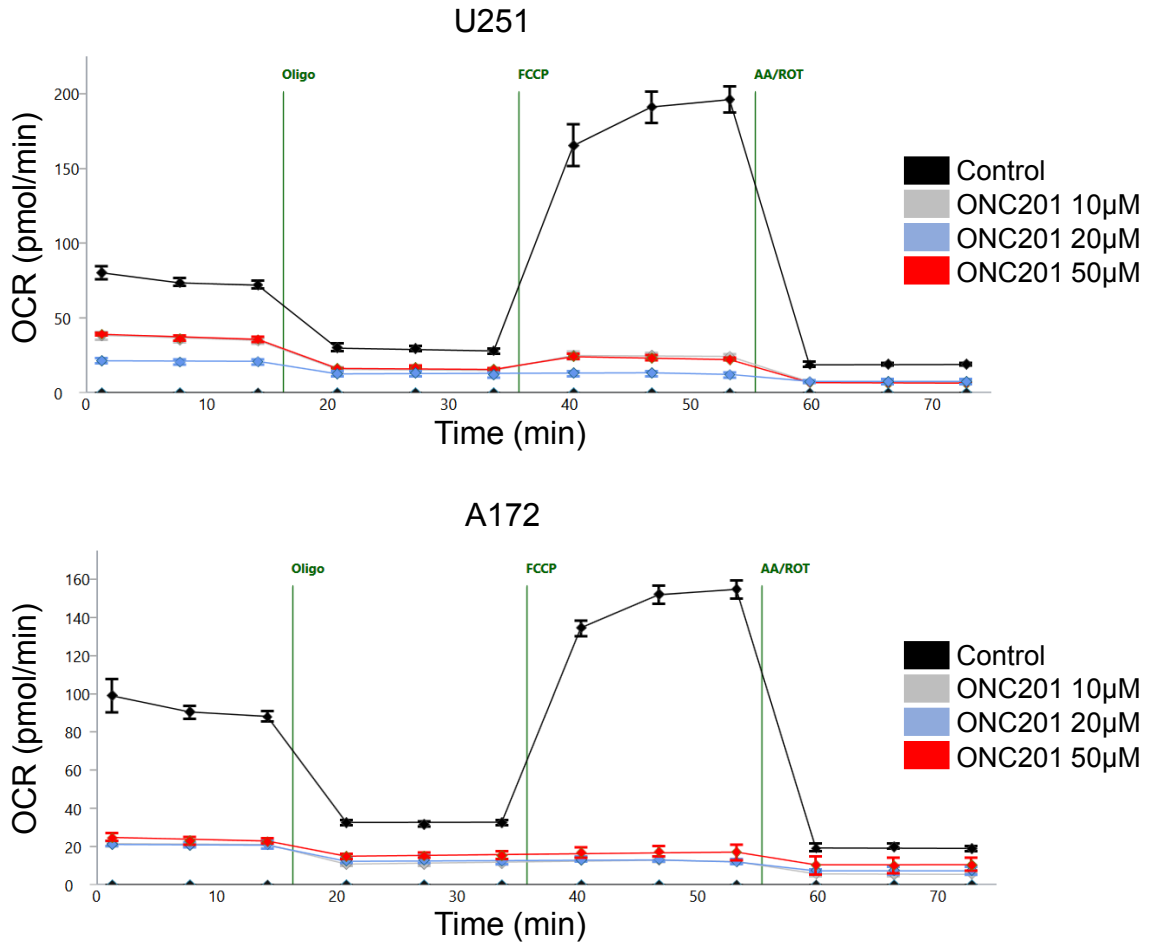

Figure 6: Treatment with ONC201/TIC10 reduces OCR. OCR graphs of U251 and A172 glioblastoma cells that were treated as indicated 24 hours prior to performing mitochondrial stress test. Oligomycin, FCCP and rotenone/antimycin A were successively injected while continuous extracellular flux analysis was recording OCR. The data shown are representative for 3 independent experiments and are displayed as mean and SD [53] (used according to CC BY 4.0 https://creativecommons.org/licenses/by/4.0/").

3.2 ONC201/TIC10 down-regulates protein expression of respiratory chain complexes

For further investigation, whether the inhibition of ONC201/TIC10 on OXPHOS is also related to the protein expression of specific complexes of the mitochondrial respiratory chain, we performed Western blot analysis (Figure 7 A and B). After treatment with ONC201/TIC10 for 24 hours, complexes I and II experienced the strongest reduction in protein expression in U251 and A172 cells. This observation was confirmed by densitometric analysis (Figure 8 A and B).

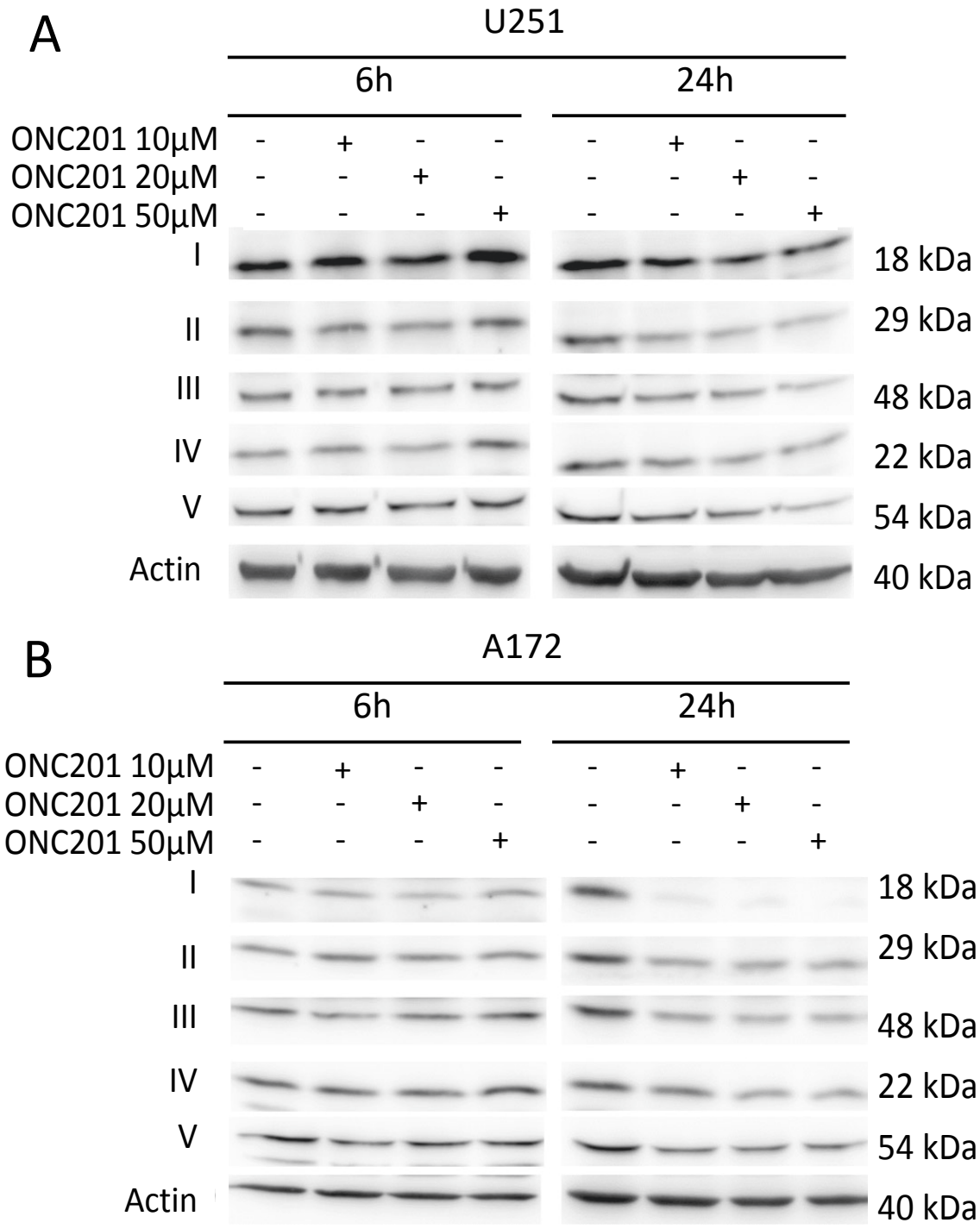

Figure 7 A and B: Treatment with ONC201/TIC10 leads to reduction in protein expression of respiratory chain complexes. A-B, U251 (A) and A172 (B) glioblastoma cells were treated for 6 hours and 24 hours as indicated.
Western blot analysis was used for examination of whole cell extracts for the expression of respiratory chain complexes I-V. Actin Western blot analysis was used to confirm equal protein loading [53] (used according to CC BY 4.0 https://creativecommons.org/licenses/by/4.0/").

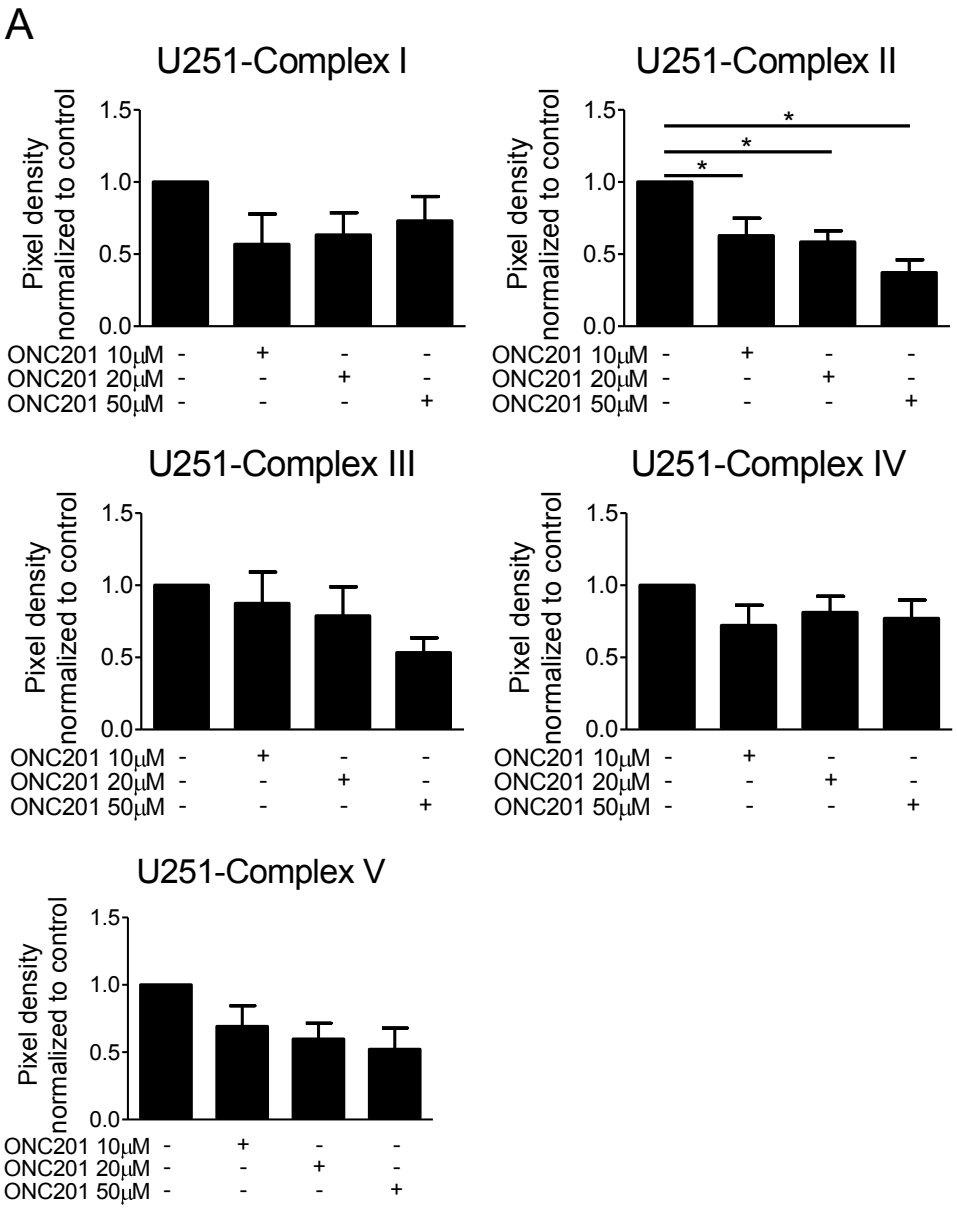

Figure 8 A: Treatment with ONC201/TIC10 for 24 hours leads to a reduction in protein expression of respiratory chain complexes. A, U251 glioblastoma cells were treated for 24 hours as indicated. Western blot analysis was used for examination of whole cell extracts for the expression of respiratory chain complexes I-V. Actin Western blot analysis was used to confirm equal protein loading. The quantification of pixel density was performed using the ImageJ software. Columns: mean; bars: SD; n=3. One-way ANOVA followed by Newman-Keuls post hoc test was used for statistical analysis [53] (used according to CC BY 4.0 https://creativecommons.org/licenses/by/4.0/").

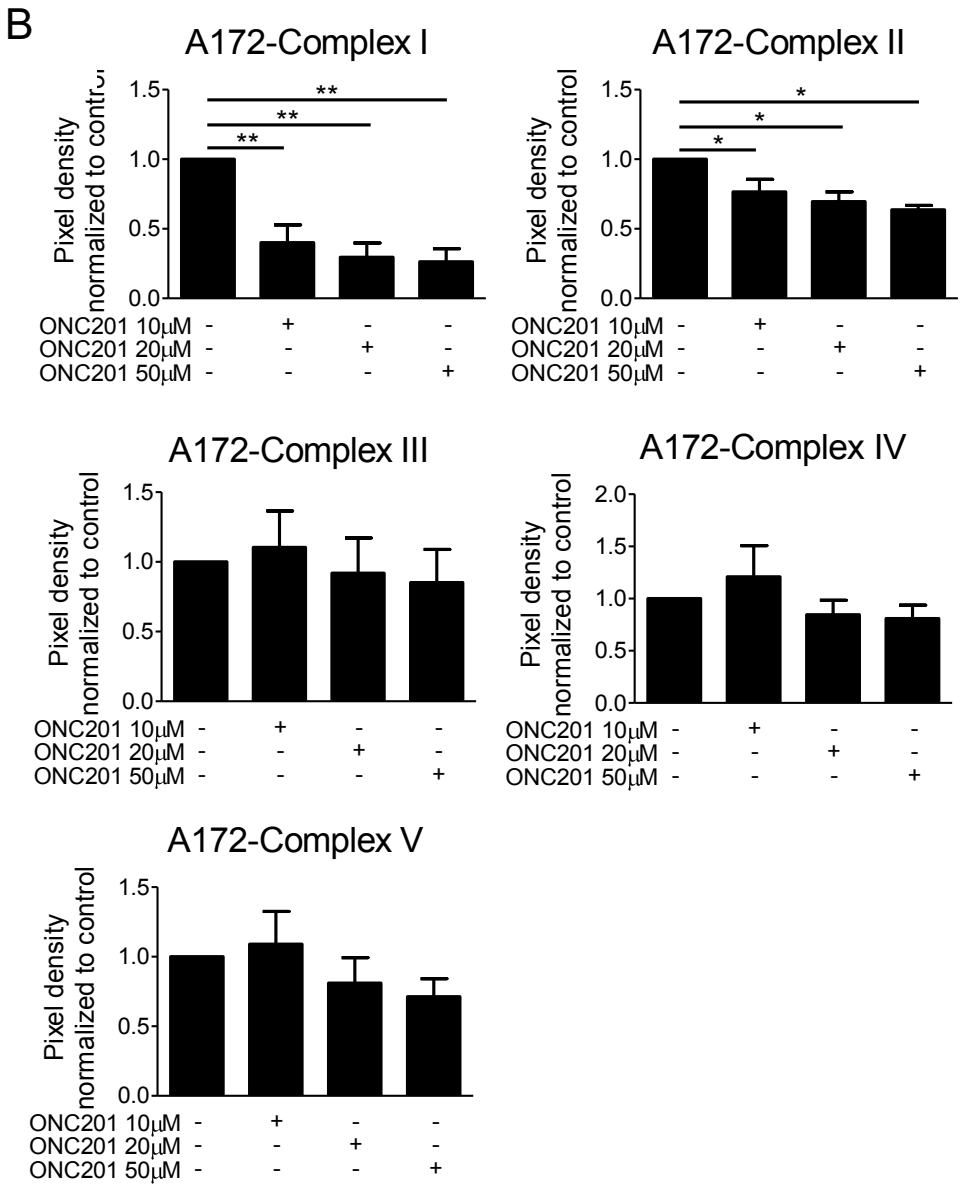

Figure 8 B: Treatment with ONC201/TIC10 for 24 hours leads to a reduction in protein expression of respiratory chain complexes. B, A172 glioblastoma cells were treated for 24 hours as indicated. Western blot analysis was used for examination of whole cell extracts for the expression of respiratory chain complexes I-V. Actin Western blot analysis was used to confirm equal protein loading. The quantification of pixel density was performed using the ImageJ software. Columns: mean; bars: SD; n=3. One-way ANOVA followed by Newman-Keuls post hoc test was used for statistical analysis [53] (used according to CC BY 4.0 https://creativecommons.org/licenses/by/4.0/").

3.3 Treatment with ONC201/TIC10 enhances the glycolytic rate of glioblastoma cells

We next investigated the effects of ONC201/TIC10 on the glycolytic activity of U251 and A172 glioblastoma cells. To this purpose, extracellular acidification rates (ECAR) were determined via extracellular flux analyses. As shown in Figure 9 A and B, while treatment with ONC201/TIC10 led to a significant reduction in OXPHOS, ECAR, as a correlate for the glycolytic rate, was markedly increased. We further analysed whether this observation creates a state of metabolic vulnerability towards glucose withdrawal. Cells were cultured with varying ambient glucose concentrations in the absence or presence of ONC201/TIC10 prior to assessing the cellular viability. As shown in Figure 10 A and B, a decreased ambient glucose concentration was associated with an enhanced response to treatment with ONC201/TIC10leading to a reduction in cellular viability in glioblastoma cells U251 and ULM-GBM-PC128 as indicated by a decrease in IC_{50} values.

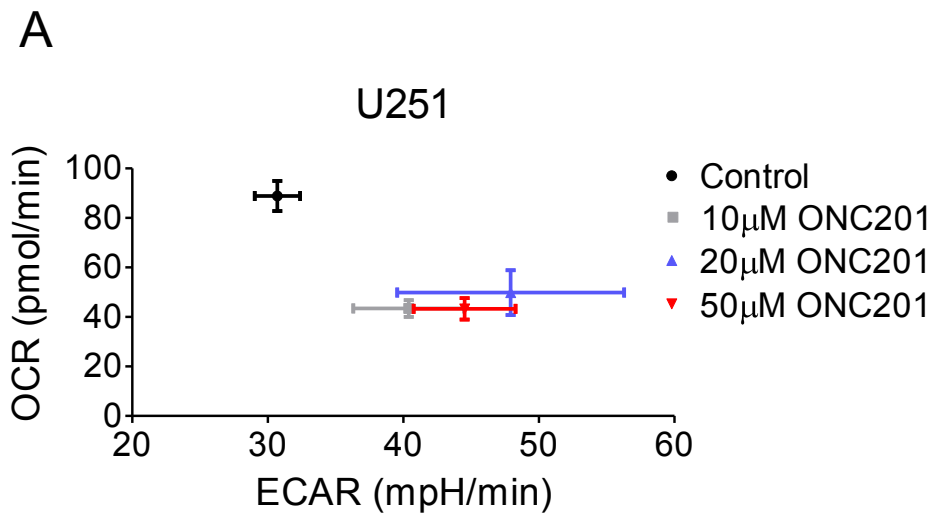

Figure 9 A: Treatment with ONC201/TIC10 for 24 hours leads to an increased glycolytic rate. A, U251 glioblastoma cells were treated for 24 hours as indicated followed by extracellular flux analysis measuring ECAR and OCR. Graphical representation of baseline OCR/ECAR-values shown as mean and SD; n=3 [53] (used according to CC BY 4.0 https://creativecommons.org/licenses/by/4.0/").

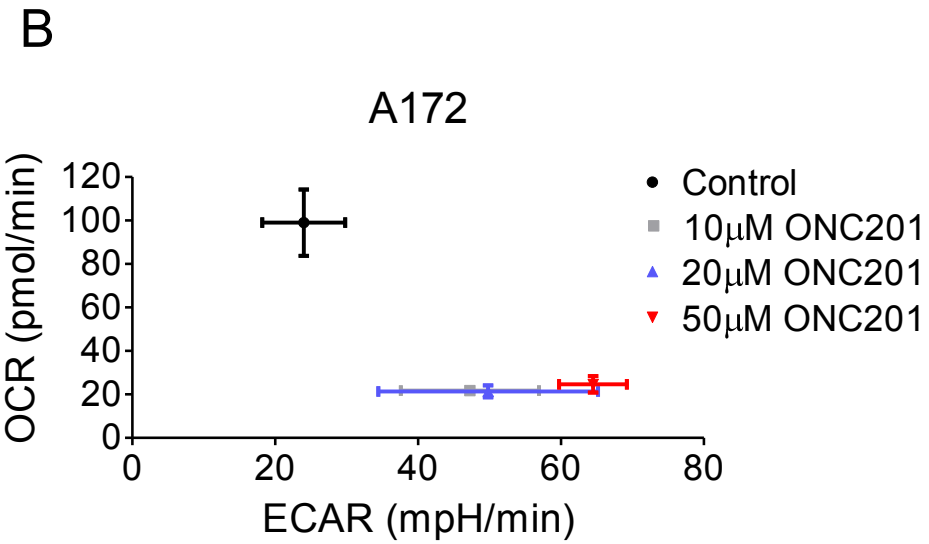

Figure 9 B: Treatment with ONC201/TIC10 for 24 hours leads to an increased glycolytic rate. B, A172 glioblastoma cells were treated for 24 hours as indicated followed by extracellular flux analysis measuring ECAR and OCR. Graphical representation of baseline OCR/ECAR-values shown as mean and SD; n=3 [53] (used according to CC BY 4.0 https://creativecommons.org/licenses/by/4.0/").

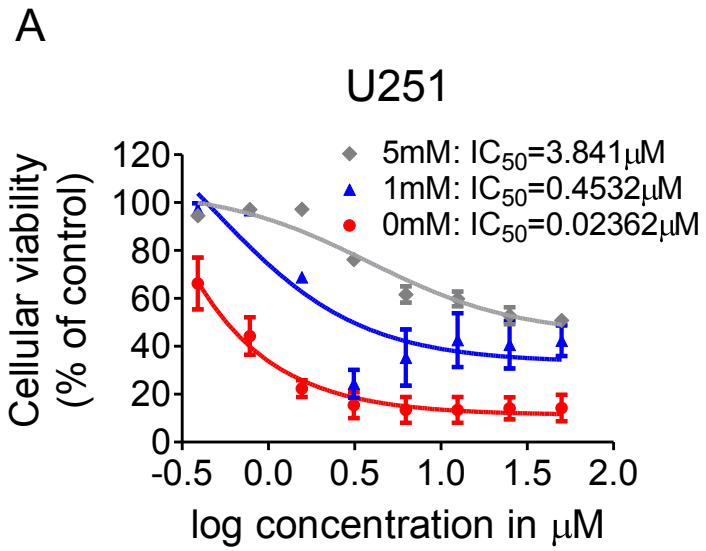

Figure 10 A: The reduction in ambient glucose concentrations leads to an increase in the response to ONC201/TIC10. A, U251 glioblastoma cells were treated for 72 hours with increasing concentrations of ONC201/TIC10 and varying concentrations of glucose present (5mM, 1mM or 0mM). Non-linear regression was performed and IC_{50}-values were calculated. Data are shown as mean and SD; n=3 [53] (used according to CC BY 4.0 https://creativecommons.org/licenses/by/4.0/").

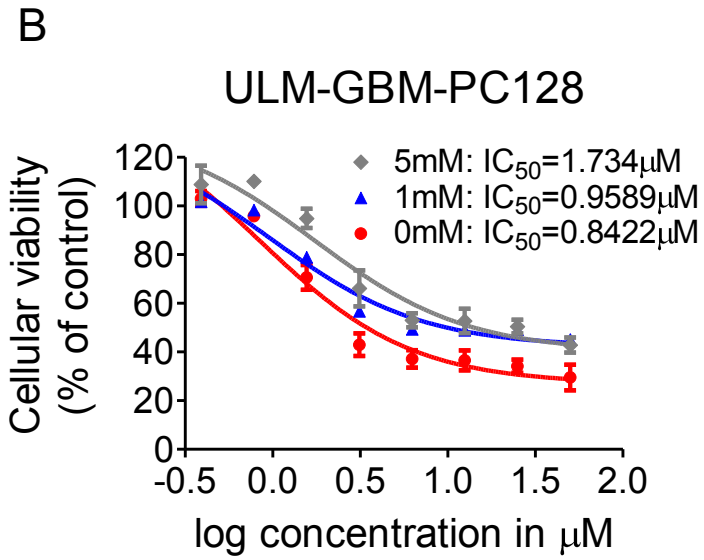

Figure 10 B: The reduction in ambient glucose concentrations leads to an increase in the response to ONC201/TIC10. B, ULM-GBM-PC128 (B) glioblastoma cells were treated for 72 hours with increasing concentrations of ONC201/TIC10 and varying concentrations of glucose present (5mM, 1mM or 0mM). Non-linear regression was performed and IC_{50}-values were calculated. Data are shown as mean and SD; n=3 [53] (used according to CC BY 4.0 https://creativecommons.org/licenses/by/4.0/").

3.4 Treatment with ONC201/TIC10 leads to an enhanced activation of the serine-one carbon-glycine (SOG) pathway

It was shown in a previous study that treatment with ONC201/TIC10 leads to an up-regulation of the SOG pathway as a compensatory mechanism in U87 glioblastoma cells [25]. We used real-time PCR analyses for mRNA expression levels of three enzymes related to the SOG pathway (PHGDH, PSAT1, PSPH) to verify whether the ONC201/TIC10-induced metabolic changes which we observed in our setting are also affecting the SOG pathway. As shown in Figure 11, treatment with ONC201/TIC10 resulted in a noticeable up-regulation of all tested enzymes in U251 and A172 glioblastoma cells.

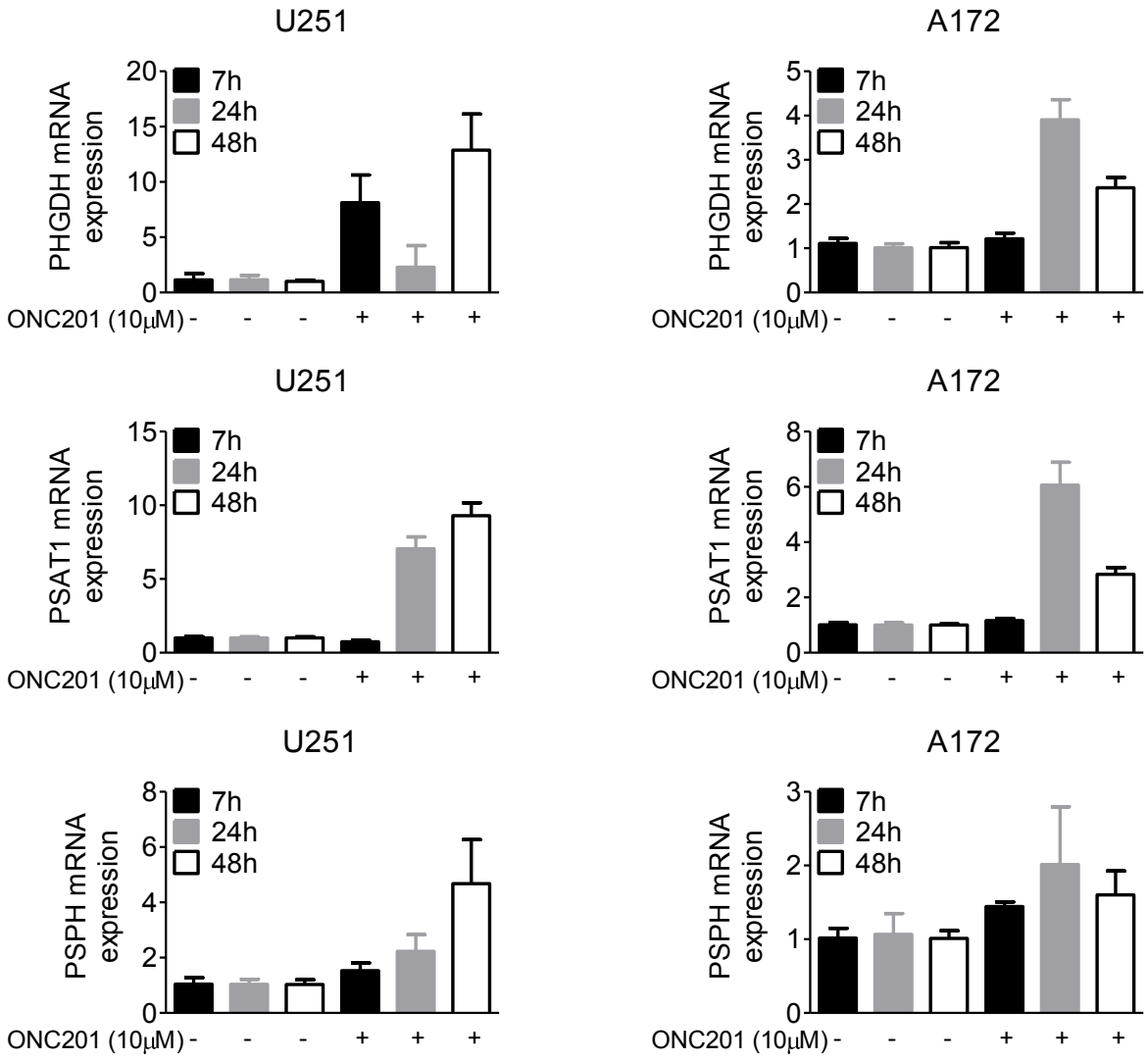

Figure 11: Treatment with ONC201/TIC10 results in an mRNA over-expression of SOG pathway enzymes PHGDH, PSAT1 and PSPH. U251 and A172 cells were treated with 10μM of ONC201/TIC10 for 7 hours, 24 hours or 48 hours. Real-time PCR was performed for PHGDH, PSAT1 and PSPH. Columns: mean; bars: SD; n=3 [53] (used according to CC BY 4.0 https://creativecommons.org/licenses/by/4.0/").

3.5 Combined treatment with ONC201/TIC10 and 2-Deoxyglucose leads to a synergistic reduction of the cell viability of glioblastoma cells

Based on our observation that treatment with ONC201/TIC10 led to a compensatory up-regulation of the glycolytic activity in response to its inhibiting effects on the mitochondrial respiration and the increased vulnerability at low glucose concentrations, we hypothesized that addition of a glycolysis inhibitor

could induce a state of energy depletion and consequently enhance the anti-neoplastic activity of ONC201/TIC10. 2-DG is an inhibitor of glycolysis, which has already been used in clinical trials before with a good safety profile and is able to cross the blood brain barrier [60]. Hence, we examined the effects of a combination therapy of ONC201/TIC10 with 2-DG and the respective substances alone. After 48 hours it is apparent on microscopic images that a combination therapy of ONC201/TIC10 with 2-DG leads to marked morphologic alterations, namely an increased rounding of cells and a decreased cellular density (Figure 12). The combination treatment was also very efficient in reducing the cellular viability of different glioblastoma cells (Figure 13). Next, we assessed whether the effects of combining ONC201/TIC10 with 2-DG are synergistic, additive or antagonistic in nature. We combined different concentrations of ONC201/TIC10 with different concentrations of 2-DG to calculate combination indices and plot isobolograms. Our findings show, that the combination of both substances acts in a predominantly synergistic manner to reduce the cellular viability of glioblastoma cells (Figure 14).

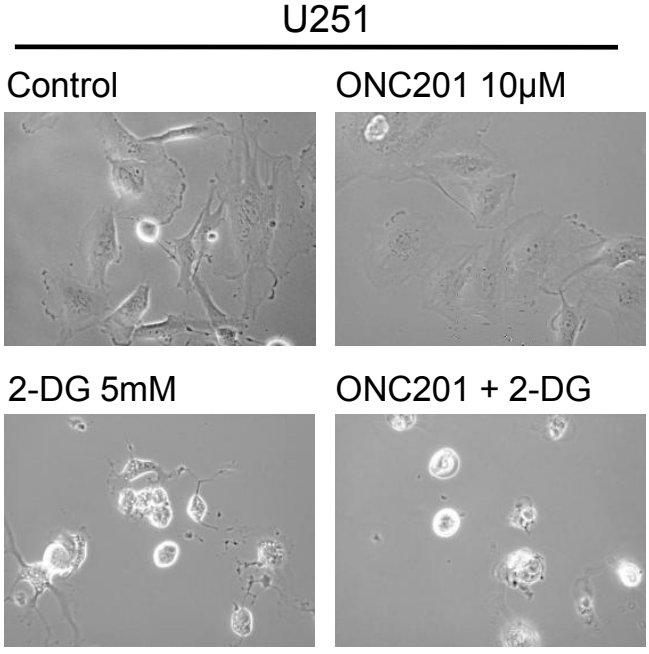

Figure 12: Treatment with ONC201/TIC10 + 2-DG alters the morphology of U251 cells and decreases the cellular density. U251 cells treated for 48 hours as indicated, representative microphotographs with 40x magnification [53] (used according to CC BY 4.0 https://creativecommons.org/licenses/by/4.0/").

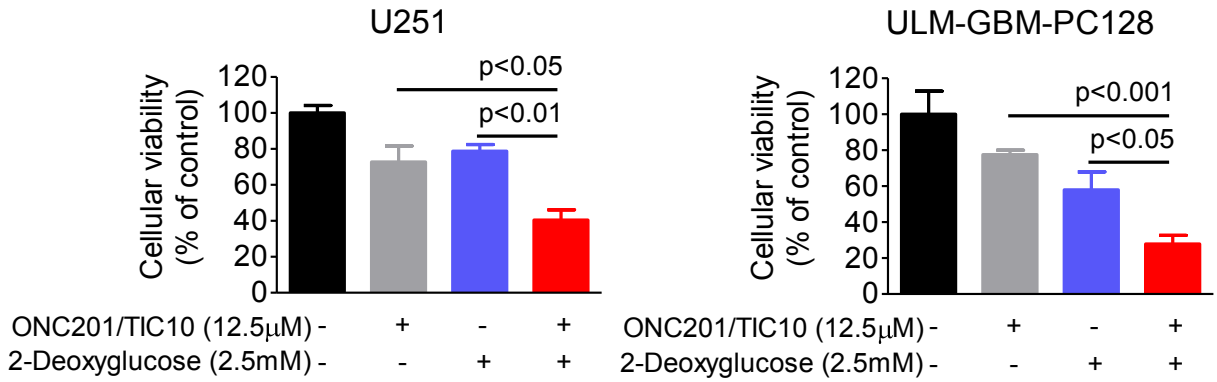

Figure 13: Treatment with the combination of ONC201/TIC10 and 2-DG leads to a significantly increased reduction in cellular viability. U251 and ULM-GBM-PC128 glioblastoma cells were treated for 72 hours as indicated and subsequently examined by MTT assay. Columns, mean; bars, SD; n=4 [53] (used according to CC BY 4.0 https://creativecommons.org/licenses/by/4.0/").

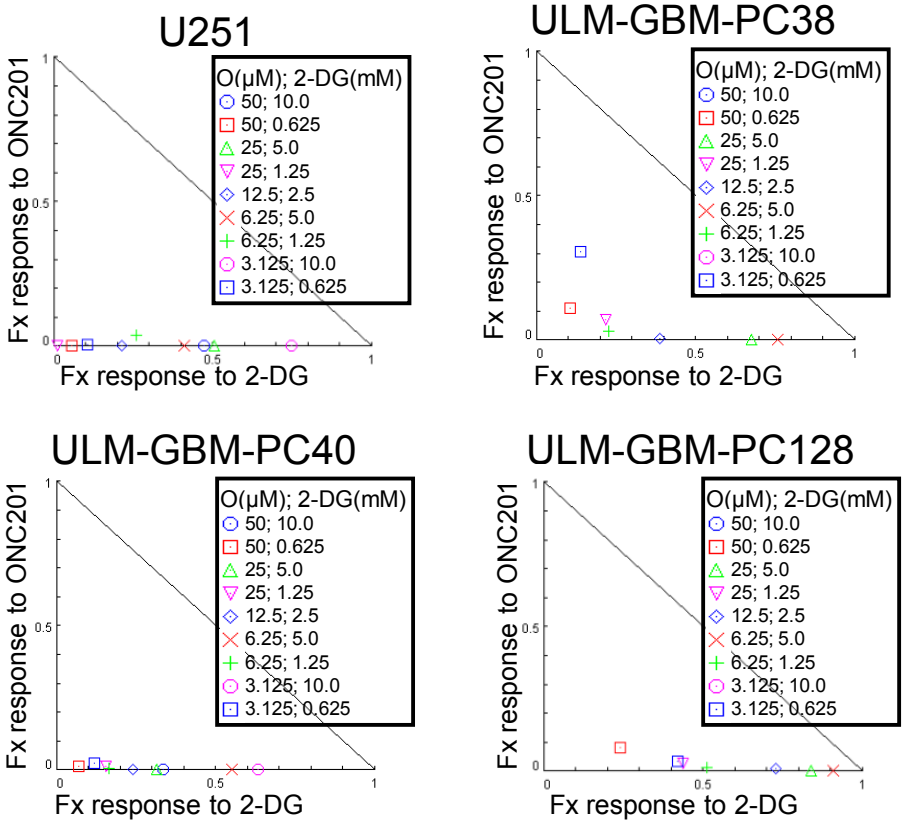

Figure 14: Combined treatment with ONC201/TIC10 and 2-DG has a synergistic drug-drug interaction. Normalized isobolograms were calculated with the data from the cellular viability assays using the CompuSyn software. The line connecting x- and y-axis represents additivity. Data points below the line indicate synergism and data points above the line stand for an antagonistic drug-drug interaction [53] (used according to CC BY 4.0 https://creativecommons.org/licenses/by/4.0/").

3.6 Combined treatment with ONC201/TIC10 and 2-DG leads to an enhanced inhibition of anchorage-independent growth

We next assessed whether the combination treatment yields enhanced inhibition on the colony forming ability. Therefore, we examined the anchorage independent growth in soft agar by treating ULM-GBM-PC128 with ONC201/TIC10 and 2-DG combined, the substances alone and their respective solvents (Figure 15 A). The number of colonies counted after 3 weeks was significantly reduced for the cells treated with the combination treatment when compared to single-agent treatment (Figure 15 B).

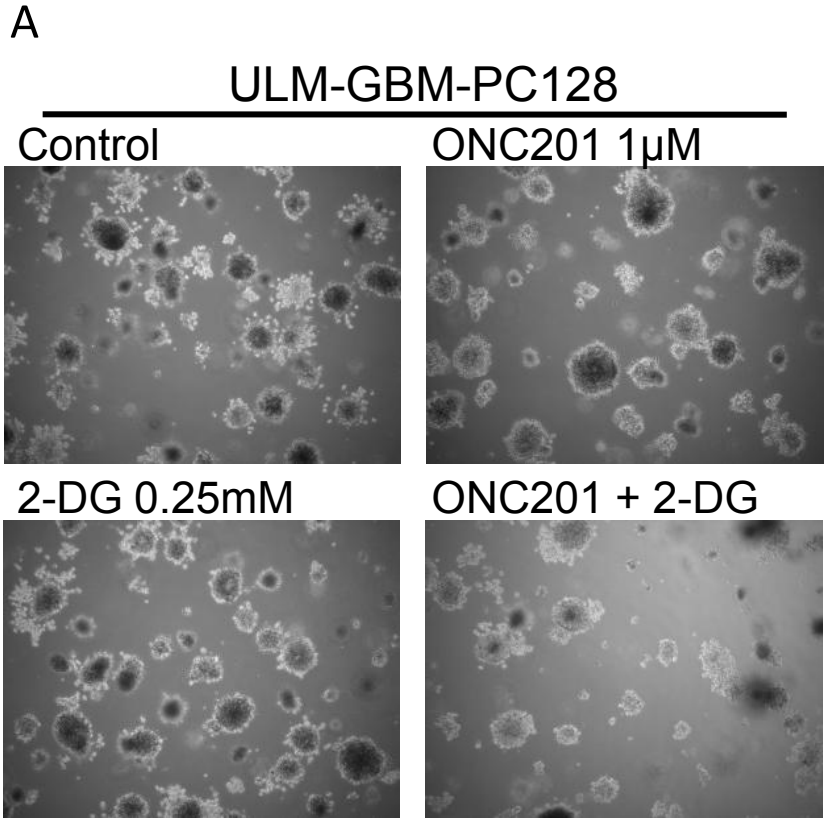

Figure 15 A: Treatment with the combination of ONC201/TIC10 and 2-DG leads to a significantly stronger inhibition of the colony forming ability of ULM-GBM-PC128 glioblastoma cells. A, ULM-GBM-PC128 glioblastoma cells were grown in agarose for 3 weeks and treated as indicated. Representative microphotographs were taken at 4x magnification [53] (used according to CC BY 4.0 https://creativecommons.org/licenses/by/4.0/").

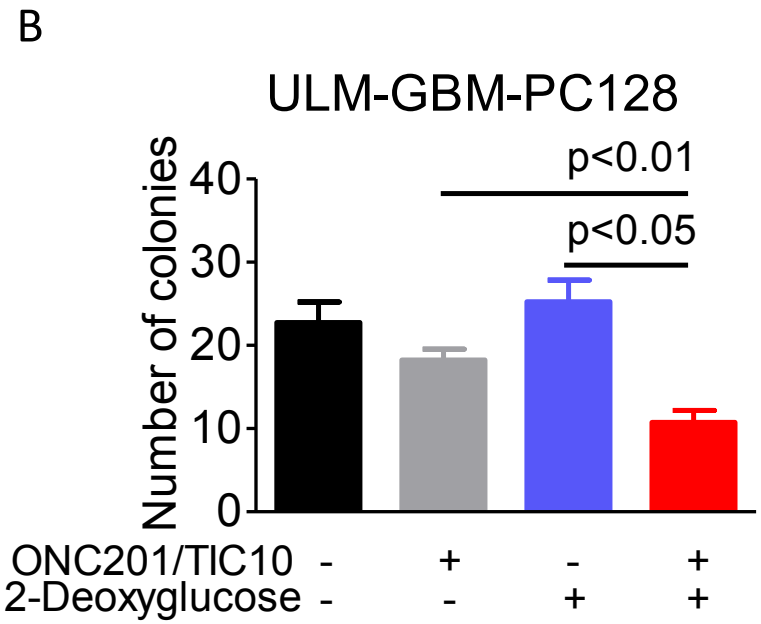

Figure 15 B: Treatment with the combination of ONC201/TIC10 and 2-DG leads to a significantly stronger inhibition of the colony forming ability of ULM-GBM-PC128 glioblastoma cells. B, Quantitative representation of the cells treated as described for A. Colonies were counted only with diameters larger than 200μm. Columns, mean; bars, SD; n=2 [53] (used according to CC BY 4.0 https://creativecommons.org/licenses/by/4.0/").

3.7 The combination treatment leads to suppression of ATP levels

Further, we investigated if the combination treatment effectively leads to an induction of a hypo-energetic state in glioblastoma cells. Thus, we assessed the ATP levels in U251 and ULM-GBM-PC128 cells. Our findings show, that the combination of ONC201/TIC10 and 2-DG leads to a significant reduction in ATP levels in the tested cells when compared to single agent treatment (Figure 16 A and B).

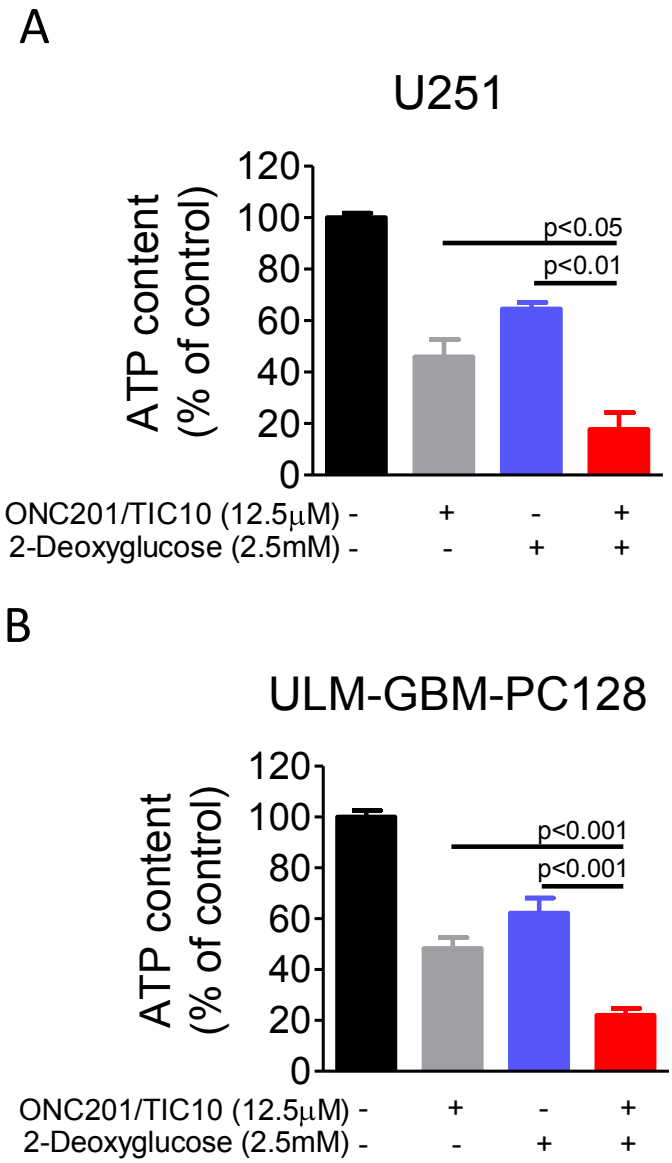

Figure 16 A and B: Treatment with ONC201/TIC10 and 2-DG leads to a state of energy depletion in glioblastoma cells. A-B, U251 (A) and ULM-GBM-PC128 (B) cells were treated as indicated for 72 hours. CellTiter-Glo® assays were performed to measure ATP levels. Columns, mean; bars, SD; n=3 [53] (used according to CC BY 4.0 https://creativecommons.org/licenses/by/4.0/").

3.8 Treatment with ONC201/TIC10 and 2-DG activates AMPK and induces a hypo-phosphorylated state

To analyze how the combination of ONC201/TIC10 and 2-DG acts on the phosphorylation status of major protein kinase signaling pathways, we performed a phospho-kinase array. Our data show, that the combination treatment leads to a marked hyper-phosphorylation of pAMPK α1, a key regulator of metabolic enzymes that is activated in energy deprived cells. This is evident after a treatment for 24 hours in ULM-GBM-PC128 cells, which after 48 hours returns to phosphorylation levels comparable to the control group (Figure 17 A, B and C). In contrast, the majority of the other signaling pathways were hypo-phosphorylated at 24 and 48 hours of treatment, including mTOR, a major regulator of protein synthesis, and the important receptor tyrosine kinases EGFR and PDGFR-β (Figure 17 A, B and C).

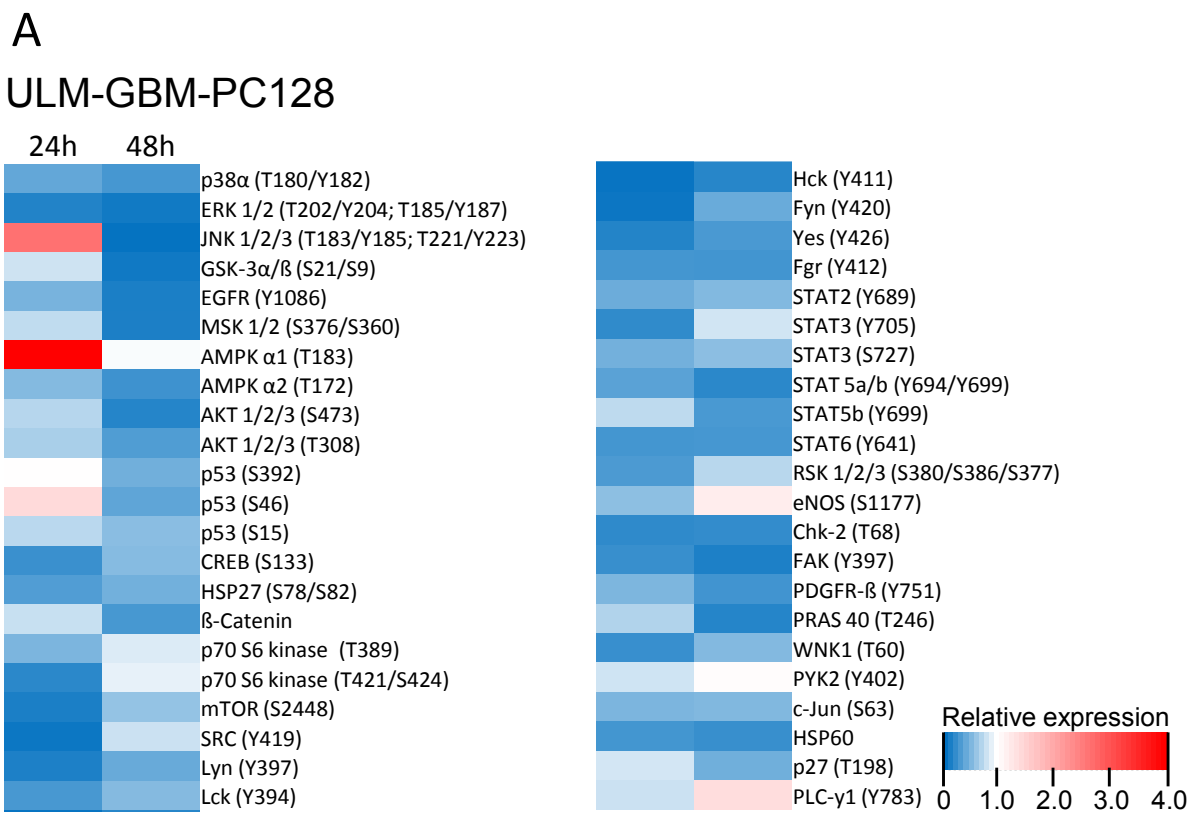

Figure 17 A: Treatment with ONC201/TIC10 and 2-DG causes a hypo-phosphorylated state. A, ULM-GBM-PC128 glioblastoma cells were treated with 10μM ONC201/TIC10 and 1.25mM 2-DG or respective solvents for 24 or 48 hours prior to the collection of the cell lysates. Incubation of the membranes with the lysates and detection of the bound phospho-proteins was performed according to the manufacturer's instructions. Each membrane contains reference spots in duplicate, that contain kinase-specific antibodies. A template to identify the coordinate of each phospho-protein on the membrane is available on the R&D System's website (http://www.rndsystems.com/pdf/ARY003b.pdf). For quantitative analysis the Bio-1D software was used and the data was firstly normalized to the respective reference spot (loading control) and secondly to the respective treatment control group. The relative phospho-kinase expression (treatment with ONC201/TIC10 and 2-DG relative to control group) is displayed in a heatmap [53] (used according to CC BY 4.0 https://creativecommons.org/licenses/by/4.0/").

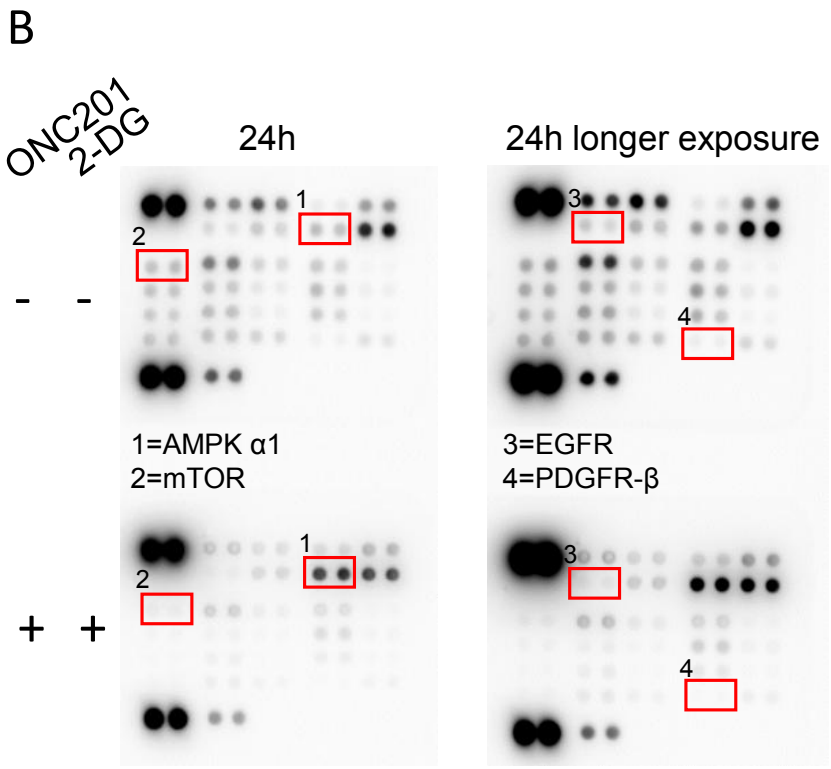

Figure 17 B: Treatment with ONC201/TIC10 and 2-DG causes a hypo-phosphorylated state. A, ULM-GBM-PC128 glioblastoma cells were treated with 10μM ONC201/TIC10 and 1.25mM 2-DG or respective solvents for 24 or 48 hours prior to the collection of the cell lysates. Incubation of the membranes with the lysates and detection of the bound phospho-proteins was performed according to the manufacturer's instructions. Each membrane contains reference spots in duplicate, that contain kinase-specific antibodies. A template to identify the coordinate of each phospho-protein on the membrane is available on the R&D System's website (http://www.rndsystems.com/pdf/ARY003b.pdf). B, Representative autoradiography of the phospho-kinase array utilized in (A) after 5 minutes and 10 minutes exposure time [53] (used according to CC BY 4.0 https://creativecommons.org/licenses/by/4.0/").

C

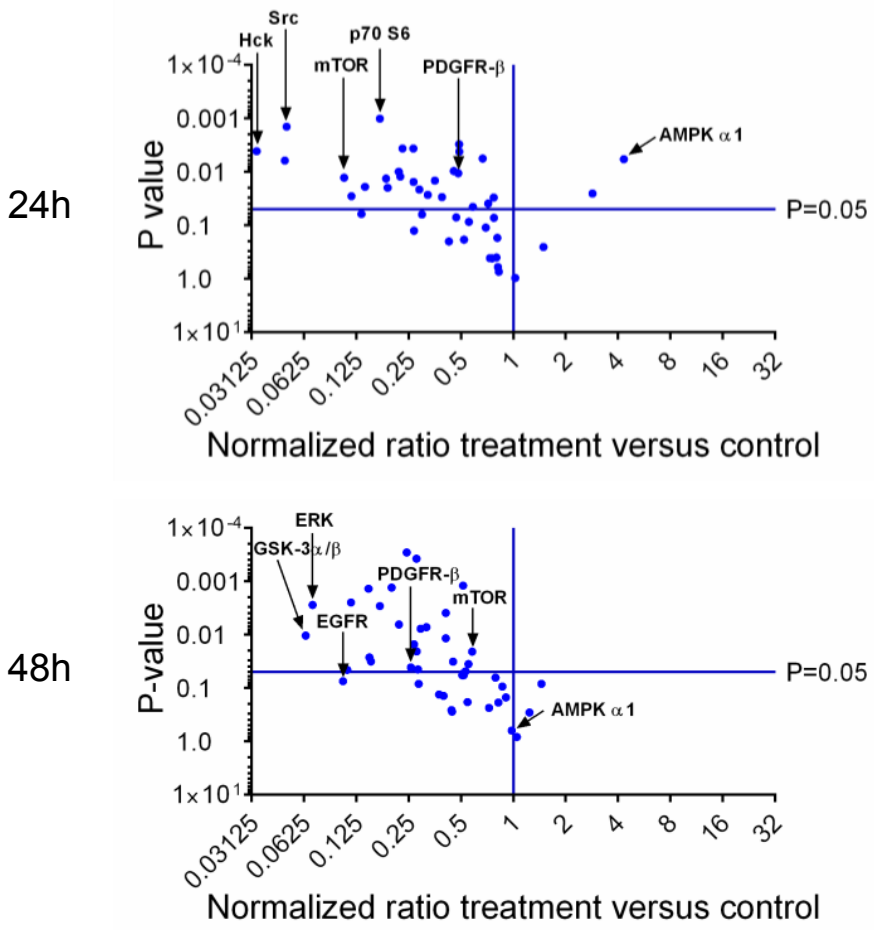

Figure 17 C: Treatment with ONC201/TIC10 and 2-DG causes a hypo-phosphorylated state. A, ULM-GBM-PC128 glioblastoma cells were treated with 10μM ONC201/TIC10 and 1.25mM 2-DG or respective solvents for 24 or 48 hours prior to the collection of the cell lysates. Incubation of the membranes with the lysates and detection of the bound phospho-proteins was performed according to the manufacturer's instructions. Each membrane contains reference spots in duplicate, that contain kinase-specific antibodies. A template to identify the coordinate of each phospho-protein on the membrane is available on the R&D System's website (http://www.rndsystems.com/pdf/ARY003b.pdf). C, Volcano plots to compare Log2 fold changes of phosphorylation status for combination treatment versus control at 24 hours and 48 hours of treatment [53] (used according to CC BY 4.0 https://creativecommons.org/licenses/by/4.0/").

3.9 The combination treatment induces cytostasis in glioblastoma cells

Next, we investigated how the combination of ONC201/TIC10 and 2-DG reduces the cellular viability of glioblastoma cells. For this purpose, we stained the cells for Propidium iodide and performed flow cytometric analysis, to analyze whether cell death is induced. Our findings show, that both the primary cultured and the established cell lines did not show enhanced DNA fragmentation (Figure 18 A and B). Furthermore, Western blot analyses did not reveal enhanced cleavage of caspase 3 and 9 following the treatment with ONC201/TIC10 and 2-DG with different concentrations (Figure 19 A and B). Thus, we next checked whether the combination treatment induces cytostasis. CFSE staining followed by flow cytometric analysis has shown that an increased fraction of the cells with a stronger CFSE signal, which was more pronounced in ULM-GBM-PC128 than in U251 cells, was present after treatment for 96 hours, indicating that those cells have a prolonged cell cycle (Figure 20 A and B). However, when performing cell cycle analysis through staining for Propidium iodide prior to flow cytometric analysis of ULM-GBM-PC38 and ULM-GBM-PC128 treated for 24, 48 and 72 hours, we did not observe a significant cell cycle arrest (Figure 21).

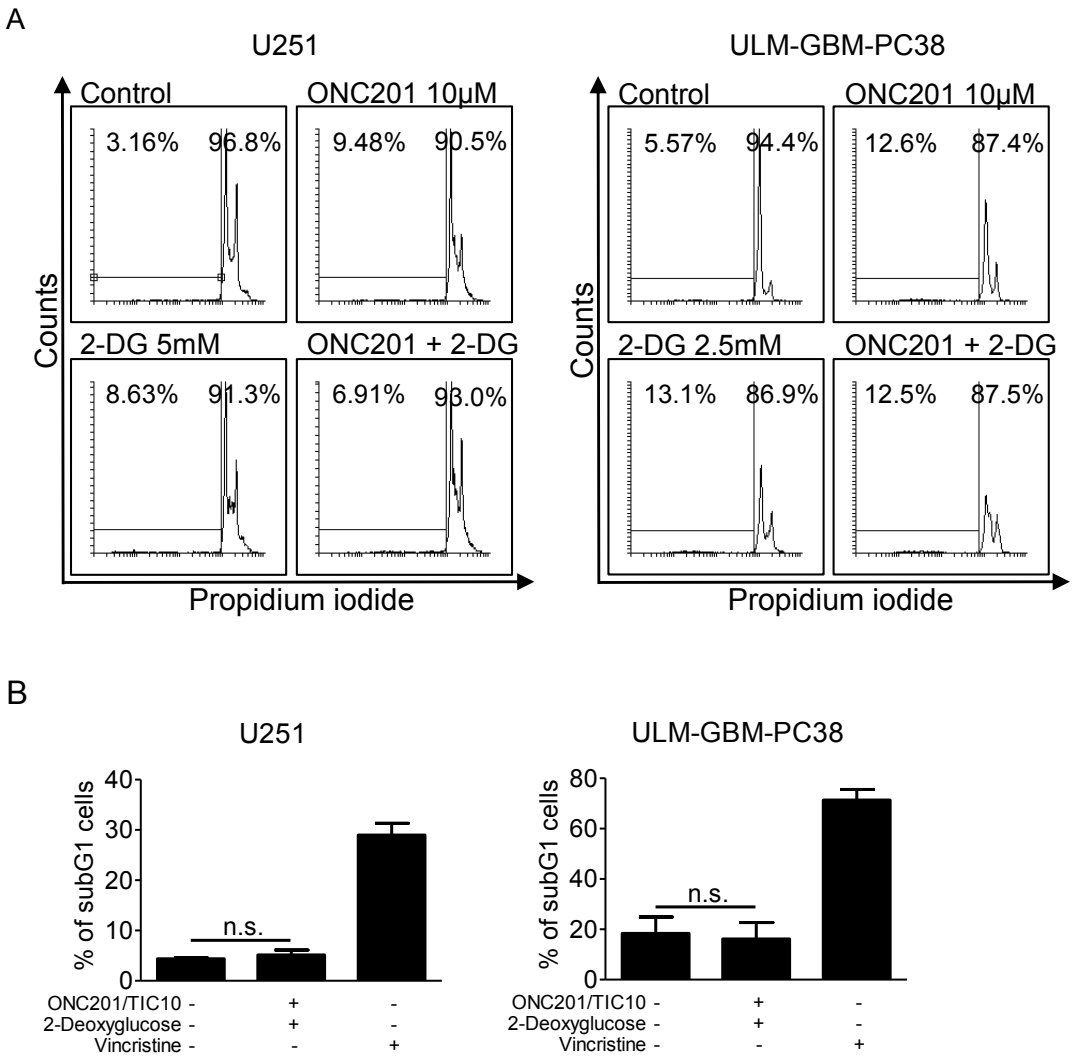

Figure 18 A and B: Combined treatment with ONC201/TIC10 and 2-DG does not cause increased DNA-fragmentation. A, U251 and ULM-GBM-PC38 cells were treated as indicated for 48 hours. Staining for Propidium iodide was performed before flow cytometric analysis. Representative histograms are shown. B, Quantitative analysis of the subG1 fraction for the experimental setting described in (A). Cells stimulated with 50nM vincristine served as a positive control for increased DNA-fragmentation. Columns, mean; bars, SEM; n=3 [53] (used according to CC BY 4.0 https://creativecommons.org/licenses/by/4.0/").

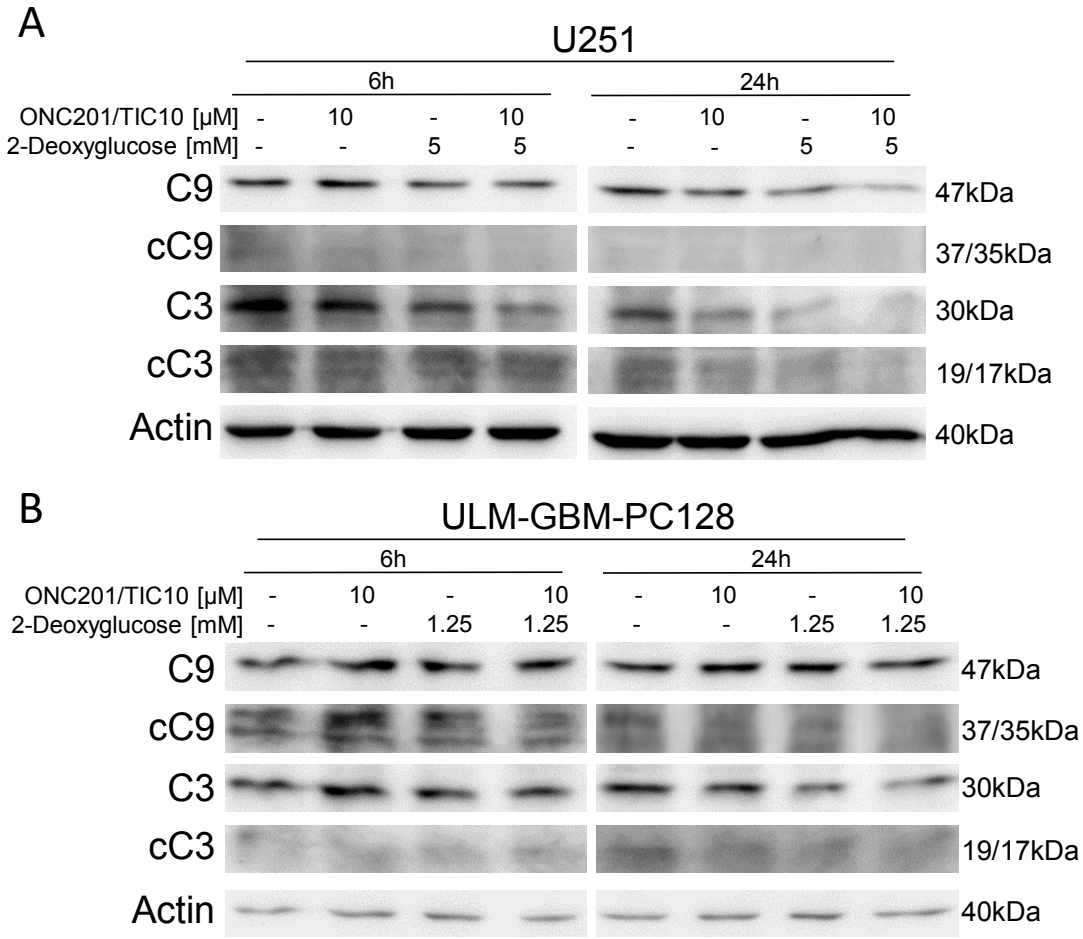

Figure 19 A and B: Treatment with ONC201/TIC10 and 2-DG does not lead to cleavage of caspase 3 or 9. A-B, U251 (A) and ULM-GBM-PC128 (B) glioblastoma cells were treated as indicated. Western blot analysis was performed for Caspase-9 (C9), cleaved Caspase-9 (cC9), Caspase-3 (C3) and cleaved Caspase-3 (cC3). Actin was used as a loading control [53] (used according to CC BY 4.0 https://creativecommons.org/licenses/by/4.0/").

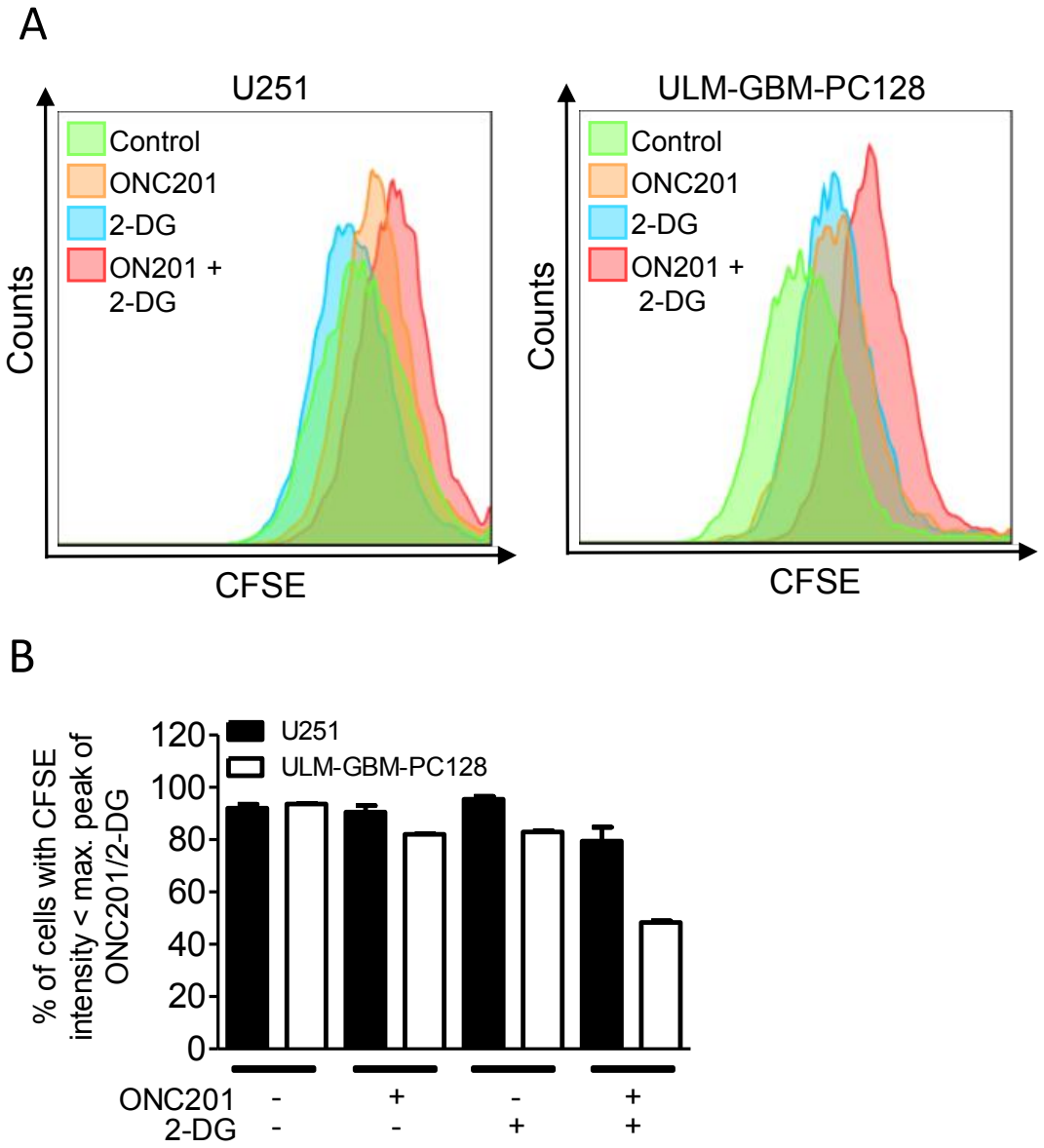

Figure 20 A and B: Treatment with ONC201/TIC10 and 2-DG prolongs cell cycle progression. A, U251 and ULM-GBM-PC128 cells were labeled with CFSE before treatment with 10μM ONC201/TIC10 and 5mM 2-DG for U251 or 1.25mM 2-DG for ULM-GBM-PC128 cells or solvent. Flow cytometric analysis was performed after 96 hours of treatment. Representative histograms are shown. B, Quantitative analysis of cells treated as described in (A). Columns, mean; bars, SD [53] (used according to CC BY 4.0 https://creativecommons.org/licenses/by/4.0/").

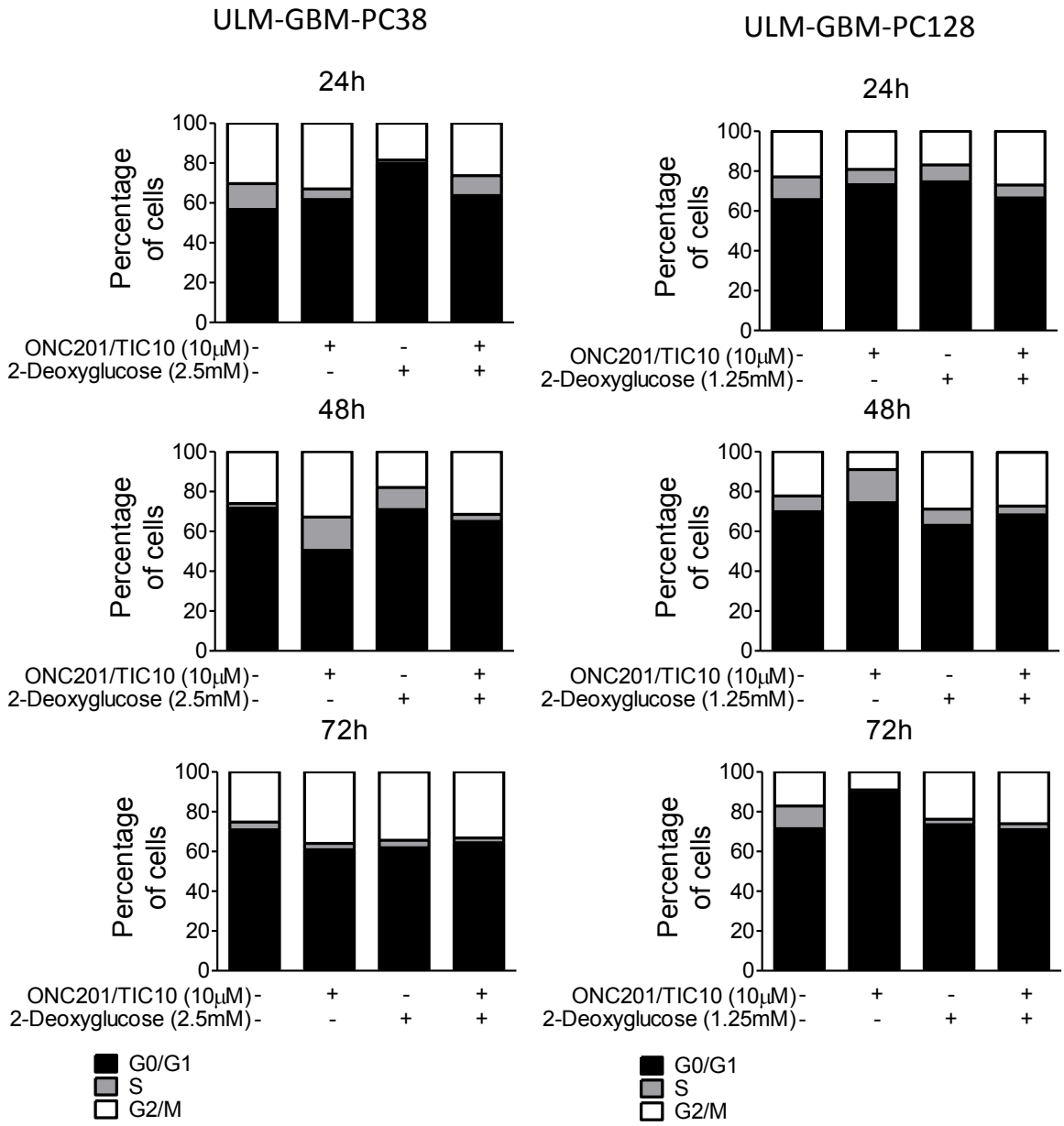

Figure 21: Combined treatment with ONC201/TIC10 and 2-DG does not induce significant cell cycle arrest. ULM-GBM-PC38 and ULM-GBM-PC128 were treated as indicated for 24, 48 or 72 hours. Propidium iodide staining was performed prior to flow cytometric analysis and subsequent cell cycle analysis. Graphs are representative for 3 independent experiments [53] (used according to CC BY 4.0 https://creativecommons.org/licenses/by/4.0/").

3.10 Combined treatment with ONC201/TIC10 and 2-DG has marked anti-migratory effects on glioblastoma cells

Glioblastoma cells are of highly migratory nature contributing to the therapeutic resistance encountered in this disease. Thus, we examined whether the combination treatment inhibits the migratory capacity of glioblastoma cells. To assess the effect of the treatment on the random cellular movement, we performed time-lapse live cell microscopy with single-cell tracking. Our findings show, that the treatment with both compounds solitarily has no significant effect on cellular migration, whereas the combination of ONC201/TIC10 with 2-DG strongly inhibited migratory capacity of the tested cells (Figure 22 A, B and C).

Next, we assessed whether the combination therapy affects the directed movement of glioblastoma cells by performing a scratch assay. The U251 established glioblastoma cell line showed a significantly reduced directed migratory capacity after 18 and 24 hours of stimulation when treated with the combination therapy compared to the control or single compound treatment (Figure 23 A and B). While subjected to the treatment the cells did not show morphological changes, that may indicate the beginning of cell death. Furthermore, we addressed the question whether the combination of ONC201/TIC10 and 2-DG also reduces the migratory capacity across a collagen-coated porous membrane along a chemoattractant gradient. Our data showed, that U251, ULM-GBM-PC38 and ULM-GBM-PC128 cells all had a clearly reduced transmigratory activity following the combination treatment compared to single compounds and control (Figure 24 A-F).

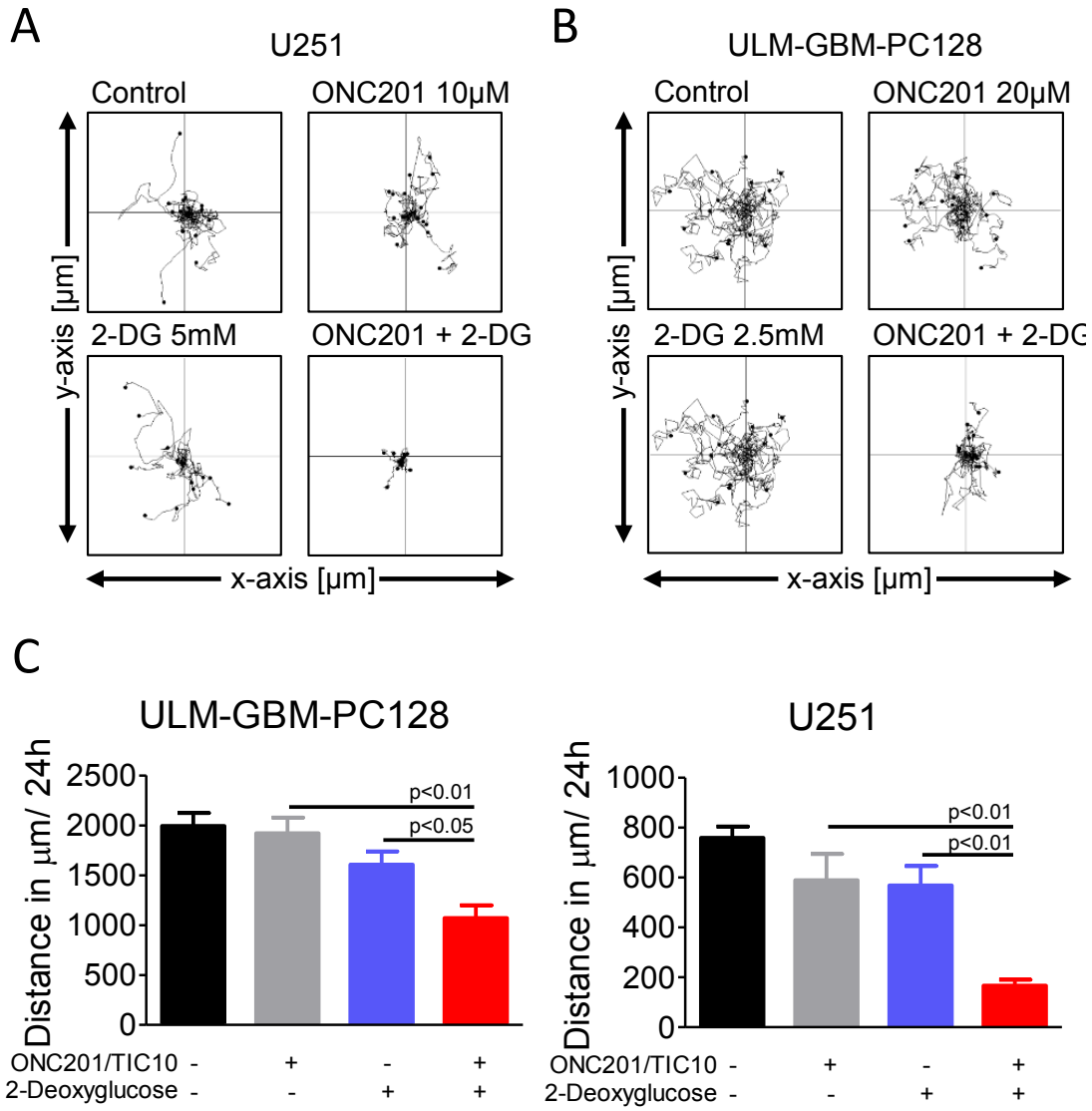

Figure 22 A, B and C: Combined treatment with ONC201/TIC10 and 2-DG had enhanced anti-migratory activity and reduced random cellular movement. A-B, U251 (A) and ULM-GBM-PC128 (B) glioblastoma cells were seeded on 24-well plates and were treated as indicated followed by consecutive microscopic imaging (10x magnification) over a period of 24 hours. Single- cell tracking was done with the MtrackJ software. The paths of 15 single cells during those 24 hours are shown in wind-rose plots. The tracks were aligned to have the same starting position to have comparative illustrations. C, the total movement of 45 cells was evaluated within the tracked 24 hours per treatment condition. Columns, mean; bars, SD; n=3 [53] (used according to CC BY 4.0 https://creativecommons.org/licenses/by/4.0/").

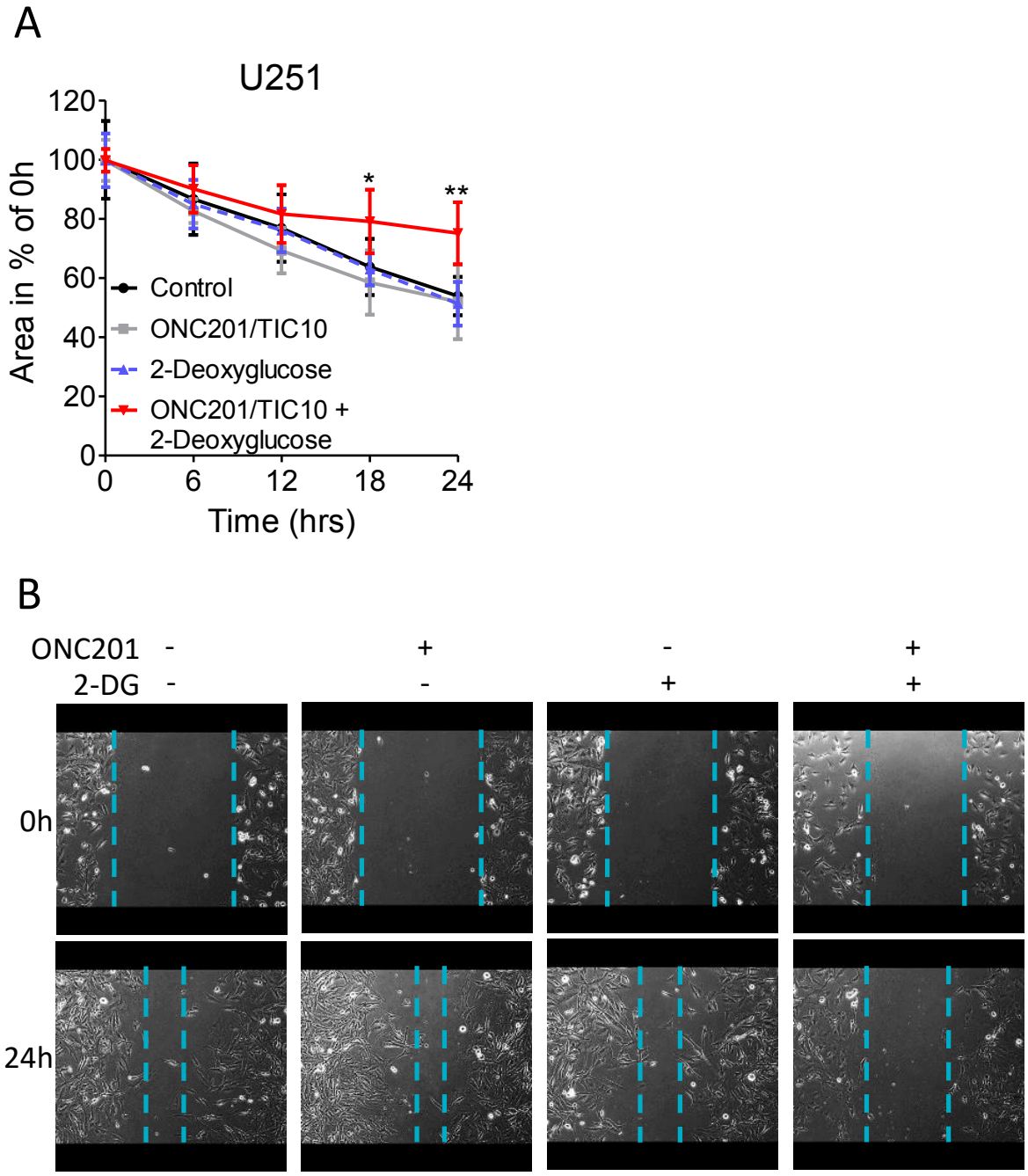

Figure 23 A and B: The combination treatment with ONC201/TIC10 has an anti-migratory effect on directed movement in scratch wound-healing assays. U251 cells were seeded as a subconfluent monolayer and were scratched prior to treatment with the solvent, ONC201/TIC10 (10µM), 2-DG (5mM) or the combination of both substances. Microscopic images were taken at the indicated time points after performing the scratch. A, Data are presented as mean and SD. One-way ANOVA followed by Tukey's post hoc test was performed to assess statistical significance. B, representative pictures at the indicated time points are shown [53] (used according to CC BY 4.0 https://creativecommons.org/licenses/by/4.0/").

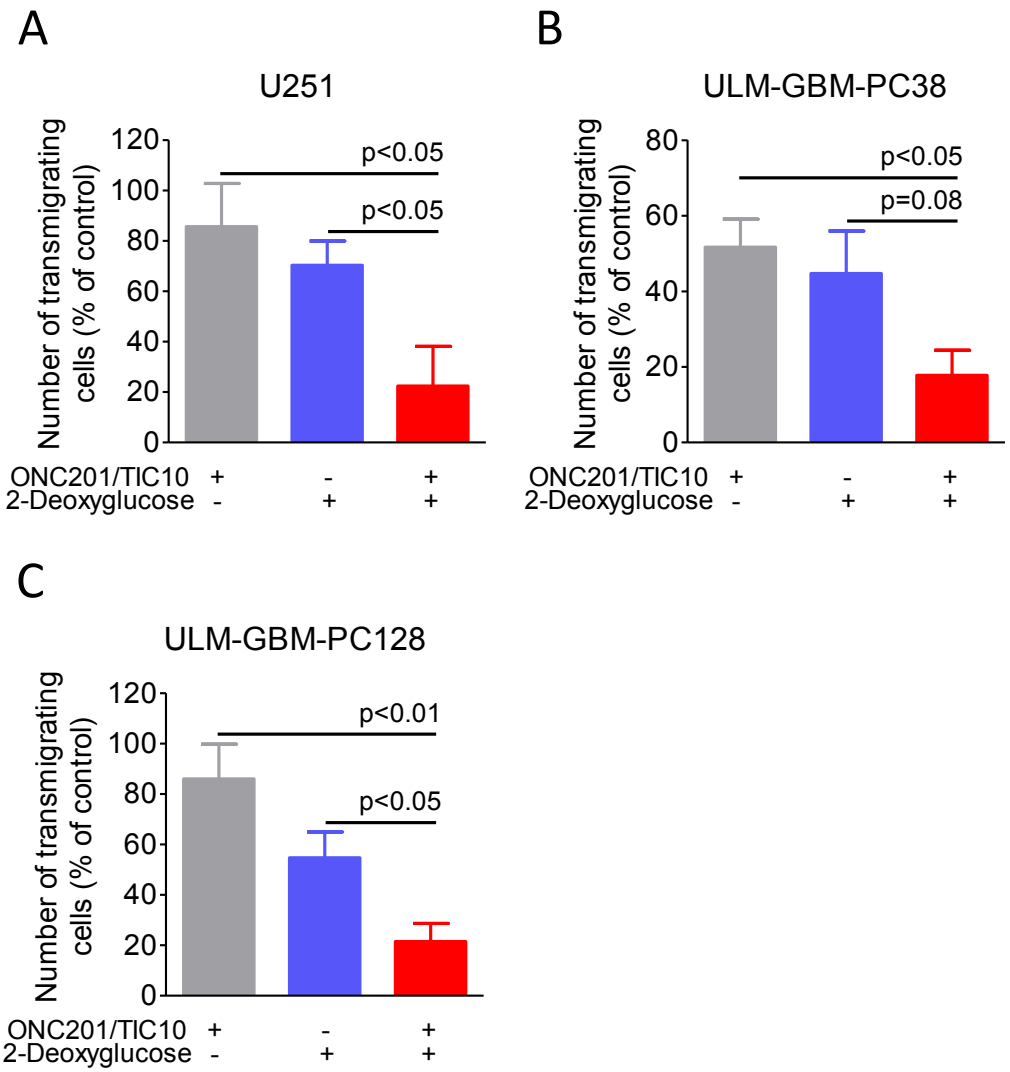

Figure 24 A – C: Combined treatment of ONC201/TIC10 and 2-DG leads to a marked reduction of the trans migratory capacity along a chemoattractant gradient. A-F, U251 (A/D), ULM-GBM-PC38 (B/E) and ULM-GBM-PC128 (C/F) were seeded onto transwell® membranes in culture medium containing 1.5% FBS and were subsequently treated with solvent, ONC201/TIC10 (10μM), 2-DG (5mM) or the combination of both substances. Culture medium containing 10-20% FBS and the corresponding treatments served as a chemoattractant. After a duration of 24 hours, the upper side of the membrane was wiped, and the lower side of the membrane was stained with DAPI. Columns, mean; bars, SD; n=4 [53] (used according to CC BY 4.0 https://creativecommons.org/licenses/by/4.0/").

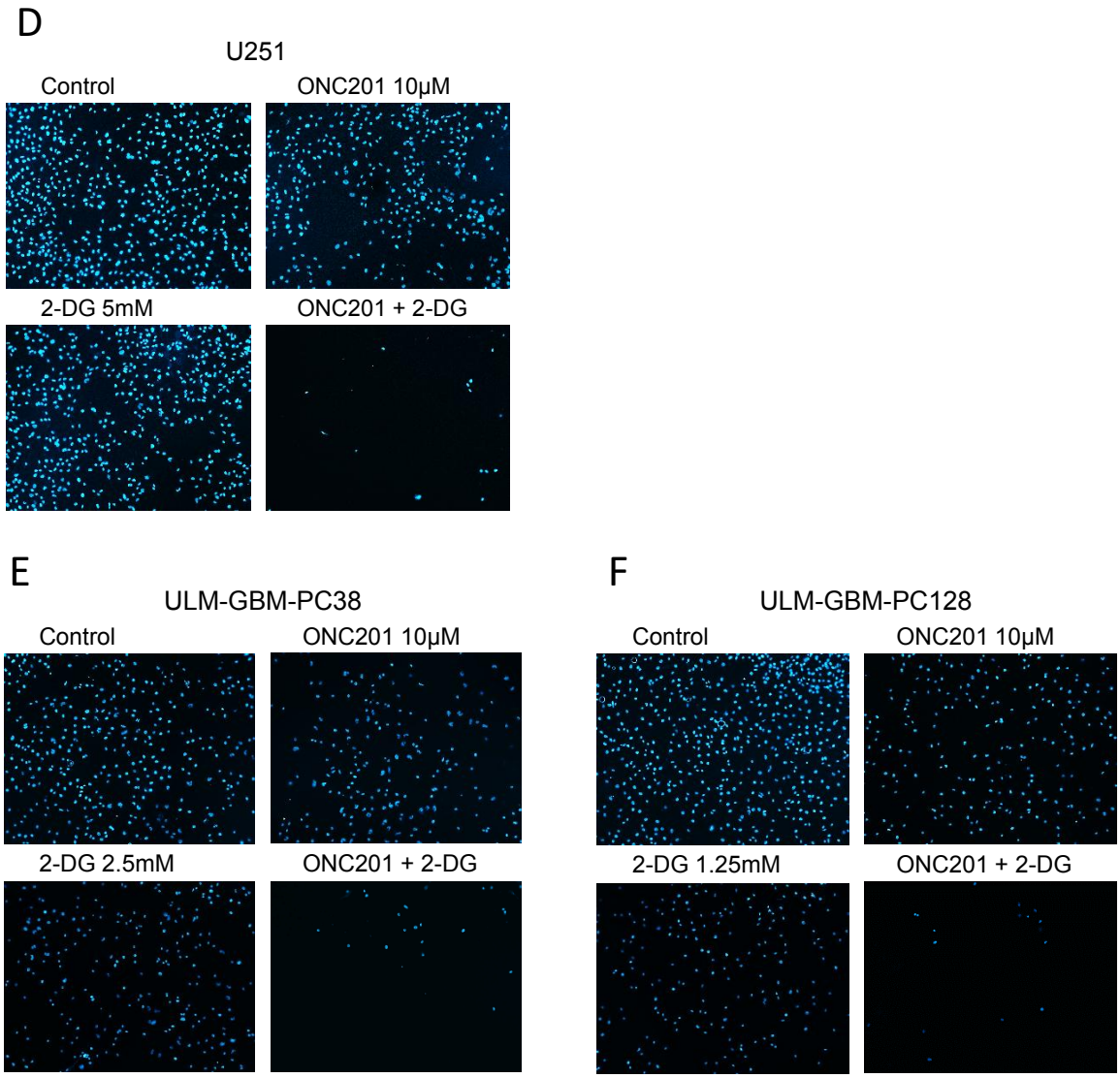

Figure 24 D – F: Combined treatment of ONC201/TIC10 and 2-DG leads to a marked reduction of the trans migratory capacity along a chemoattractant gradient. A-F, U251 (A/D), ULM-GBM-PC38 (B/E) and ULM-GBM-PC128 (C/F) were seeded onto transwell® membranes in culture medium containing 1.5% FBS and were subsequently treated with solvent, ONC201/TIC10 (10µM), 2-DG (5mM) or the combination of both substances. Culture medium containing 10-20% FBS and the corresponding treatments served as a chemoattractant. After a duration of 24 hours, the upper side of the membrane was wiped, and the lower side of the membrane was stained with DAPI. D-F, images of a representative part of the membrane were taken at 10x magnification and transmigrated cells were counted [53] (used according to CC BY 4.0 https://creativecommons.org/licenses/by/4.0/").

3.11 Combined treatment with ONC201/TIC10 and 2-DG leads to an inhibition of tumor growth on the chorion allantoic membrane

To approximate the effects of the combination therapy to an *in vivo* setting, we used the CAM assay as an "in vivo-near" setup to assess the three-dimensional tumor growth of U251 and ULM-GBM-PC128 cells following treatment. For this purpose, the glioblastoma cells were seeded onto the CAM of fertilized chicken eggs and were treated, starting 24 hours later, twice per day for three days with ONC201/TIC10, 2-DG, both substances combined or the solvents. Our data show, that the combination therapy induced a significant reduction in tumor size for both, U251 and ULM-GBM-PC128 tumor models (Figure 25 A-F). Furthermore, the combination of the substances led to a reduced cellularity compared to the singular treatment and control (Figure 25 B). Moreover, singular treatment with 2-DG seemed to increase the vascular supply of the tumor, whereas the addition of ONC201/TIC10 led to a negation of this result (Figure 25 C and D). Interestingly, treatment with 2-DG only led to an increased three-dimensional tumor growth compared to the control group (Figure 25 E and F).

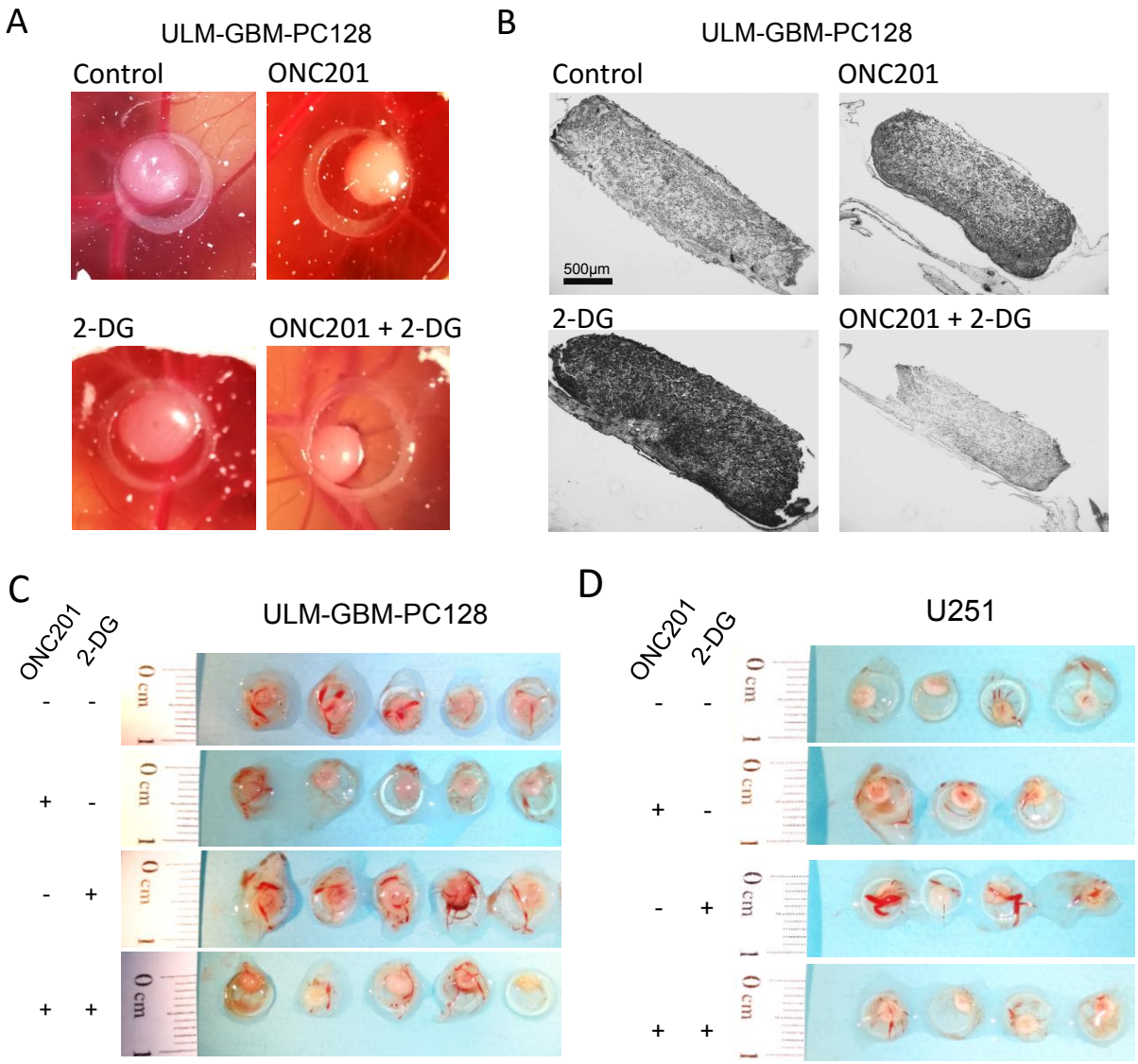

Figure 25 A – D: Combined treatment with ONC201/TIC10 inhibits three-dimensional tumor growth on the CAM. A-F, 1x10^6 ULM-GBM-PC128 cells or 2x10^6 U251 cells were seeded onto each CAM. 24 hours later, cells were treated with ONC201/TIC10 (50µM), 2-DG (25mM), both compounds or the solvents twice per day for three days. On day 5, the tumors were extracted, and photographs were taken before fixation with 10% formalin and subsequent histological processing. A, Representative photographs on day 5 of ULM-GBM-PC128 tumors. The ring has a diameter of 5mm. B, Representative histological images of ULM-GBM-PC128 tumors stained with hematoxylin and eosin at 4-fold magnification (scale bar = 500µm). C-D, Photographs of the extracted tumors, which were treated as indicated. Three to five replicates are shown [53] (used according to CC BY 4.0 https://creativecommons.org/licenses/by/4.0/").

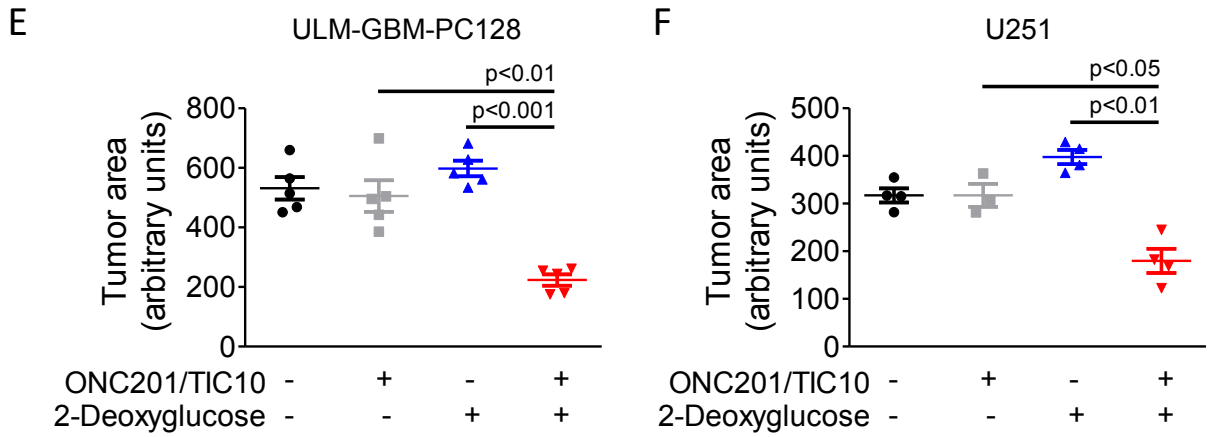

Figure 25 E – F: Combined treatment with ONC201/TIC10 inhibits three-dimensional tumor growth on the CAM. A-F, 1x10^6 ULM-GBM-PC128 cells or 2x10^6 U251 cells were seeded onto each CAM. 24 hours later, cells were treated with ONC201/TIC10 (50µM), 2-DG (25mM), both compounds or the solvents twice per day for three days. On day 5, the tumors were extracted, and photographs were taken before fixation with 10% formalin and subsequent histological processing. E-F, Quantitative analysis of the tumor area assessed with the ImageJ software. Data are presented as mean of at least three tumors for each treatment group with SD [53] (used according to CC BY 4.0 https://creativecommons.org/licenses/by/4.0/").

3.12 The combination treatment with ONC201/TIC10 and 2-DG has a low toxicity in normal human cells and shows no organ toxicity in chicken embryos

Finally, we investigated the toxicity profile of both compounds used together. We assessed the side effects for non-pathological human cells by testing the effect of the combined treatment with ONC201/TIC10 and 2-DG on fibroblasts, primary-astrocyte-enriched brain cells and mesenchymal stem cells. Our data show, that the combination therapy did affect the cellular viability of all cells to some extent, nevertheless those effects were notably weaker compared to the ones evident in glioblastoma cells. Interestingly, the effect of the combination was not significantly stronger compared to the single-compound treatment on the non-pathological cells (Figure 26 A-C). Furthermore, we examined if the combination therapy shows effects of hematotoxicity or organ toxicity in chicken embryos. Our

results show, that the combination therapy of ONC201/TIC10 with 2-DG did not affect leucocyte or erythrocyte counts in a significant manner (Figure 26 D-E). In addition, at microscopic inspection of the blood cell morphology, no notable differences were seen between the treated and untreated group (Figure 26 F). Lastly, when analyzing tissue samples form heart, lung, liver, kidney and spleen histologically, no enhanced injury was observed with the combination therapy of ONC201/TIC10 and 2-DG in comparison to the control groups (Figure 26 G).

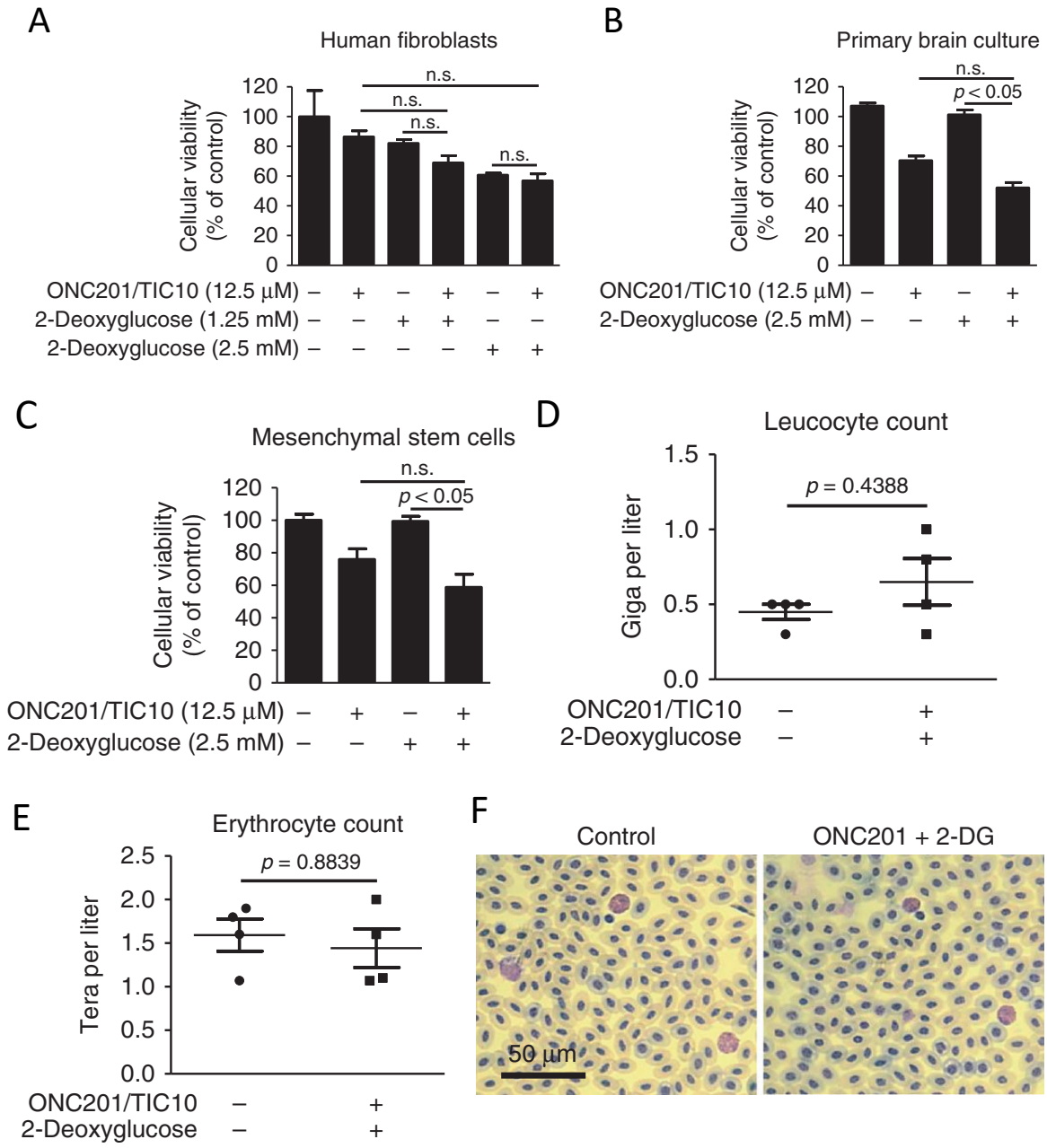

Figure 26 A-F: Combination therapy with ONC201/TIC10 and 2-DG does not show increased toxicity in healthy human cells or chicken embryos. A-C, Human fibroblasts (A), primary astrocyte-enriched brain cells (B) and mesenchymal stem cells (C) were treated with ONC201/TIC10, 2-DG, the combination of both substances or the solvents with indicated concentrations. 72 hours later, MTT assays were performed. Columns, mean; bars, SD; n=3. For statistical analysis one-way ANOVA followed by Newman-Keuls post hoc test were used. D-E, Five-day-old chicken embryos were subjected to treatment twice per day, five days a week for 11 days topically with 15µl of 50µM ONC201/TIC10 and 25mM 2-DG or the solvents. Afterwards blood samples were collected for analysis of leucocyte (D) and erythrocyte (E) counts. Data are shown as mean and SEM. n=4. F, Representative microscopic images at 40-fold magnification of blood smears derived from the chicken embryos described in D and E are shown [53] (used according to CC BY 4.0 https://creativecommons.org/licenses/by/4.0/").

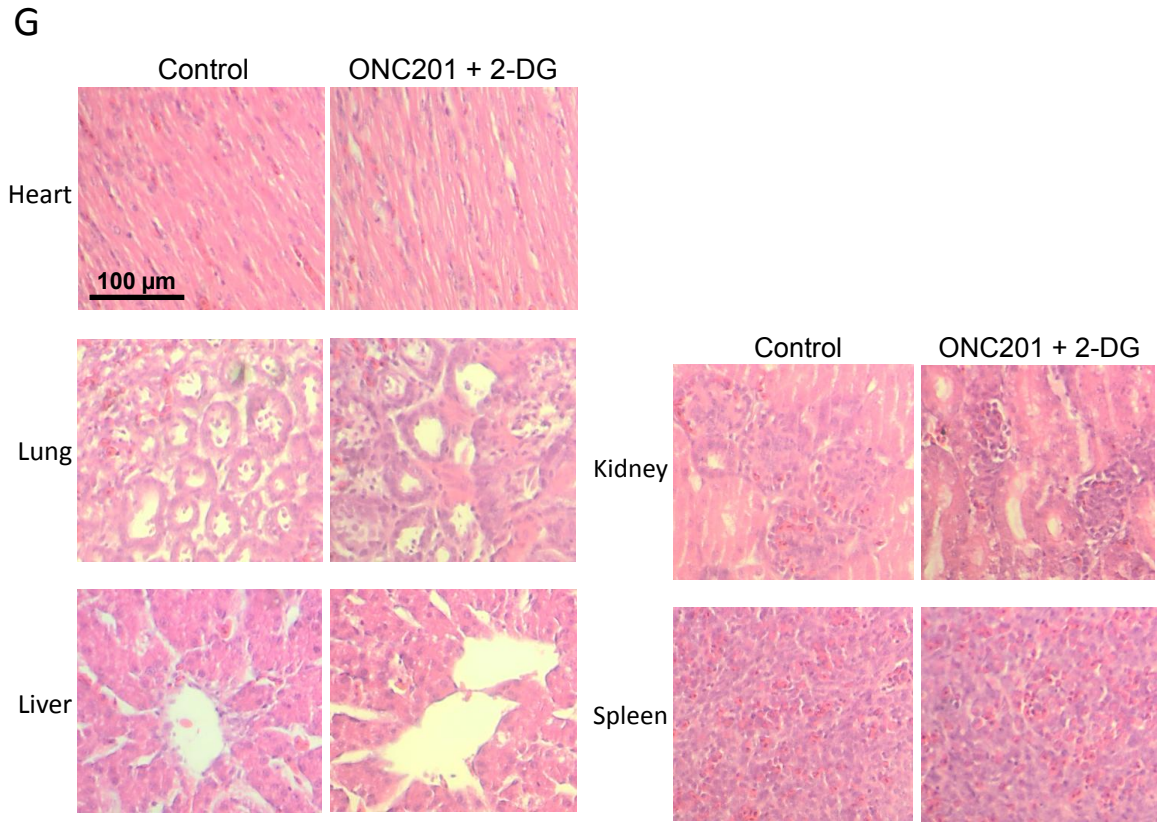

Figure 26 G: Combination therapy with ONC201/TIC10 and 2-DG does not show increased toxicity in healthy human cells or chicken embryos. Five-day-old chicken embryos were subjected to treatment twice per day, five days a week for 11 days topically with 15µl of 50µM ONC201/TIC10 and 25mM 2-DG or the solvents. G, Representative microphotographs of histological analysis of indicated organs taken from chicken embryos treated as described, stained with hematoxylin and eosin [53] (used according to CC BY 4.0 https://creativecommons.org/licenses/by/4.0/").

4. Discussion

When Otto Warburg first observed the occurrence of aerobic glycolysis in cancer in 1927, he described that cancer cells will utilize the pathway of glycolysis, in disregard of the abundance of oxygen, instead of the more energetically preferential mitochondrial oxidative phosphorylation [75]. Pavlova and Thompson then favorized the hypothesis of proliferating cancer cells using the Warburg effect to generate metabolic intermediates for biosynthetic processes and reducing equivalents to maintain those high glycolytic rates, whereas quiescent subpopulations utilize primarily the mitochondrial respiration to synthesize an increased amount of ATP. This flexible metabolism, that is adapted to the different needs of the heterogenous cancer cell populations, was therefore highlighted as one possible cause of the common therapeutic resistance of multiple malignancies [49].

In this study, we have shown that treatment with the imipridone compound ONC201/TIC10 resulted in a significant reduction of oxidative phosphorylation, that led to a compensatory increase in glycolytic activity revealing a potential target of further inhibition. We took advantage of this vulnerability by adding 2-DG which induced a state of energy deprivation and has shown synergistic anti-cancer activity overall.

Ishida and colleagues however have shown in a previous study, that a treatment with imipridones alone already induced a reduction of both mitochondrial respiration and glycolysis [25]. Whereas in this study we showed an upregulation of the glycolytic rate following the treatment with just ONC201/TIC10, supposedly in a compensatory manner. The reason for those contradicting results is probably the heterogeneity of the different glioblastoma cellular systems used, further advocating the importance of combination therapies to target multiple metabolic pathways of cancer cells and therefore closing down possible escape pathways of cancer. In our study, we showed that a concomitant inhibition of the oxidative phosphorylation and glycolysis by treatment with ONC201/TIC10 and 2-DG led to a synergistic reduction of the cellular viability of tested established and primary-

cultured glioblastoma cell lines. Kim and colleagues have shown that targeting OXPHOS and glycolysis in glioblastoma cells with a combination of 2-DG and the antidiabetic drug metformin effectively decreased the stemness and invasive capacity of glioblastoma tumor spheres in both an *in vitro* and *in vivo* setting [33]. The biological effects described in their study were linked to significantly reduced ATP levels and a downregulation of stemness-related genes and proteins such as CD133, Sox-2 and Notch2 to different degrees. Although we haven't investigated the effect of a combined treatment with ONC201/TIC10 and 2-DG on stemness-related markers, it would be interesting to investigate whether the energy depletion resulting from the combination therapy has a similar effect. This hypothesis is supported by a previous study reported by Prabhu and colleagues. In this study, ONC201/TIC10 was shown to target both, cancer stem cells (CSC) that were resistant to the standard chemotherapy and non-CSCs in colorectal cancer. Hereby their data show that the treatment with ONC201/TIC10 led to a suppression of multiple markers of CSCs in *in vitro* and *in vivo* models. These effects were described to be in a Foxo3a and TRAIL-dependent manner [51]. In addition, Prabhu and colleagues have described in another study that ONC201/TIC10 affected the cancer cell stemness at the transcription level at time points that preceded cell death. Further analyses have shown that the CSC gene expression profiles targeted by ONC201/TIC10 in colorectal cancer cells are also genes involved in prostate cancer and glioblastoma. This finding was confirmed by testing the effect of ONC201/TIC10 on cancer self-renewal in prostate cancer cell lines and patient-derived glioblastoma cells [52]. Although we have not investigated the effect of the combination of ONC201/TIC10 with 2-DG on the stemness of glioblastoma cells and the influence on TRAIL expression and Foxo3a transcription, it seems possible that those effects could be even more enhanced by the combination treatment.

Our data show that targeting the glycolytic pathway alone with 2-DG or OXPHOS with ONC201/TIC10 alone had no significant effect on the migratory capacity of the glioblastoma cells we examined. In contrast, the combination therapy exhibited a notable and significant anti-migratory effect. Other groups have shown similar results. Kennedy and colleagues presented data displaying even enhanced motility

of glioblastoma cell lines following the suppression of OXPHOS alone using oligomycin. These observations go in line with the hypothesis that cell migration is connected to hypoxia as an adaptive response to evade the nutrient-deficient microenvironment. In the same study, the authors described that a concomitant use of 2-DG and oligomycin, thus a combined inhibition of glycolysis and OXPHOS, led to a synergistic suppression of cell migration [32]. Similar, Shukla and coworkers have provided evidence that treatment with 2-DG led to an increased migratory capacity of GB cells by suppressing miR-t-5p and thus upregulating TFF3, a PI3K/Akt signaling pathway activator. This led to glioma growth and enhanced invasion, therefore, promoting disease progression [59]. Whether the addition of ONC201/TIC10 leads to a different effect on the miR-t-5p expression levels than a singular treatment with 2-DG remains to be investigated in future projects.

Furthermore, as Karpel-Massler and colleagues have shown in a previous study, some tumors are more vulnerable to treatments targeting the metabolome of the tumor. IDH1-mutated glioblastomas display said mutation in practically all glioblastoma cells, even though the tumor itself remains highly heterogenous. Those mutations lead to an increased accumulation of the oncometabolite 2-R-2-hydroxyglutarate (2-HG) which interferes with the ATP-synthase complex of oxidative phosphorylation, leaving the metabolic activity already compromised [29]. Targeting an already vulnerable metabolism of glioblastomas, such as the one of IDH1-mutated tumors, for instance with the combination therapy presented in this work, might yield promising results. Therefore, a screening for metabolic vulnerabilities in tumor samples from patients might prove advantageous for implementing a personalized treatment approach. Furthermore, Muller and colleagues have examined The Cancer Genome Atlas glioblastoma data set for homozygous deletions and identified a homozygous deletion at the 1p36 tumor-suppressor locus which includes the ENO1 gene. Enolase is an essential enzyme catalyzing the conversion of 2-phosphoglyceric acid into phosphoenolpyruvate, which is the second to last step of glycolysis. This enzyme is encoded by three homologous genes: ENO1, which is expressed in all cells; ENO2, that is expressed

in neural tissue and ENO3, expressed in muscular tissue, which is not particularly important in the context of glioblastoma therapy. The said homozygous deletion at the 1p36 locus is present in 1-5% of glioblastomas, making this subset of glioblastoma potentially sensitive to a therapy inhibiting ENO2 due to the absence of ENO1 and the importance of glycolysis for the tumoral energy production and generation of byproducts. Their data show that ENO1-deleted glioblastoma cells are particularly vulnerable to ENO2 inhibition, while the surrounding healthy neural tissue can compensate the ENO2 inhibition through the available ENO1 activity [44]. This group of patients might prove to be particularly responsive to a combined therapy with ONC201/TIC10 and an ENO2 inhibitor due to the already vulnerable metabolome of this glioblastoma subset.

The above-mentioned examples demonstrate the importance of screenings for molecular alterations of brain tumors or tumors in general. The group around Brat of the cIMPACT-NOW project therefore suggests to incorporate potential morphologic, proliferative or molecular markers that correlate with aggressive clinical behavior into the grading system for brain tumors. As an example, homozygous deletion of CDKN2A/B for was shown to be associated with a shorter overall survival in patients with IDH-mutant astrocytomas correlating with the clinical behavior of a WHO grade IV tumor. Based on histological criteria alone these tumors would be rather classified as grade II or III tumors. Differences in biological behavior also prompted the suggestion to clearly distinguish IDH-mutant from IDH-wildtype diffuse astrocytic gliomas in the grading system. The term glioblastoma could then be used solely for diffuse astrocytic gliomas that are IDH-wildtype and correspond histologically and genetically to an aggressive clinical behavior, therefore being included into WHO grade IV. Those diffuse astrocytic gliomas that are IDH-mutant would be graded based on their morphologic and genetic features and most importantly their clinical behavior into WHO grade II, III or IV [8]. In addition, defining just the IDH-mutation status of diffuse astrocytic gliomas is not sufficient and should also include EGFR amplification level, whole chromosome 7 gain/ whole chromosome 10 loss (+7/-10)

and TERT promoter mutations to include a tumor into the WHO grade IV category [9].

These suggestions mark a path towards more personalized treatment strategies based on molecular features which could in the future also include the profile of tumoral metabolic activity.

After all, the results of this preclinical study need to be critically viewed with respect to a potential clinical translation. Two important factors that are in favor of a potential clinical application of our combination therapy is the ability of both substances, ONC201/TIC10 and 2-DG, to cross the blood-brain barrier and to have shown to be well tolerated by patients [4,60]. Arrillaga-Romany and colleagues showed that when patients received weekly single agent treatment with ONC201/TIC10 at 625mg, the intratumoral concentration approximately 24 hours following the second weekly dose reached up to 9.3μM, a concentration that is close to the concentrations used in most of our experiments [5]. Whether 2-DG can reach similar concentrations, compared to our experimental setting, with good tolerability, remains to be investigated in future clinical trials.

The good tolerability and ability to reach efficacious concentrations at the tumor site offer a prospect, that our experimental approach is a potentially viable option for a clinical trial. Nevertheless, side effects of a therapy targeting the metabolism of possibly all cells in the human organism cannot be ruled out, yet. Although we have investigated the toxicity profile of the combination therapy for some normal human cells and organs of chicken embryos, this still remains a preliminary testing method and requires further investigation. Ultimately, the therapeutic efficacy remains to be studied in an *in vivo* orthotopic glioblastoma model, to see if the effects on tumor formation in our *in vivo near* CAM-assay are comparable.

In summary, our work suggests that a profound inhibition of the cancer cell metabolism can be achieved by the combined use of imipridones with a glycolysis inhibitor, such as 2-DG, to yield potent anti-cancer activity in a synergistic manner. Nevertheless, some questions remain to be addressed regarding the mechanism of how our suggested combination therapy specifically induces its effects on the cancer cell metabolome. One option to further look into this aspect, is the use of

coupled liquid chromatography-mass spectrometry to identify in treated cells precisely which metabolites are accumulating or lacking compared to cells not treated with our combination. As a result, further metabolic vulnerabilities or activated compensatory pathways could be unveiled and additionally targeted, augmenting the anti-neoplastic effect.

5. Summary

Metabolic dysregulation poses one of the complexities of battling brain malignancies such as glioblastoma. In this work we investigated, if a multi-targeting approach to reprogram the metabolome of glioblastoma leads to an enhanced anti-neoplastic activity.

Preclinical tests were performed using a combined treatment with ONC201/TIC10 and 2-Deoxyglucose in established and primary-cultured glioblastoma cells. Real-time effects on the oxidative phosphorylation (OXPHOS) and glycolysis were examined through the use of extracellular flux analysis. Further, Western blot analysis was used to determine protein expression of respiratory chain complexes. Biological effects on tumour growth were examined on the chorioallantoic membrane (CAM).

As a result, treatment with ONC201/TIC10 shows an impairment of the mitochondrial respiration leading to an increased glycolytic activity. Combined with 2-Deoxyglucose, both substances together induce a state of energy depletion, evident through the significant decrease in ATP levels and a generalized hypophosphorylative state. Additionally, synergistic anti-proliferative and anti-migratory activity were observed in different glioblastoma cell-lines. Furthermore, the combined therapy led to a significantly reduced tumour formation on the CAM. Consequently, combined therapy with ONC201/TIC10 and 2-Deoxyglucose leads to a metabolic reprogramming of glioblastoma cells yielding a synergistic anti-cancer activity. Lastly, due to the ability of both agents to readily cross the blood-brain barrier and the fact that a good safety profile was shown in clinical trials, when used solitarily, a further clinical evaluation of this therapeutic strategy is warranted.

6. Bibliography

1. Allen JE, Kline CLB, Prabhu V V., Wagner J, Ishizawa J, Madhukar N, Lev A, Baumeister M, Zhou L, Lulla A, Stogniew M, Schalop L, Benes C, Kaufman HL, Pottorf RS, Rao Nallaganchu B, Olson GL, Al-Mulla F, Duvic M, Wu GS, Dicker DT, Talekar MK, Lim B, Elemento O, Oster W, Bertino J, Flaherty K, Wang ML, Borthakur G, Andreeff M, Stein M, El-Deiry WS. Discovery and clinical introduction of first-in-class imipridone ONC201. *Oncotarget*. 2016;7:74380-74392. doi:10.18632/oncotarget.11814
2. Allen JE, Krigsfeld G, Mayes PA, Patel L, Dicker DT, Patel AS, Dolloff NG, Messaris E, Scata KA, Wang W, Zhou JY, Wu GS, El-Deiry WS. Dual inactivation of Akt and ERK by TIC10 signals Foxo3a nuclear translocation, TRAIL gene induction, and potent antitumor effects. *Sci Transl Med*. 2013;5:171ra17. doi:10.1126/scitranslmed.3004828
3. Allen JE, Krigsfeld G, Patel L, Mayes PA, Dicker DT, Wu GS, El-Deiry WS. Identification of TRAIL-inducing compounds highlights small molecule ONC201/TIC10 as a unique anti-cancer agent that activates the TRAIL pathway. *Mol Cancer*. 2015;14:99. doi:10.1186/s12943-015-0346-9
4. Arrillaga-Romany I, Chi AS, Allen JE, Oster W, Wen PY, Batchelor TT. A phase 2 study of the first imipridone ONC 201, a selective DRD 2 antagonist for oncology, administered every three weeks in recurrent glioblastoma. *Oncotarget*. 2017;8:79298-79304. doi:10.18632/oncotarget.17837
5. Arrillaga-Romany I, Odia Y, Allen JE, Prabhu V V., Tarapore R, Oster W, Mehta MP, Wen PY, Batchelor T. Intratumoral activity of ONC201 in adult recurrent glioblastoma patients. *J Clin Oncol*. 2018;36:e14034-e14034. doi:10.1200/jco.2018.36.15_suppl.e14034
6. Bachelard HS. Glucose as a fuel for the brain. *Biochem Soc Trans*. 1978;6:520-524. doi:10.1042/bst0060520
7. Binabaj MM, Bahrami A, ShahidSales S, Joodi M, Joudi Mashhad M, Hassanian SM, Anvari K, Avan A. The prognostic value of MGMT promoter methylation in glioblastoma: A meta-analysis of clinical trials. *J Cell Physiol*.

2018;233:378-386. doi:10.1002/jcp.25896

8. Brat DJ, Aldape K, Colman H, Figrarella-Branger D, Fuller GN, Giannini C, Holland EC, Jenkins RB, Kleinschmidt-DeMasters B, Komori T, Kros JM, Louis DN, McLean C, Perry A, Reifenberger G, Sarkar C, Stupp R, van den Bent MJ, von Deimling A, Weller M. cIMPACT-NOW update 5: recommended grading criteria and terminologies for IDH-mutant astrocytomas. *Acta Neuropathol*. 2020;139:603-608. doi:10.1007/s00401-020-02127-9
9. Brat DJ, Aldape K, Colman H, Holland EC, Louis DN, Jenkins RB, Kleinschmidt-DeMasters BK, Perry A, Reifenberger G, Stupp R, von Deimling A, Weller M. cIMPACT-NOW update 3: recommended diagnostic criteria for "Diffuse astrocytic glioma, IDH-wildtype, with molecular features of glioblastoma, WHO grade IV." *Acta Neuropathol*. 2018;136:805-810. doi:10.1007/s00401-018-1913-0
10. Chi AS, Tarapore RS, Hall MD, Shonka N, Gardner S, Umemura Y, Sumrall A, Khatib Z, Mueller S, Kline C, Zaky W, Khatua S, Weathers SP, Odia Y, Niazi TN, Daghistani D, Cherrick I, Korones D, Karajannis MA, Kong XT, Minturn J, Waanders A, Arillaga-Romany I, Batchelor T, Wen PY, Merdinger K, Schalop L, Stogniew M, Allen JE, Oster W, Mehta MP. Pediatric and adult H3 K27M-mutant diffuse midline glioma treated with the selective DRD2 antagonist ONC201. *J Neurooncol*. 2019;145:97-105. doi:10.1007/s11060-019-03271-3
11. Christofk HR, Vander Heiden MG, Harris MH, Ramanathan A, Gerszten RE, Wei R, Fleming MD, Schreiber SL, Cantley LC. The M2 splice isoform of pyruvate kinase is important for cancer metabolism and tumour growth. *Nature*. 2008;452:230-233. doi:10.1038/nature06734
12. DeBerardinis RJ, Chandel NS. Fundamentals of cancer metabolism. *Sci Adv*. 2016;2:e1600200. doi:10.1126/sciadv.1600200
13. Dianat-Moghadam H, Heidarifard M, Mahari A, Shahgolzari M, Keshavarz M, Nouri M, Amoozgar Z. TRAIL in oncology: From recombinant TRAIL to nano- and self-targeted TRAIL-based therapies. *Pharmacol Res*. 2020;155.

doi:10.1016/j.phrs.2020.104716

14. Dranoff, Glenn; Elion, Gertrude B.; Friedman, Henry S.; Bigner DD. Combination chemotherapy in vitro exploiting glutamine metabolism of human glioma and medulloblastoma - PubMed. Cancer Research. Published 1985. https://pubmed.ncbi.nlm.nih.gov/4028000/
15. Estrella V, Chen T, Lloyd M, Wojtkowiak J, Cornnell HH, Ibrahim-Hashim A, Bailey K, Balagurunathan Y, Rothberg JM, Sloane BF, Johnson J, Gatenby RA, Gillies RJ. Acidity Generated by the Tumor Microenvironment Drives Local Invasion. *Cancer Res*. 2013;73:1524-1535. doi:10.1158/0008-5472.CAN-12-2796
16. Falschlehner C, Schaefer U, Walczak H. Following TRAIL's path in the immune system. *Immunology*. 2009;127:145-154. doi:10.1111/j.1365-2567.2009.03058.x
17. Frankenberg-Schwager M, Harbich R, Frankenberg D, Jain V. 2-deoxy-d-glucose inhibits rejoining of radiation-induced DNA double-Strand breaks in yeast. *Int J Radiat Biol*. 1992;61:185-190. doi:10.1080/09553009214550801
18. Giese A, Bjerkvig R, Berens ME, Westphal M. Cost of Migration: Invasion of Malignant Gliomas and Implications for Treatment. *J Clin Oncol*. 2003;21:1624-1636. doi:10.1200/JCO.2003.05.063
19. Greer EL, Brunet A. FOXO transcription factors at the interface between longevity and tumor suppression. *Oncogene*. 2005;24:7410-7425. doi:10.1038/sj.onc.1209086
20. Hanif F, Muzaffar K, Perveen K, Malhi SM, Simjee SU. Glioblastoma Multiforme: A Review of its Epidemiology and Pathogenesis through Clinical Presentation and Treatment. *Asian Pac J Cancer Prev*. 2017;18:3-9. doi:10.22034/APJCP.2017.18.1.3
21. Hasslacher S, Schneele L, Stroh S, Langhans J, Zeiler K, Kattner P, Karpel-Massler G, Siegelin M, Schneider M, Zhou S, Grunert M, Halatsch ME, Nonnenmacher L, Debatin KM, Westhoff MA. Inhibition of PI3K signalling increases the efficiency of radiotherapy in glioblastoma cells. *Int J Oncol*.

2018;53:1881-1896. doi:10.3892/ijo.2018.4528

22. Hochhaus A, Ernst T, Eigendorff E, La Rosée P. Causes of resistance and treatment choices of second- and third-line treatment in chronic myelogenous leukemia patients. *Ann Hematol*. 2015;94:133-140. doi:10.1007/s00277-015-2323-1

23. Holland EC. Glioblastoma multiforme: the terminator. *Proc Natl Acad Sci U S A*. 2000;97:6242-6244. http://www.ncbi.nlm.nih.gov/pubmed/10841526

24. Inda M d. M, Bonavia R, Mukasa A, Narita Y, Sah DWY, Vandenberg S, Brennan C, Johns TG, Bachoo R, Hadwiger P, Tan P, DePinho RA, Cavenee W, Furnari F. Tumor heterogeneity is an active process maintained by a mutant EGFR-induced cytokine circuit in glioblastoma. *Genes Dev*. 2010;24:1731-1745. doi:10.1101/gad.1890510

25. Ishida CT, Zhang Y, Bianchetti E, Shu C, Nguyen TTT, Kleiner G, Sanchez-Quintero MJ, Quinzii CM, Westhoff MA, Karpel-Massler G, Prabhu V V., Allen JE, Siegelin MD. Metabolic reprogramming by dual AKT/ERK inhibition through imipridones elicits unique vulnerabilities in glioblastoma. *Clin Cancer Res*. 2018;24:5392-5406. doi:10.1158/1078-0432.CCR-18-1040

26. Jamal-Hanjani M, Quezada SA, Larkin J, Swanton C. Translational Implications of Tumor Heterogeneity. *Clin Cancer Res*. 2015;21:1258-1266. doi:10.1158/1078-0432.CCR-14-1429

27. Jang M, Kim SS, Lee J. Cancer cell metabolism: implications for therapeutic targets. *Exp Mol Med*. 2013;45:e45. doi:10.1038/emm.2013.85

28. Karpel-Massler G, Bâ M, Shu C, Halatsch ME, Westhoff MA, Bruce JN, Canoll P, Siegelin MD. TIC10/ONC201 synergizes with Bcl-2/Bcl-xL inhibition in glioblastoma by suppression of Mcl-1 and its binding partners in vitro and in vivo. *Oncotarget*. 2015;6:36456-36471. doi:10.18632/oncotarget.5505

29. Karpel-Massler G, Ishida CT, Bianchetti E, Zhang Y, Shu C, Tsujiuchi T, Banu MA, Garcia F, Roth KA, Bruce JN, Canoll P, Siegelin MD. Induction of synthetic lethality in IDH1-mutated gliomas through inhibition of Bcl-xL. *Nat Commun*. 2017;8:1067. doi:10.1038/s41467-017-00984-9

30. Karpel-Massler G, Shu C, Chau L, Banu M, Halatsch ME, Westhoff MA, Ramirez Y, Ross AH, Bruce JN, Canoll P, Siegelin MD. Combined inhibition of Bcl-2/Bcl-xL and Usp9X/Bag3 overcomes apoptotic resistance in glioblastoma in vitro and in vivo. *Oncotarget*. 2015;6:14507-14521. doi:10.18632/oncotarget.3993
31. Karpel-Massler G, Westhoff MA, Zhou S, Nonnenmacher L, Dwucet A, Kast RE, Bachem MG, Wirtz CR, Debatin KM, Halatsch ME. Combined Inhibition of HER1/EGFR and RAC1 Results in a Synergistic Antiproliferative Effect on Established and Primary Cultured Human Glioblastoma Cells. Published online 2013. doi:10.1158/1535-7163.MCT-13-0052
32. Kennedy CR, Tilkens SB, Guan H, Garner JA, Or PMY, Chan AM. Differential sensitivities of glioblastoma cell lines towards metabolic and signaling pathway inhibitions. *Cancer Lett*. 2013;336:299-306. doi:10.1016/j.canlet.2013.03.020
33. Kim EH, Lee JH, Oh Y, Koh I, Shim JK, Park J, Choi J, Yun M, Jeon JY, Huh YM, Chang JH, Kim SH, Kim KS, Cheong JH, Kim P, Kang SG. Inhibition of glioblastoma tumorspheres by combined treatment with 2-deoxyglucose and metformin. *Neuro Oncol*. Published online August 29, 2016:now174. doi:10.1093/neuonc/now174
34. Kline CLB, Ralff MD, Lulla AR, Wagner JM, Abbosh PH, Dicker DT, Allen JE, El-Deiry WS. Role of Dopamine Receptors in the Anticancer Activity of ONC201. *Neoplasia (United States)*. 2018;20:80-91. doi:10.1016/j.neo.2017.10.002
35. Law M, Yang S, Wang H, Babb JS, Johnson G, Cha S, Knopp EA, Zagzag D. Glioma grading: sensitivity, specificity, and predictive values of perfusion MR imaging and proton MR spectroscopic imaging compared with conventional MR imaging. *AJNR Am J Neuroradiol*. 2005;24:1989-1998. http://www.ncbi.nlm.nih.gov/pubmed/14625221
36. Lee M, Ko H, Yun M. Cancer Metabolism as a Mechanism of Treatment Resistance and Potential Therapeutic Target in Hepatocellular Carcinoma. *Yonsei Med J*. 2018;59:1143. doi:10.3349/YMJ.2018.59.10.1143

37. Liberti M V, Locasale JW. The Warburg Effect: How Does it Benefit Cancer Cells? *Trends Biochem Sci*. 2016;41:211-218. doi:10.1016/j.tibs.2015.12.001
38. Louis DN, Ohgaki H, Wiestler OD, Cavenee WK, Burger PC, Jouvet A, Scheithauer BW, Kleihues P. The 2007 WHO classification of tumours of the central nervous system. *Acta Neuropathol*. 2007;114:97-109. doi:10.1007/s00401-007-0243-4
39. Mao H, Lebrun DG, Yang J, Zhu VF, Li M. Deregulated signaling pathways in glioblastoma multiforme: molecular mechanisms and therapeutic targets. *Cancer Invest*. 2012;30:48-56. doi:10.3109/07357907.2011.630050
40. Martin MJ, Eberlein C, Taylor M, Ashton S, Robinson D, Cross D. Inhibition of oxidative phosphorylation suppresses the development of osimertinib resistance in a preclinical model of EGFR-driven lung adenocarcinoma. *Oncotarget*. 2016;7:86313-86325. doi:10.18632/oncotarget.13388
41. McGranahan N, Swanton C. Biological and Therapeutic Impact of Intratumor Heterogeneity in Cancer Evolution. *Cancer Cell*. 2015;27:15-26. doi:10.1016/j.ccell.2014.12.001
42. Mohanti BK, Rath GK, Anantha N, Kannan V, Das BS, Chandramouli BAR, Banerjee AK, Das S, Jena A, Ravichandran R, Sahi UP, Kumar R, Kapoor N, Kalia VK, Dwarakanath BS, Jain V. Improving cancer radiotherapy with 2-deoxy-D-glucose: Phase I/II clinical trials on human cerebral gliomas. *Int J Radiat Oncol Biol Phys*. 1996;35:103-111. doi:10.1016/S0360-3016(96)85017-6
43. Molenaar RJ, Verbaan D, Lamba S, Zanon C, Jeuken JWM, Boots-Sprenger SHE, Wesseling P, Hulsebos TJM, Troost D, van Tilborg AA, Leenstra S, Vandertop WP, Bardelli A, van Noorden CJF, Bleeker FE. The combination of IDH1 mutations and MGMT methylation status predicts survival in glioblastoma better than either IDH1 or MGMT alone. *Neuro Oncol*. 2014;16:1263-1273. doi:10.1093/neuonc/nou005
44. Muller FL, Colla S, Aquilanti E, Manzo VE, Genovese G, Lee J, Eisenson D, Narurkar R, Deng P, Nezi L, Lee MA, Hu B, Hu J, Sahin E, Ong D, Fletcher-Sananikone E, Ho D, Kwong L, Brennan C, Wang YA, Chin L, Depinho RA.

Passenger deletions generate therapeutic vulnerabilities in cancer. *Nature*. 2012;488:337-342. doi:10.1038/nature11331

45. Muñoz-Pinedo C, Ruiz-Ruiz C, De Almodóvar CR, Palacios C, López-Rivas A. Inhibition of glucose metabolism sensitizes tumor cells to death receptor-triggered apoptosis through enhancement of death-inducing signaling complex formation and apical procaspase-8 processing. *J Biol Chem*. 2003;278:12759-12768. doi:10.1074/jbc.M212392200
46. Ohgaki H, Kleihues P. Epidemiology and etiology of gliomas. *Acta Neuropathol*. 2005;109:93-108. doi:10.1007/s00401-005-0991-y
47. Pardridge WM, Crane PD, Mietus LJ, Oldendorf WH. Kinetics of Regional Blood–Brain Barrier Transport and Brain Phosphorylation of Glucose and 2-Deoxyglucose in the Barbiturate–Anesthetized Rat. *J Neurochem*. 1982;38:560-568. doi:10.1111/j.1471-4159.1982.tb08663.x
48. Patel AP, Tirosh I, Trombetta JJ, Shalek AK, Gillespie SM, Wakimoto H, Cahill DP, Nahed B V, Curry WT, Martuza RL, Louis DN, Rozenblatt-Rosen O, Suvà ML, Regev A, Bernstein BE. Single-cell RNA-seq highlights intratumoral heterogeneity in primary glioblastoma. *Science (80-)*. 2014;344:1396-1401. doi:10.1126/science.1254257
49. Pavlova NN, Thompson CB. The Emerging Hallmarks of Cancer Metabolism. *Cell Metab*. 2016;23:27-47. doi:10.1016/j.cmet.2015.12.006
50. Potter M, Newport E, Morten KJ. The Warburg effect: 80 years on. *Biochem Soc Trans*. 2016;44:1499-1505. doi:10.1042/BST20160094
51. Prabhu V V., Allen JE, Dicker DT, El-Deiry WS. Small-molecule ONC201/TIC10 targets chemotherapy-resistant colorectal cancer stem-like cells in an akt/Foxo3a/TRAIL-Dependent manner. *Cancer Res*. 2015;75:1423-1432. doi:10.1158/0008-5472.CAN-13-3451
52. Prabhu V V., Lulla AR, Madhukar NS, Ralff MD, Zhao D, Kline CLB, Van Den Heuvel APJ, Lev A, Garnett MJ, McDermott U, Benes CH, Batchelor TT, Chi AS, Elemento O, Allen JE, El-Deiry WS. Cancer stem cell-related gene expression as a potential biomarker of response for first-in-class imipridone ONC201 in solid tumors. *PLoS One*. 2017;12.

doi:10.1371/journal.pone.0180541

53. Pruss M, Dwucet A, Tanriover M, Hlavac M, Kast RE, Debatin KM, Wirtz CR, Halatsch ME, Siegelin MD, Westhoff MA, Karpel-Massler G. Dual metabolic reprogramming by ONC201/TIC10 and 2-Deoxyglucose induces energy depletion and synergistic anti-cancer activity in glioblastoma. *Br J Cancer 2020 1228*. 2020;122:1146-1157. doi:10.1038/s41416-020-0759-0

54. Raez LE, Papadopoulos K, Ricart AD, Chiorean EG, Dipaola RS, Stein MN, Rocha Lima CM, Schlesselman JJ, Tolba K, Langmuir VK, Kroll S, Jung DT, Kurtoglu M, Rosenblatt J, Lampidis TJ. A phase i dose-escalation trial of 2-deoxy-d-glucose alone or combined with docetaxel in patients with advanced solid tumors. *Cancer Chemother Pharmacol*. 2013;71:523-530. doi:10.1007/s00280-012-2045-1

55. Rong Y, Durden DL, Van Meir EG, Brat DJ. "Pseudopalisading" necrosis in glioblastoma: a familiar morphologic feature that links vascular pathology, hypoxia, and angiogenesis. *J Neuropathol Exp Neurol*. 2006;65(6):529-539. http://www.ncbi.nlm.nih.gov/pubmed/16783163

56. Rybinski B, Yun K. Addressing intra-tumoral heterogeneity and therapy resistance. *Oncotarget*. 2016;7:72322-72342. doi:10.18632/oncotarget.11875

57. Salah Uddin ABM JT. Neurologic Manifestations of Glioblastoma Multiforme Clinical Presentation: History, Physical, Causes. Published 2015. https://emedicine.medscape.com/article/1156220-clinical

58. Sequist L V., Soria JC, Goldman JW, Wakelee HA, Gadgeel SM, Varga A, Papadimitrakopoulou V, Solomon BJ, Oxnard GR, Dziadziuszko R, Aisner DL, Doebele RC, Galasso C, Garon EB, Heist RS, Logan J, Neal JW, Mendenhall MA, Nichols S, Piotrowska Z, Wozniak AJ, Raponi M, Karlovich CA, Jaw-Tsai S, Isaacson J, Despain D, Matheny SL, Rolfe L, Allen AR, Camidge DR. Rociletinib in EGFR -Mutated Non–Small-Cell Lung Cancer . *N Engl J Med*. 2015;372:1700-1709. doi:10.1056/nejmoa1413654

59. Shukla A, Gupta P, Singh R, Mishra DP. Glycolytic inhibitor 2-Deoxy-D-Glucose activates migration and invasion in glioblastoma cells through modulation of the miR-7-5p/TFF3 signaling pathway. *Biochem Biophys Res*

Commun. 2018;499:829-835. doi:10.1016/j.bbrc.2018.04.001

60. Singh D, Banerji AK, Dwarakanath BS, Tripathi RP, Gupta JP, Mathew TL, Ravindranath T, Jain V. Optimizing cancer radiotherapy with 2-deoxy-D-glucose: Dose escalation studies in patients with glioblastoma multiforme. *Strahlentherapie und Onkol*. 2005;181:507-514. doi:10.1007/s00066-005-1320-z
61. Singh SP, Singh S, Jain V. Effects of 5-bromo-2-deoxyuridine and 2-deoxy-d-glucose on radiation-induced micronuclei in mouse bone marrow. *Int J Radiat Biol*. 1990;58:791-797. doi:10.1080/09553009014552171
62. Smith C, Ironside JW. Diagnosis and pathogenesis of gliomas. *Curr Diagnostic Pathol*. 2007;13:180-192. doi:10.1016/j.cdip.2007.04.002
63. Sols A, Crane R. Substrate specificity of brain hexokinase. *J Biol Chem*. 1954;210:581-595. http://www.ncbi.nlm.nih.gov/pubmed/13211595
64. Songtao Q, Lei Y, Si G, Yanqing D, Huixia H, Xuelin Z, Lanxiao W, Fei Y. IDH mutations predict longer survival and response to temozolomide in secondary glioblastoma. *Cancer Sci*. 2012;103:269-273. doi:10.1111/j.1349-7006.2011.02134.x
65. Sottoriva A, Spiteri I, Piccirillo SGM, Touloumis A, Collins VP, Marioni JC, Curtis C, Watts C, Tavare S. Intratumor heterogeneity in human glioblastoma reflects cancer evolutionary dynamics. *Proc Natl Acad Sci*. 2013;110:4009-4014. doi:10.1073/pnas.1219747110
66. Stein M, Lin H, Jeyamohan C, Dvorzhinski D, Gounder M, Bray K, Eddy S, Goodin S, White E, Dipaola RS. Targeting tumor metabolism with 2-deoxyglucose in patients with castrate-resistant prostate cancer and advanced malignancies. *Prostate*. 2010;70:1388-1394. doi:10.1002/pros.21172
67. Stupp R, Mason WP, van den Bent MJ, Weller M, Fisher B, Taphoorn MJB, Belanger K, Brandes AA, Marosi C, Bogdahn U, Curschmann J, Janzer RC, Ludwin SK, Gorlia T, Allgeier A, Lacombe D, Cairncross JG, Eisenhauer E, Mirimanoff RO, European Organisation for Research and Treatment of Cancer Brain Tumor and Radiotherapy Groups, National Cancer Institute of

Canada Clinical Trials Group. Radiotherapy plus Concomitant and Adjuvant Temozolomide for Glioblastoma. *N Engl J Med*. 2005;352:987-996. doi:10.1056/NEJMoa043330

68. Sun L, Liu X, Fu H, Zhou W, Zhong D. 2-Deoxyglucose Suppresses ERK Phosphorylation in LKB1 and Ras Wild-Type Non-Small Cell Lung Cancer Cells. *PLoS One*. 2016;11:e0168793. doi:10.1371/journal.pone.0168793
69. Swamy RK, Manickam J, Adhikari JS, Dwarakanath BS. Glycolytic inhibitor, 2-deoxy-D-glucose, does not enhance radiation-induced apoptosis in mouse thymocytes and splenocytes in vitro. *Indian J Exp Biol*. 2005;43:686-692. http://www.ncbi.nlm.nih.gov/pubmed/16121709
70. Tamimi AF, Juweid M. *Epidemiology and Outcome of Glioblastoma*. Codon Publications; 2017. doi:10.15586/CODON.GLIOBLASTOMA.2017.CH8
71. Tateishi K, Iafrate AJ, Ho Q, Curry WT, Batchelor TT, Flaherty KT, Onozato ML, Lelic N, Sundaram S, Cahill DP, Chi AS, Wakimoto H. Myc-Driven glycolysis is a therapeutic target in glioblastoma. *Clin Cancer Res*. 2016;22:4452-4465. doi:10.1158/1078-0432.CCR-15-2274
72. Le Tourneau C, Delord JP, Gonçalves A, Gavoille C, Dubot C, Isambert N, Campone M, Trédan O, Massiani MA, Mauborgne C, Armanet S, Servant N, Bièche I, Bernard V, Gentien D, Jezequel P, Attignon V, Boyault S, Vincent-Salomon A, Servois V, Sablin MP, Kamal M, Paoletti X, SHIVA investigators. Molecularly targeted therapy based on tumour molecular profiling versus conventional therapy for advanced cancer (SHIVA): a multicentre, open-label, proof-of-concept, randomised, controlled phase 2 trial. *Lancet Oncol*. 2015;16:1324-1334. doi:10.1016/S1470-2045(15)00188-6
73. Venneti S, Thompson CB. Metabolic Reprogramming in Brain Tumors. *Annu Rev Pathol Mech Dis*. 2017;12:515-545. doi:10.1146/annurev-pathol-012615-044329
74. Walczak H, Miller RE, Ariail K, Gliniak B, Griffith TS, Kubin M, Chin W, Jones J, Woodward A, Le T, Smith C, Smolak P, Goodwin RG, Rauch CT, Schuh JCL, Lynch DH. Tumoricidal activity of tumor necrosis factor–related apoptosis–inducing ligand in vivo. *Nat Med*. 1999;5:157-163.

doi:10.1038/5517

75. Warburg O, Wind F, Negelein E. The metabolism of tumors in the body. *J Gen Physiol*. 1927;8:519-530. doi:10.1085/jgp.8.6.519

76. Ward PS, Thompson CB. Metabolic Reprogramming: A Cancer Hallmark Even Warburg Did Not Anticipate. *Cancer Cell*. 2012;21:297-308. doi:10.1016/j.ccr.2012.02.014

77. Westhoff MA, Brühl O, Nonnenmacher L, Karpel-Massler G, Debatin KM. Killing me softly--future challenges in apoptosis research. *Int J Mol Sci*. 2014;15:3746-3767. doi:10.3390/ijms15033746

78. Wick A, Drury D, Nakada H, Wolfe J. Localization of the primary metabolic block produced by 2-deoxyglucose. *J Biol Chem*. 1957;224:963-969. http://www.ncbi.nlm.nih.gov/pubmed/13405925

79. Yan H, Parsons DW, Jin G, McLendon R, Rasheed BA, Yuan W, Kos I, Batinic-Haberle I, Jones S, Riggins GJ, Friedman H, Friedman A, Reardon D, Herndon J, Kinzler KW, Velculescu VE, Vogelstein B, Bigner DD. IDH1 and IDH2 Mutations in Gliomas . *N Engl J Med*. 2009;360:765-773. doi:10.1056/nejmoa0808710

80. Yang JY, Zong CS, Xia W, Yamaguchi H, Ding Q, Xie X, Lang JY, Lai CC, Chang CJ, Huang WC, Huang H, Kuo HP, Lee DF, Li LY, Lien HC, Cheng X, Chang KJ, Hsiao CD, Tsai FJ, Tsai CH, Sahin AA, Muller WJ, Mills GB, Yu D, Hortobagyi GN, Hung MC. ERK promotes tumorigenesis by inhibiting FOXO3a via MDM2-mediated degradation. *Nat Cell Biol*. 2008;10:138-148. doi:10.1038/ncb1676

81. Zhang L, Sorensen MD, Kristensen BW, Reifenberger G, McIntyre TM, Lin F. D-2-Hydroxyglutarate Is an Intercellular Mediator in IDH-Mutant Gliomas Inhibiting Complement and T Cells. *Clin Cancer Res*. 2018;24:5381-5391. doi:10.1158/1078-0432.CCR-17-3855

82. Zhang Y, Li X, Tan S, Liu X, Zhao X, Yuan Z, Nie C. Mcl-1 expression and JNK activation induces a threshold for apoptosis in Bcl-xL-overexpressing hematopoietic cells. *Oncotarget*. 2017;8:11042-11052. doi:10.18632/oncotarget.14223

83. Zhu J, Zheng Y, Zhang H, Sun H. Targeting cancer cell metabolism: The combination of metformin and 2-Deoxyglucose regulates apoptosis in ovarian cancer cells via p38 MAPK/JNK signaling pathway. *Am J Transl Res*. 2016;8:4812-4821. http://www.ncbi.nlm.nih.gov/pubmed/27904682

Statutory declaration

Hereby, I declare that I wrote the present dissertation with the topic:
"Tumor cell metabolism as a therapeutic target in glioblastoma
– Characterization of the anti-neoplastic activity of a combined treatment with ONC201/TIC10 and 2-Deoxyglucose"
independently and used no other aids than those cited. In each individual case, I have clearly identified the source of the passages that are taken word for word or paraphrased from other works.
Furthermore, I hereby declare that I have carried out my scientific work according to the principles of good scientific practice in accordance with the current "Satzung der Universität Ulm zur Sicherung guter wissenschaftlicher Praxis" [Rules of the Ulm University for Assuring Good Scientific Practice].

Düsseldorf, 25.04.2021

Maximilian Pruss

Acknowledgements

Firstly, and most of all, I would like to thank Prof. Dr. med. Georg Karpel-Massler for giving me the opportunity to work on this dissertation. At every step of the process, he provided intellectual guidance and had an availability every student could only wish for. Through him I got a deep interest and insight in the field of laboratory medicine. He taught me the importance of research as a pillar of medicine, and I feel honored to have taken my baby steps in this field with such an accomplished scientist and clinician. Without him, I might not have the job I have today, which I truly love, and through him I might have the opportunity to continue my work in laboratory medicine in the future.

Secondly and equally, I would like to thank PD Dr. Mike-Andrew Westhoff, who taught me how to approach scientific questions and always had the time to explain everything that I ever asked. The atmosphere and the mood in his laboratory are absolutely incredible, welcoming and friendly. I am thankful to have gathered my experience with him and his team.

I am grateful to Annika Dwucet, who taught me all the basic laboratory skills and supported me with every experiment along the way. Additionally, I would like to thank Andrea Schuster and Daniela Zerrinius for teaching me and lending me a helpful hand whenever I needed one. Without them and without everybody else in the laboratory of Prof. Dr. med. Georg Karpel-Massler and PD Dr. Mike-Andrew Westhoff, this project would not have been possible.

Lastly, I would like to thank my partner Stephanie for always being by my side and my mother, brother and uncle without who I couldn’t have been able to pursue my dream of becoming a medical doctor.

Curriculum vitae

Personal dates

Name	Maximilian Pruss
Date of birth	1993
Place of birth	Frankfurt am Main
Marital status	unmarried
Nationality	German

Educational training

2008-2003	Heinrich-von-Gagern-Gymnasium, Frankfurt am Main Graduation: general higher education entrance qualification